KU LEUVEN

BPS
Belgian Physical Society

General Scientific Meeting
Belgian Physical Society

KU Leuven, Belgium
Leuven, May 27, 2026

Abstract Book

Plenary Talks

Plenary1

Taking quantum bits from the lab to 300 mm cmos fab: overcoming materials and interface limitations through advanced semiconductor manufacturing

Kristiaan De Greve[1,2]

[1]*imec, 3001 Leuven, Belgium*
[2]*Department of Electrical Engineering, KU Leuven, 3001 Leuven, Belgium*

In this talk, I will present recent work performed in my group at imec pertaining the fabrication of superconducting and spin qubits in an industry-level 300 mm CMOS pilot fabrication line. Through the careful modification of dedicated CMOS fabrication processes, interface and materials limitations to qubit performance can be tackled in a way that is in principle conducive to yielding large scale quantum circuits. For superconducting qubits, overcoming surface-oxide based limitations [1] recently resulted in the first demonstration of subtractively etched qubits in an advanced 300 mm manufacturing process [2], with high yield and high coherence. Innovations in materials and interfacial treatment further widen the toolbox of materials and processes available for superconducting qubit manufacturing [3].

For quantum dot qubits in silicon (MOS) and silicon/silicon-germanium (Si/SiGe), our effort has focused on optimizing processes and designs to create very low noise and low disorder quantum dots in both MOS [4] and Si/SiGe [5], using dedicated tooling and processes. Our quantum dot effort is validated by experimental studies demonstrating statistically low disorder [6] and reproducibly high qubit coherence and fidelity [7] in test devices – in line with theoretical models linking defectivity to noise and disorder in quantum dots [8].

In addition to the qubit optimization effort, I will present recent results on the development of modules that allow for upscaling of quantum dot arrays, that will allow larger scale processors to be manufactured. Bringing together quantum dot control, high qubit quality and large scale arrays should enable the realization of quantum dot spin qubit architectures into functional systems, such as the recently proposed trilinear array with shuttling enhanced qubit connectivity [9]. Time permitting, I will briefly digress on recent efforts to couple microwave photons to optical photons [10], to allow long-distance connectivity of cryogenic qubits.

[1] Van Damme et al., Argon-Milling-Induced Decoherence Mechanisms in Superconducting Quantum Circuits, 2023 *Phys Rev Appl* **20**, 014034
[2] J. Van Damme et al., Advanced CMOS manufacturing of superconducting qubits on 300 mm wafers, 2024 *Nature* **634**, 74
[3] DP Lozano et al., Low-loss α-tantalum coplanar waveguide resonators on silicon wafers: fabrication, characterization and surface modification, 2024 *Mater Quantum Tech* **4**, 025801
[4] A. Elsayed et al., Low charge noise quantum dots with industrial CMOS manufacturing, 2024 *NPJ Quantum* **10**, 70
[5] T. Koch et al., Industrial 300 mm Industrial 300 mm wafer processed spin qubits in natural silicon/silicon-germanium, 2025 *NPJ Quantum* **11**, 59
[6] K.-C. Chen et al., Statistical analysis of spurious dot formation in silicon metal-oxide-semiconductor single electron transistors, 2025 *Phys Rev B* **111**, 125301
[7] P. Steinacker et al., A 300 mm foundry silicon spin qubit unit cell exceeding 99% fidelity in all operations, 2025 *Nature* **646**, 81
[8] M. Shehata et al., Modeling semiconductor spin qubits and their charge noise environment for quantum gate fidelity estimation, 2023 *Phys Rev B* **108**, 045305
[9] R. Li et al., A trilinear quantum dot architecture for semiconductor spin qubits, 2025 *arXiv* 2501.17841 (*Scientific Reports*, in press).
[10] A. Ulrich et al., Engineering high Pockels coefficients in thin-film strontium titanate for cryogenic quantum electro-optic applications, 2025 *Science* **390**, 390

Plenary2

Laser-cooled molecules for quantum science and tests of fundamental physics

M. R. Tarbutt[1]

[1]*Centre for Cold Matter, Blackett Laboratory, Imperial College London, London SW7 2BW, UK*

Over the last decade, there has been rapid progress in laser cooling and trapping of polar molecules. This progress has been driven by the many exciting applications of ultracold molecules. They can be used to study many-body quantum physics, process quantum information and improve our understanding of chemical processes at the quantum level. They can also be used to test physics beyond the Standard Model [1].

In this talk, I will first introduce our methods for cooling and trapping polar molecules, then describe how we use these ultracold molecules to probe fundamental physics. In one experiment, we are developing a molecular lattice clock based on ultracold CaF molecules and using it to test the hypothesis that the fundamental constants may vary in time. Our clock will be especially sensitive to variations of the electron-to-proton mass ratio [2]. In a second experiment, we aim to use ultracold YbF molecules to measure the electron's electric dipole moment (EDM) with precision beyond the current state of the art [3]. This experiment is a molecular interferometer [4] and some example interference fringes are shown in Figure 1. The measurement is a test of time-reversal symmetry violation and an extremely sensitive probe of new physics, including models of supersymmetry. I will present the status of these experiments and our plans for future developments.

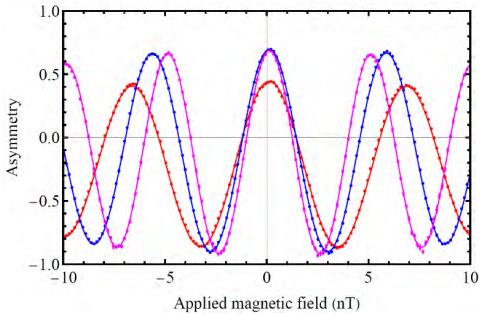

Figure 1: Interference fringes as a function of applied magnetic field in a spin interferometer using a beam of ultracold YbF molecules. The three datasets correspond to molecules travelling at three different speeds.

[1] DeMille D, Hutzler N R, Rey A M and Zelevinsky T 2024 *Nature Physics* **20**, 741
[2] Barontini G *et al.* 2022 *EPJ Quantum Technol.* **9**, 12
[3] Roussy T S *et al.* 2023 *Science* **381**, 46
[4] Jenkins R A *et al.* 2026 *arXiv:2602.00713*

YSC1

Precise Nuclear Charge Radii of Silicon Isotopes Using Muonic X-ray Spectroscopy

M. Deseyn[1] for the ReferenceRadii collaboration

[1]*Instituut voor Kern- en Stralingsfysica, KU Leuven, Leuven, Belgium*

The nuclear charge radius quantifies the spatial distribution of electric charges inside the nucleus. As a fundamental property of atomic nuclei, it provides a direct benchmark for nuclear-structure models, allows for searches for physics beyond the standard model [1], and constrains the properties of neutron stars through the equation of state [2]. Accurate charge radius determination is therefore essential for both tests of fundamental interactions and for constraining the properties of the nuclear equation of state using the slope of the symmetry energy *L*.

Since silicon isotopes are of particular interest for this, dedicated laser spectroscopy has been performed to extract its charge radii [2], which are currently being expanded upon. However, laser spectroscopy relies on the so-called atomic mass- and field-shift parameters to extract charge radii, which are currently a limiting factor. This limits the reliability of the extracted radii and reduces the sensitivity to new physics and to nuclear equation of state constraints. Therefore, a model-independent calibration using a King-plot analysis is needed, which in turn requires the absolute nuclear charge radius of 3 isotopes. In this contribution, we will report on the absolute charge radii of ^{28,29,30}Si using muonic x-ray spectroscopy.

When a negative muon is captured into an atomic orbit, the increased mass (∼207 times the electron mass) reduces the Bohr radius (by that same factor). Consequently, the overlap between the muon and the nucleus is increased substantially compared to its electronic counterparts, re-sulting in a sensitivity increase of about seven orders of magnitude. The emitted muonic x-ray transition energies hence provide a precise probe of the nuclear charge radius.

The experiment on ^{28,29,30}Si was performed in 2024 at the Paul Scherrer Institute using the high-resolution GIANT HPGe detector array [3]. By combining the measured transition energies with QED and nuclear-structure calculations, improved absolute charge radii were extracted. The achieved precision represents an improvement of a factor 3 compared to previous literature values, while also increasing the reliability.

The improved reference radii enable experimental determination of the mass- and field-shift parameters through a King-plot analysis. With these improved parameters, laser spectroscopy isotope shifts of radioactive isotopes can be translated towards high precision charge radii along the Si isotopic chain. Those improved charge radii allow for an enhanced accuracy on the determination of the slope of the symmetry energy in the neutron equation of state, allowing investigation of the slight tension between the *L* parameter extracted from [1] and PREX-II [4].

This work is part of the broader effort by the muX/ReferenceRadii collaboration at PSI, which is reviving the field of muonic x-ray spectroscopy in the medium to heavy mass nuclei.

[1] Mikhail Gorchtein and Chien-Yeah Seng. Superallowed nuclear beta decays and precision tests of the standard model. 2024 *Ann. Rev. Nucl. Part. Sci.* **74,** 23-47

[2] Kristian König *et al.*. Nuclear charge radii of silicon isotopes. 2024 *Phys. Rev. Lett.* **132**, 162502.

[3] Lars Gerchow *et al.*, Germanium array for non-destructive testing (GIANT) setup for muon-induced x-ray emission (MIXE) at the Paul Scherrer Institute. 2023 *Rev. Sci. Instrum.* **94**, 045106.

[4] Brendan T. Reed, *et al.* Implications of PREX-2 on the equation of state of neutron-rich matter. 2021 *Phys. Rev. Lett.* **126**, 172503.

YSC2

Radar Signal Properties and Reconstruction for the Radar Echo Telescope for Neutrinos

Jannes Loonen[1] on behalf of the Radar Echo Telescope Collaboration

[1]*Vrije Universiteit Brussel, Brussel, 1050, België*

The Radar Echo Telescope (RET) aims to observe the cosmic neutrino flux at the highest energies ($> 10^{16}$ eV) using radar. Neutrinos are known to have a small interaction probability and a rapidly decreasing flux at high energies. Consequently, they are hard to detect on Earth. However, they can travel over large cosmological distances unharmed and will therefore help reveal the nature of the most energetic astrophysical events in the universe and allow us to probe particle interactions at the highest energies. Radio wave detection methods can instrument the large effective volumes required for observing these high-energy neutrinos in a cost-effective manner. We discuss the radar method as a possible radio-based approach. The in-ice interaction of neutrinos creates a cascade of high-energy secondary particles that ionise their surroundings, leaving behind a dense trail of free electrons that can be detected using radar. We will present the rich phenomenology of the expected radar signals and show that their time evolution and frequency content can be predicted using two simple analytical expressions. We discuss how these new insights regarding signal properties can be used to reconstruct neutrino properties, such as their arrival direction, and help in detector optimisation for RET.

Thermal waves as messengers to image heat dissipation in 3D-integrated cryogenic-CMOS structure

Valentin Fonck, Pascal Gehring

UCLouvain, IMCN-NAPS

Quantum computers have recently emerged as vessels capable of solving problems, in cryptography, pharmaceutical industry and others, that would be intractable for normal computers. As companies and universities strive for the achievement of the first commercial quantum computer, recent advancements have pushed the number of qubits in a single system beyond the one-thousand mark [1] but have also highlighted significant challenges in scalability, integration, and thermal management. In particular, connecting each qubit to room-temperature equipment via individual cables would result in thermal loads and space requirements exceeding the capacity of current dilution refrigerators. Positioning certain measurement and control electronics at cryogenic temperatures (e.g. cryo-CMOS) in direct proximity to the qubits would thus open new avenues towards scalable quantum computers.
In this work, we implement a new derivative of Scanning Thermal Microscopy, called Sideband Scanning Thermal Wave microscopy which exploits the mixing of thermal and electrical signals in the form of sidebands to improve the temperature sensitivity and phase stability during the scan. This extra phase stability provides us access to the information contained in the phase of the thermal excitation of a buried element which reveals the thermal wave velocity within the material.
We employ this novel method to explore the heat flows within a complex, 3D-integrated, commercial cryoCMOS component. We image simultaneously the temperature oscillations created by a buried diode thermometer, here excited with an AC signal which induces self-heating, on the sample's surface and the thermal wave velocity which reveals the thermal diffusivity. These quantities can be combined to obtain the thermal conductivity as well and paint a full picture of the heat paths within this multilayered structure. This new method could be adapted at cryogenic temperatures to accelerate iterative cryogenic CMOS design by directly imaging the electronic component's dissipation at their base temperature.

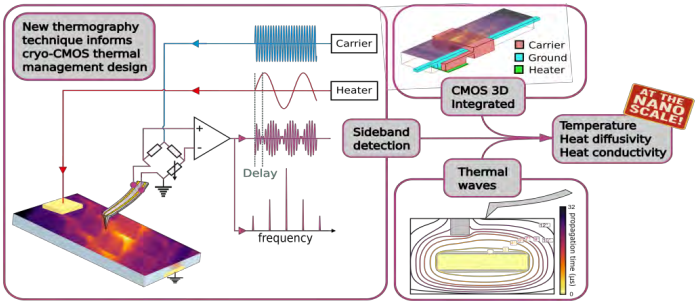

Figure 1: three key aspects of the showcased work : A new scanning technique leveraging the sideband detection of thermal signals is introduced. The technique allows the imaging of thermal waves at nanometric scales on CMOS 3D integrated structures. This reveals the local temperature, heat diffusivity and heat conductivity of the self-heating device at the nanoscale.

[1] M. AbuGhanem, "IBM quantum computers: evolution, performance, and future directions," 2025 *The Journal of Supercomputing*, **81,** 687

Invited Talks

INV1

Fast radio bursts as precursor radio emission from monster shocks

A. Vanthieghem[1] and A. Levinson[2]

[1]*Sorbonne Université, Observatoire de Paris, Université PSL, CNRS, LUX, F-75005 Paris, France*
[2]*School of Physics and Astronomy, Tel Aviv University, Tel Aviv 69978, Israel*

arno.vanthieghem@obspm.fr

Fast Radio Bursts (FRBs) are bright millisecond flashes of radio waves, mainly from outside our galaxy. These signals display a wide range of properties that have never been observed before and are challenging to interpret. Although several distinct origins are conceivable, there are indications that some of these bursts are associated with magnetars.

Given the diversity of observed bursts, it is likely that the underlying emission mechanism is not unique. Nevertheless, recent observations support a magnetospheric origin for a fraction of them. Evidence includes scintillation patterns, polarization angle swings, and burst morphology pointing to emission occurring within a magnetar's magnetosphere. In such extreme environments, where magnetic fields routinely reach 10^{15}G within a dilute electron-positron plasma, the shock wave is mediated by collective plasma effects, such as fast magnetosonic solitons, which may emit in the radio band and be interpreted as FRBs.

It has been proposed recently that the breaking of MHD waves in the inner magnetosphere of strongly magnetized neutron stars can power different types of high-energy transients. Motivated by these considerations, we study the steepening and dissipation of a strongly magnetized fast magnetosonic wave propagating in a declining background magnetic field using particle-in-cell simulations that span MHD scales. Our analysis confirms the formation of a monster shock and, for the first time, reveals the generation of a high-frequency precursor wave by a synchrotron maser instability at the monster shock, accounting for 0.1% of the total energy dissipated at the shock. We further discuss theoretical developments in shock physics, including the effect of radiative drag on the shock transition and signature.

[1] A. Vanthieghem & A. Levinson, "Fast Radio Bursts as Precursor Radio Emission from Monster Shocks," 2025 *Phys. Rev. Lett.* **134,** 035201
[2] A. Vanthieghem & A. Levinson, "Relativistically magnetized collisionless shocks in pair plasma: Solitons, chaos, and thermalization," 2025 *Phys. Rev. E* **111,** 045209

INV2

Overview of Wendelstein 7-X

Dirk Hartmann

Max-Planck-Institut für Plasmaphysik, Wendelsteinstrasse 1, Greifswald, 17491, Germany

Wendelstein 7-X is fusion experiment located in Greifswald, Germany, employing toroidal plasma confinement on the basis of optimized stellarator magnetic fields. The device has been developed to generate and confine hydrogen plasmas at temperatures and densities relevant for fusion reactors for up to 30 minutes. It started operation in 2015 and since then has achieved some remarkable milestones on technical operation, on understanding aspects that influence plasma confinement and on achieving record triple products for stellarator plasmas.

The talk will give an overview on the magnetic confinement of fusion plasmas, optimizations that led to the design of the device, its principle technical elements, in particular the megawatt power electron cyclotron heating system, and on achievements, records and challenges of plasma operation. The talk will conclude with an outlook on future goals of this device and other devices that pursue similar goals and are presently in design or in preparation.

INV3

Testing the Standard Model with Molecules

A. Borschevsky

The Van Swinderen Institute for Particle Physics and Gravity, University of Groningen, Nijenborgh 4, 9747 AG Groningen, The Netherlands

Search for violation of fundamental symmetries provides a unique opportunity for testing the Standard Model. Atomic and molecular experiments offer a low energy and comparatively inexpensive alternative to high energy accelerator research in this field. As the observable effects (such as parity violation, PV) are expected to be very small, highly sensitive systems and extremely precise measurements are required for the success of such experiments. Atomic and molecular theory can provide crucial support for these experiments.

An important task of theoretical research is to identify optimal molecular and atomic systems for measurements and to understand the mechanisms behind the enhanced sensitivity, which is strongly dependent on the electronic structure. Thus, accurate computational methods are needed in order to provide reliable predictions rather than estimates, and to obtain the various parameters that are required for the interpretation of the experiments.

I will present the results of our recent investigations of molecules in the context of search for parity violating effects. An overview of the theoretical methods will be provided, including the recently developed scheme for assigning error bars on theoretical predictions. Then, I will focus on showcasing the different types of systems (diatomic, triatomic, and chiral molecules) that are promising candidates for experiments that aim to test the Standard Model and perhaps detect new physical phenomena [1-3].

[1] Y. Hao, P. Navratil, E. B. Norrgard, M. Ilias, E. Eliav, R.G.E. Timmermans, V. V. Flambaum, and A.Borschevsky, Nuclear spin-dependent parity-violating effects in light polyatomic molecules, 2020 *Phys. Rev. A* **102**, 052828
[2] Eduardus, Y. Shagam, A. Landau, S. Faraji, P. Schwerdtfeger, A. Borschevsky and L. F. Pasteka,Large vibrationally induced parity violation effects in CHDBrI, 2023 *Chem. Commun.* **59**, 14579
[3] M. R. Fiechter, P. A. B. Haase, N. Saleh, P. Soulard, B. Tremblay, R. W. A. Havenith, R. G. E. Timmermans, P. Schwerdtfeger, J. Crassous, B. Darquié, L. F. Pašteka, and A. Borschevsky, Toward Detection of the Molecular Parity Violation in Chiral Ru(acac)3 and Os(acac)3, 2022 *J. Phys. Chem. Lett.* **13**, 10011

INV4

Probing structure and reactivity of metal clusters by IR spectroscopy using free-electron lasers

Olga V. Lushchikova[1], Deepak Pradeep[1], Piero Ferrari[1] and Joost M. Bakker[1]

[1]*HFML-FELIX, Nijmegen, 6525 ED, The Netherlands*

Metal clusters in the sub-nanometer regime, composed of only a few atoms, lie at the boundary between the classical and quantum regimes, bridging the gap between isolated atoms and bulk materials. In this regime, every atom plays an important role and can significantly influence the overall properties. This extreme sensitivity makes both their geometric and electronic structures highly tunable, making them not only fundamentally interesting but also highly relevant for materials science, in particular for the rational design of catalytic materials.[1]

To access the intrinsic properties of few-atom particles, we investigate them isolated in the gas phase, where they are free from perturbations induced by solvents or supporting surfaces. In our experiments, charged or neutral clusters are produced in a molecular beam apparatus via laser ablation and subsequent aggregation in a helium buffer gas environment.[2] Optionally, react the formed clusters with small molecules such as CO_2, H_2 and CH_4, to gain insight into reaction mechanisms at the molecular level.[3]

To characterize the structures of clusters and the binding nature of their reaction products, we employ action spectroscopy using intense, tunable infrared radiation from the FELICE laser at HFML-FELIX in Nijmegen, the Netherlands.[2] Upon resonant absorption of infrared light, clusters can undergo fragmentation, which is detected by mass spectrometry, providing indirect access to their vibrational spectra. The broad tunability and high pulse energy of FELICE (100–2000 cm^{-1}, up to 5 J/pulse) allow us to probe both the molecular fingerprint spectral region even of tightly bound systems and, uniquely, low-frequency vibrational modes associated with metal–metal bonding in clusters.[4]

[1] Lang S. M. and Bernhardt T.M. 2012 *Phys. Chem. Chem. Phys.* **14** 9255–9269
[2] Bakker J. M. *et al*. 2010 *J. Chem. Phys.* **132** 074305
[3] Lushchikova O. V. *et al.* 2021 *J. Phys. Chem. A* **125** 2836
[4] Lushchikova O. V. *et al*. 2019 *Phys. Chem. Chem. Phys.* **10(9)** 2151–2155

INV5

Local probing of transverse thermoelectric effects in meso- and nano scale devices

Mohammadali Razeghi[1], Jean Spiece[1], Valentin Fonck[1], Yao Zhang[2], Michael Rohde[1], Rikkie Joris[3], Philip S. Dobson[4], Jonathan M.R. Weaver[4], Lino M.C. Pereira[3], Simon Granville[2], **Pascal Gehring[1]**

[1]*Institute of Condensed Matter and Nanosciences, Université catholique de Louvain (UCLouvain), Louvain-la-Neuve, 1348, Belgium*
[2]*Robinson Research Institute, Victoria University of Wellington, Wellington, PO Box 600, New Zealand*
[3]*Quantum Solid State Physics, KU Leuven, Leuven, 3001, Belgium*
[4]*James Watt School of Engineering, University of Glasgow, Glasgow, G12 8LT, UK*

Solid-state cooling offers compact, silent, and eco-friendly solutions but remains limited by the low efficiency of classical thermoelectrics. We explore *transverse thermoelectric effects* as an alternative pathway for on-chip cooling. Using our unique scanning thermal microscopy [1,2,3], we locally probe nanoscale transverse effects—anomalous Ettingshausen, Nernst, and spin Seebeck—and directly assess the impact of defects, interfaces, and magnetic textures on performance. We show that the anomalous Ettingshausen effect (AEE) is strongly enhanced in materials with non-trivial band topology, such as the Heusler alloy Co_2MnGa, where *in situ* mapping reveals a record-high room-temperature AEE coefficient in µm-sized devices [4]. Furthermore, nanoribbon geometries induce a *geometrical Peltier effect*, increasing the figure of merit by 170%. The combined action of anomalous Ettingshausen and Peltier effects produces a nanoscale spot cooler, highlighting the potential of magnetic Weyl semimetals for efficient solid-state thermal management.

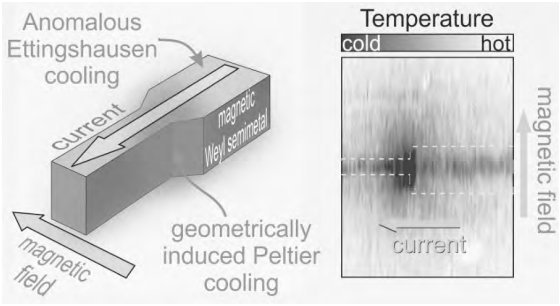

Figure 1: Left: Schematic of the Hybrid Longitudinal-Transverse thermoelectric cooling device. Right: Scanning thermal microscopy map on a Co_2MnGa device.

[1] Harzheim A *et al.* (2018) *Nano Letters* **18**(12) 7719–7725
[2] Harzheim A *et al.* (2020) *2D Materials* **7** 041004
[3] Spièce J *et al.* (2025) *Small Methods* **9** 2401715
[4] Razeghi M *et al.* (2025) *ACS Nano*, **19**(46) 39725–39734

INV6

Thermodynamics of near-extreme black holes

Chiara Toldo[1]

[1]*Theoretical and Mathematical Physics, Université Libre de Bruxelles*

From the perspective of classical gravity, a black hole is the simplest object we know of. At the same time, it possesses huge entropy, hinting at an incredibly complex microstructure: understanding this fact falls in the realm of quantum gravity. In this talk I will review recent results concerning the microscopics and the thermodynamics of black holes close to extremality. I will describe how recently developed techniques allow to compute the quantum corrections to the entropy of near-extremal black holes, both by making use of an effective near-horizon theory (Jackiw-Teitelboim gravity) and by regularizing certain zero-modes appearing in the gravitational path integral. I then will show that the quantum-corrected near-extremal entropy of the Kerr black hole exhibits 3/2logT behavior characteristic of the Schwarzian model, and predicts the lifting of the ground state degeneracy.

INV7

From the Monopole Paradox to Perfect Transmission: Topological String Attachment in Scattering

Atsushi Ueda[1]

[1]*Department of Physics and Astronomy, Ghent University, Krijgslaan 281, 9000 Gent, Belgium*

A magnetic monopole is not just an exotic object; it can fundamentally change the identity of the particles that scatter from it. In high-energy physics, Callan showed that when a charged chiral fermion scatters off a monopole, the outgoing particle need not be the original fermion. It may even appear to carry a fractional charge. This puzzle, known as the *monopole paradox,* has challenged our understanding of charge, symmetry, and locality for decades [1-2].

Recent work suggests a new interpretation: the outgoing fermion is dressed by a hidden topological string attached to the monopole. This string places the particle in a twisted sector, allowing it to behave as if it carries fractional charge [3-6]. In this sense, the monopole does not merely scatter the particle; it changes the language in which the particle is described.

In this talk, I will discuss a lattice analogue of this phenomenon in condensed matter systems. By coupling a pair of dual theories, one can build an interface that perfectly transmits any incoming wave packet. Yet the particle emerging on the other side is transformed, effectively disguised by a topological line. I will explain how to construct such interfaces within a tensor network framework, and discuss their possible applications, including what they may teach us about the monopole paradox itself [7].

[1] C. G. Callan, Jr., 1982 *Phys. Rev. D* **25**, 2141
[2] V. A. Rubakov, 1982 *Nucl. Phys. B* **203**, 311-348
[3] M. van Beest, P. Boyle Smith, D. Delmastro, Z. Komargodski, and D. Tong, *JHEP* 03, 014, arXiv:2306.07318.
[4] V. Loladze, T. Okui, and D. Tong, 2025, *arXiv*:2508.21059.
[5] V. Loladze and T. Okui, 2025 *Phys. Rev. Lett.* **134**, 051602
[6] M. van Beest, P. Boyle Smith, D. Delmastro, R. Mouland, and D. Tong, *JHEP* 08, 004, *arXiv*:2312.17746.
[7] A. Ueda, V. V. Linden, L. Lootens, J. Haegeman, P. Fendley, and F. Verstraete *arXiv:* 2510.26780.

INV8

Stretching the physical boundaries of DNA hybridization for mutation detection

Jef Hooyberghs[1]

[1]*UHasselt, Data Science Institute, Theory Lab, Agoralaan, Diepenbeek, 3590, Belgium*

DNA hybridization, i.e. the formation of the double helix from two single stranded sequences, is a fundamental reaction used across various disciplines, applications and technologies. E.g. in clinical applications somatic genomic testing of circulating tumor DNA (ctDNA) in blood samples is important for cancer therapy [1]. The scientific-technical challenge lies in accurately determining the proportion of mutated ctDNA in a sample predominantly containing non-mutated circulating free DNA. To achieve sensitive detection of minimal residual disease, there is a need to develop and adopt new and affordable detection principles with enhanced analytical capabilities.

The affinity with which DNA probes hybridize with their complementary sequence is determined by the sequence-dependent free energy, ΔG. The selectivity toward mutations is determined by the free energy penalty, $\Delta\Delta G$, that a mutation entails. This sets a lower limit on the fraction of mutated DNA that can be detected in a background of unmutated DNA. Since $\Delta\Delta G$ is a physical property of the DNA molecule, it appears to impose a hard limit on the detection threshold.

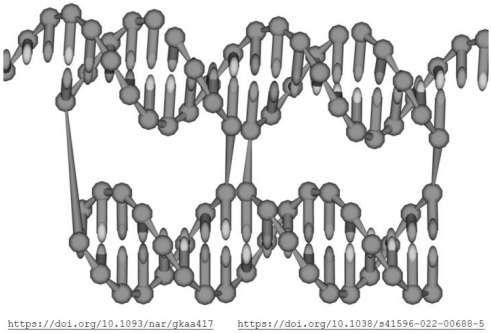

Figure 1: Example of strain-containing multi-strand structure with increased sequence selectivity.

This presentation explains how the limit of detection can be decomposed into a technology-dependent factor and a fundamental factor governed entirely by the physics of DNA. Subsequently, we discuss various strategies that allow this fundamental factor to be pushed beyond the traditional physical limit, supported by experimental results [2]. We detail how these effects can be quantified, showing how the different scenarios are all encapsulated within an elegant expression for the detection limit. We discuss the extent to which these effects can be interpreted from the perspective of statistical physics and conclude with open questions.

[1] Cohen S.A., Liu M.C. and Aleshin A., 2023. *Nature* **619** (7969), 259–268
[2] Stulens Y., Van Hoof R., Hollanders K., Nelissen I., Szymonik M., Wagner P., Froyen G., Maes B. and Hooyberghs J., 2025. *Biosens. Bioelectron.* **281**, 117342

INV9

Taking the NEXT steps towards the northeast of the nuclear landscape

J.Even[1]

[1]*University of Groningen, Faculty of Science and Engineering, Van Swinderen Institute for Particle Physics and Gravity Groningen, 9474AA, the Netherlands*

Over the past decades more than 3300 nuclides have been discovered.[1] Isotopes along the proton dripline even up to the actinide region are known. However, at the neutron-rich side the area towards the dripline remains largely a *terra incognita* especially in the heavy and superheavy element region (see Figure 1). The discovery of very heavy and superheavy nuclei has been driven by fusion evaporation reaction. Due to the limited number of available beam and target combinations heavy neutron-rich nuclei remain inaccessible through fusion reactions. In my talk I will explore alternative options which can provide access to the northeastern part of the nuclear landscape. In the recent year the use of multinucleon transfer reaction in deep inelastic collision gained more and more attention as a potential way to synthesize heavy nuclei (see e.g. [2,3]) . This method comes along with several technical challenges such as a large energy and angular distribution of the reaction products.

I will introduce the NEXT setup that has recently been installed at the PARTREC facility in Groningen in order to study Neutron-rich, Exotic, heavy nuclei produced in multinucleon Transfer reactions. NEXT consists of a solenoid pre-separator which provides a large angular acceptance of the transfer products and a MultiReflection Time-of-Flight Mass Spectrometer (MR ToF MS) for their isobaric separation and precision studies. NEXT will open the door to the discovery of new isotopes and studies or rare decay modes.

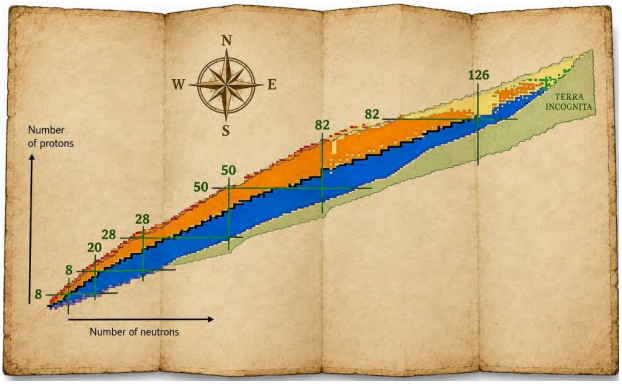

Figure 1: The chart of nuclides. The green shaded area indicates the region of so-far undiscovered nuclei.

[1] M. Thoennessen 2023, *Int. J. Mod. Phys E* **32** 2330001
[2] W. D. Loveland 2019, *Front. Phys.* **7** 23
[3] S. Heinz, H. M. Devaraja 2022 *Eur. Phys. J. A* **58** 114
[4] J. Even et al 2022, Atoms **10** 59

Plot Twists and Unexpected Turns in Physics Reasoning

P. van Kampen[1]

[1]*CASTeL & School of Physical Sciences, Dublin City University, D09 KWA2, Ireland*

Physics education research (PER) has been a vibrant field of research for half a century. I will start the talk with an overview of the field, including some key studies that documented how students learn physics in the classroom, and some theoretical frameworks that help us interpret and connect these empirical findings. This sets the scene for the main focus of the talk—how students use graphical representations to display and extract information about physical phenomena in various contexts.

A substantial body of foundational PER has shown that students' difficulties with interpreting physics concepts often stem from deep-seated reasoning patterns and intuitive ideas. Early work by McDermott and colleagues (e.g. [1]) revealed that students retained persistent conceptual and representational challenges after traditional introductory university level physics instruction. Beichner developed the Test of Understanding Graphs in Kinematics (TUG-K), a multiple-choice diagnostic instrument [2]. Elby interpreted students interactions with various graphs in terms of epistemological resources [3]. In the mathematics education literature, Carlsen *et al* [4] mapped out the coordination steps involved in the covariational reasoning that Cartesian graphs represent.

Building on this foundation, more recent research has examined how students interpret and construct graphs across a variety of contexts and representations [5–8]. Work by Van den Eynde *et al* [8] has illuminated how students coordinate—or don't coordinate—between algebraic expressions and Cartesian graphs. Recent studies by Condon *et al* [10, 11] have shown that many students find it hard to represent equal spatial intervals in an experiment as equal intervals on a Cartesian graph.

[1] McDermott L, Rosenquist M and van Zee E 1987 *Am. J. Phys.* **55** 505
[2] Beichner R J 1994 *Am. J. Phys.* **62** 750
[3] Elby A 2000 *J. Math. Behav.* **19** 481
[4] Carlsen M *et al* 2002 *J. Res. Math. Educ.* **33** 352
[5] Wemyss T and van Kampen P 2013 *Phys. Rev. ST Phys. Educ. Res.* **9** 020119
[6] Ivanjek L *et al* 2016 *Phys. Rev. Phys. Educ. Res.* **12** 010106
[7] Bollen L *et al* 2016 *Phys. Rev. Phys. Educ. Res.* **12** 010108
[8] Rodriguez J-M G *et al* 2018 *J. Chem. Educ.* **95** 2114
[9] Van den Eynde S *et al* 2019 *Phys. Rev. Phys. Educ. Res.* **15** 020113
[10] Condon O *et al* 2024 *Phys. Educ.* **59** 025001
[11] Condon O *et al* 2026 *Eur. J. Phys.* **47** 015703

Contributed Oral Presentations

O1

Exploring radar echoes from high-energy particle cascades with RET-CR

I. Loudon[1], on behalf of the Radar Echo Telescope (RET) collaboration

[1]*Université Libre de Bruxelles, Science Faculty CP230, B-1050 Brussels, Belgium*

High energy particles interacting in ice produce relativistic particle cascades, detectable via radar, as the ionisation trails left in their wake scatter incident radio waves. Therefore, cascades passing through an ice volume illuminated with radio frequency transmitters produce a radar echo, allowing the cascade to be spotted, and recorded by surrounding receivers in order to obtain information on the cascade and progenitor particle. The RET experiment aims to utilise this method to probe the >PeV cosmic neutrino flux, providing insight into the highest energy astrophysical processes.

To this end, the RET collaboration has been working to demonstrate the radar method insitu with the Radar Echo Telescope for Cosmic Rays (RET-CR) experiment. Deployed in Greenland in 2023 and 2024, RET-CR utilised secondary in-ice particle cascades - produced by high-energy cosmic ray air showers impinging on the ice surface - as a test beam for the radar method. Additionally, modelling and simulation studies have been undertaken in order to obtain an in-depth understanding of the radar signal properties. In this work we will discuss the radar detection method and RET-CR experiment, exploring the experimental and simulation-based efforts to investigate the expected signal features and first data.

Integral dielectric kernel modelling approach to wave heating in toroidal plasmas

P. U. Lamalle[1], B. C. G. Reman[1], Chr. Slaby[2a], D. Van Eester[1], Chr. Geuzaine[3], J. Zaleski[3], M. Campos Pinto[2b], Y. Güçlü[2b], E. Moral Sánchez[2b]

[1]*Laboratory for Plasma Physics, Royal Military Academy, Brussels, Belgium*
[2]*Max-Planck-Institut für Plasmaphysik,* [2a]*Greifswald and* [2b]*Garching, Germany*
[3]*Dept. of Electrical Engineering and Computer Science, University of Liège, Belgium*

Current magnetic fusion experiments and future reactors require multi-megawatt auxiliary heating systems in order to bring the plasma to relevant operating temperatures. Plasma heating by means of high-frequency electromagnetic waves is one of the main approaches and is carried out in different frequency ranges such as ion cyclotron (ICRF), electron cyclotron and lower hybrid resonance frequencies. In the ICRF range, the relevant wavelengths are comparable with the characteristic lengths of the configuration, and Maxwell's equations must be solved as a boundary value problem inside the plasma-filled vacuum chamber of the tokamak ("full-wave" treatment). To accurately model the radiofrequency dielectric properties of warm tokamak plasmas in presence of rotational transform (i.e. of a poloidal component of the equilibrium magnetic field), most of the Vlasov-Maxwell kinetic theoretical models and codes addressing full-wave propagation and absorption are based on toroidal and poloidal Fourier expansions of the RF fields. A significant drawback of this field representation is its lack of flexibility, in that it does not allow local refinements of numerical discretizations on a given magnetic surface.

As a remedy to this, novel theoretical expressions have been obtained for the dielectric response of Maxwellian tokamak and stellarator plasmas in the form of integral operators [1-2] which are free from the traditional spectral expansions, i.e. fully expressed in configuration space. These results involve mildly singular integral kernels, which incorporate the non-local nature of wave-particle interactions along the equilibrium magnetic field lines and the associated spatial wave dispersion. They are independent of the RF field representation inside the plasma volume and therefore amenable to three-dimensional finite element discretizations. The present contribution will highlight our new approach and its key advantages. We will then summarize the theoretical results and their analytical exploitation in view of efficient numerical implementation. Applications to ICRH modelling [3] are vigorously proceeding and discussed in the companion contribution [4].

[1] P. U. Lamalle *et al* (2024), Joint Varenna - Lausanne International Workshop on Theory of Fusion Plasmas, Varenna, Italy.
[2] P. U. Lamalle *et al* (2025), 20th RF Power in Plasmas Conference, Hohenkammer, Germany.
[3] B. C. G. Reman *et al* (2025), EPJ Web of Conferences **346** 01019 (2026).
[4] B. C. G. Reman *et al*, this Meeting.

Thermal and plasma modelling of a hot cavity ion source for radioactive ion beam production at ISOL@MYRRHA

L. Quanjel[1, 2], K. Rijpstra[1], J. P. Ramos[1], A. Koszorus[1, 2], T. E. Cocolios[2], and L. Popescu[1]

[1]*Belgian Nuclear Research Centre, SCK CEN, Mol, Belgium*
[2]*Institute for Nuclear and Radiation Physics (IKS), Leuven, Belgium*

ISOL@MYRRHA [1], currently under construction at the Belgian Nuclear Research Centre SCK CEN, will be an isotope-separation facility producing radioactive ion beams (RIBs) using 100-MeV protons at beam intensities up to 500 µA. These RIBs will support applications in fundamental research, medical science, and materials science [2]. A key component of the facility is the hot-cavity ion source, which relies on surface and/or resonance-laser ionisation. The cavity is resistively heated above 2000 °C, where thermionic electrons and ionised atoms interact to form a low-density, partially-ionised plasma. The behaviour of this plasma critically influences ion confinement, transport, and extraction efficiency.

A central challenge is that the cavity volume must remain small to preserve low beam emittance. This constraint amplifies space-charge effects, enhances plasma–wall interactions, and makes stable ion confinement and efficient extraction particularly difficult at high neutral loads. To characterise this unconventional plasma environment, we combine thermal–electrical finite-element modelling with Particle-In-Cell (PIC) simulations. The temperature distribution and voltage drop calculated with Ansys [3] provide boundary conditions for the PIC code Pantera [4], which self-consistently resolves thermionic emission, surface/laser ionisation, and multispecies ion–neutral transport. The simulations predict electron densities of $\sim 10^{15}$ m^{-3} near the wall and the formation of a confining potential of a few volts. At increased neutral flux, however, positive-ion accumulation leads to space-charge saturation and, in extreme cases, reversal of the confining potential, reducing ion survival and extraction efficiency.

The simulations further show how variations in cavity geometry and wall-temperature profiles strongly modify the plasma state through changes in electron and ion dynamics. These insights allow us to identify operational thresholds beyond which plasma confinement breaks down and extraction becomes inefficient.

Experimental studies using a prototype cavity, measuring ion-extraction time profiles, ionisation efficiencies, and emittance, serve as validation inputs for the modelling framework. Although direct plasma diagnostics inside the hot cavity are not feasible, the combined modelling–empirical approach enables us to infer plasma behaviour indirectly and to guide future optimisation of the ion source geometry and operating conditions. Ultimately, this optimisation aims to minimise space-charge saturation and maintain high extraction efficiencies under the elevated ion loads required for ISOL@MYRRHA's future operation.

[1] L. Popescu et al., The Belgian Nuclear Research Centre (SCK CEN), 2025 *Nucl. Phys. News* **32**.2, pp. 4–8
[2] SCK CEN / MYRRHA, *ISOL@MYRRHA*, https://www.myrrha.be/myrrha-applications/nuclear-science/isolmyrrha (accessed: March 2026)
[3] Ansys, *Academic Research Mechanical*, Release 20.1, https://www.ansys.com/
[4] P. Parodi et al., *Pantera: A PIC-MCC-DSMC software for the simulation of rarefied gases and plasmas*, SoftwareX, 31, 102244, https://doi.org/10.1016/j.softx.2025.102244

O4

From Polarization Dynamics to Heat Flow in Nanoscale Ferroelectrics

Jean Spièce

Institute of Condensed Matter and Nanosciences, UCLouvain

jean.spiece@uclouvain.be

Ferroelectric materials provide a unique platform to explore the interplay between electrical, mechanical, and thermal degrees of freedom. This coupling is particularly rich in low-dimensional systems and polymer thin films, where reduced dimensionality, spatial inhomogeneities, and confinement effects give rise to complex polarization behavior. Understanding how these different channels interact at the nanoscale remains a central challenge.

In this contribution, I will present an overview of recent efforts to probe ferroelectricity in two-dimensional materials and polymer films from the perspective of coupled physical responses. We investigate how polarization evolves under electrical stimuli, focusing on the dynamics of switching, the role of local heterogeneities, and the influence of device-like geometries. At the same time, we examine how these polarization processes are accompanied by local temperature variations, providing direct insight into electrocaloric and pyroelectric responses. Taken together, these observations reveal how electrical, mechanical, and thermal effects are intertwined, and how energy is locally converted and redistributed in these systems.

We observe that polarization switching proceeds through highly localized, nanosecond-scale events with pronounced nanoscale variability, which in turn generate spatially inhomogeneous thermal responses. The strong correlation between switching pathways and local electrocaloric and pyroelectric signals highlights a direct coupling between polarization dynamics and heat flow. These findings provide concrete insight into energy conversion at the nanoscale and raise fundamental questions about the role of disorder and dimensionality in coupled ferroelectric phenomena.

Towards rovibrationally resolved photochemistry in H_2O-CO_2

A.S. Bogomolov[1], S. Collignon[1], N. Moazzen-Ahmadi[2], M. Herman[3], and C. Lauzin[1]

[1]*Université Catholique de Louvain, Louvain-la-Neuve, 1348, Belgium*
[2]*University of Calgary, Calgary, T2N 1N4, Canada*
[3]*Université libre de Bruxelles, Brussels, B-1050, Belgium*

Water and CO_2 are the most important greenhouse gases in our atmosphere. The solvation of CO_2 is a decisive process in the chemistry of clouds and oceans. A precise characterization of the interaction of these two molecules is thus of prime importance. In the present work, we recorded a rotationally resolved spectrum of the triple excitation of the OH stretch in the H_2O-CO_2 molecular complex. This represents a further step in our longstanding effort to better characterize the dynamics of CO_2-H_2O interactions, notably through a systematic increase in vibrational excitation [1–4]. Increasing excitation will ultimately drive the isomerization of the complex into carbonic acid H_2CO_3. The complexes were formed from an 8 cm-long pulsed slit supersonic jet and probed by the CRDS technique in the spectral range of the second OH overtone of H_2O, using the FANTASIO setup [5,6]. A home-built external cavity diode laser (ECDL), stabilized to the frequency comb, was used as the light source. The recorded spectrum was vibrationally assigned to the (v_1,v_2,v_3) ← (v_1',v_2',v_3') = (2,0,1) ← (0,0,0) and (2,0,1) + intermolecular mode ← (0,0,0) where the v_1,v_2,v_3 vibrational quantum numbers of the isolated H_2O molecule are used to assign the involved states. In this talk, I will present the experimental spectrum and the improvements to the experimental setup that enabled the recording of this spectral signature. I am going to present our progress in the analysis of this spectrum using group theory and the effective Hamiltonian. Finally, perspectives on going across the isomerization barrier will be presented.

[1] C. Lauzin, A.C. Imbreckx, T. Foldes, T. Vanfleteren, N. Moazzen-Ahmadi, and M. Herman, Mol. Phys. 118, e1706776 (2020).
[2] A.S. Bogomolov, A. Roucou, R. Bejjani, M. Herman, N. Moazzen-Ahmadi, and C. Lauzin, Chem. Phys. Lett. 774, 138606 (2021).
[3] T. Gartner, C. Lauzin, A.R.W. McKellar, and N. Moazzen-Ahmadi, J. Phys. Chem. A 127, 3668 (2023).
[4] A.S. Bogomolov, S. Collignon, R. Glorieux, N. Moazzen-Ahmadi, M. Herman, C. Lauzin, Rotationally resolved triple vibrational excitation in D_2O-CO_2 van der Waals complex, in preparation (2026).
[5] M. Herman, K. Didriche, D. Hurtmans, B. Kizil, P. Macko, A. Rizopoulos, and P.V. Poucke, Mol. Phys. 105, 815 (2007).
[6] A.S. Bogomolov, R. Glorieux, M. Herman, T. Corbo, S. Collignon, B.M. Hays, D. Lederer, N. Moazzen-Ahmadi, A. Libert, B. Tomasetti, J. Fréreux, and C. Lauzin, Mol.Phys. 123, e2413417 (2025).

O6

Lamb-Dip and Two-Photon Absorption measurements using wave-modulated NICE-OHMS for Precision Spectroscopy on Water

Arthémise Altman[1], Frank M. J. Cozijn[1], Alexandr S. Bogomolov[1], Roland Tóbiás[2], Attila G. Császár[3], Wim Ubachs[4], Clément Lauzin[1]

1. *Institute of Condensed Matter and Nanosciences, Université catholique de Louvain, Louvain-la-Neuve, Belgium*
2. *Department of Chemistry, University of Vermont, Burlington, VT, USA*
3. *Institute of Chemistry, ELTE Eötvös Loránd University, Budapest, Hungary*
4. *Department of Physics and Astronomy, LaserLab, Vrije Universiteit, Amsterdam, The Netherlands*

Water is a critical molecule in chemistry, radio astronomy and fundamental physics. This talk presents high-precision measurements of $H_2^{16}O$ using wave-modulated noise-immune cavity-enhanced optical heterodyne molecular spectroscopy (NICE-OHMS). Our instrument is used to perform Doppler-free measurements either through Lamb-dip saturation or two-photon absorption (TPA) measurements.

To enhance the accuracy of protected radio lines between 750 GHz and 3 THz, we performed high-precision Lamb-dip measurements of rovibrational lines in the 1.2-1.4 µm range. These measurements, featuring an accuracy of 2 kHz, were utilized within a spectroscopic network to improve 51 purely rotational microwave lines crucial for radio astronomy. The precision of these transitions, formerly at the 10-200 kHz level, has been improved to well below 10 kHz for all lines. This ensures that the frequency allocations defined by the International Astronomical Union are supported by unprecedented experimental precision.

Additionally, in this talk, we report several TPA transitions in $H_2^{16}O$ measured with kHz accuracy in the near infrared. This work marks the first TPA measurement in the water overtone range. By utilizing TPA's selectivity to disentangle dense state energies and reach high-parity levels, these results enable a precise metrological determination of overtone transitions.

TPA offers a unique probe for high-energy, same-parity states inaccessible via single-photon absorption. Combined, these methods provide a rigorous metrological characterization of water transitions, serving the needs of international astronomical bodies and advancing our understanding of molecular energy levels.

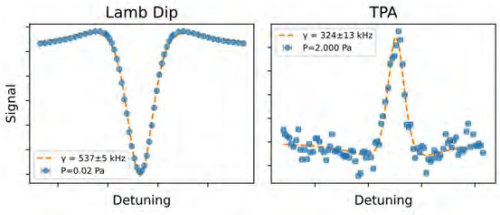

Examples of a scan on a Lamb Dip (left panel) and on a two-photon absorption (right panel).

Inertial sensing based on GPS disciplined oscillator

C. Bragard[1,2], A. Altman[1], A. Bogomolov[1], A. Goodwin-Jones[1], and C. Lauzin[1]

[1]*Univesité Catholique de Louvain, Louvain-La-Neuve, 1348, Belgium*
[2]*Univesité de Namur, Namur, 5000, Belgium*

Inertial sensors are essential tools for gravitational-wave detectors. These detectors typically rely on Fabry-Pérot cavities that are actively stabilized to minimize mechanical noises in the frequency range of interest. This stabilization demands precise monitoring of the mirrors motion using displacement sensors. Various techniques have been developed for such inertial sensing, achieving impressive sensitivities using Fabry-Pérot cavities [1] or Michelson interferometers [2][3].

Heterodyne cavity tracking relies on measuring the beating between two optical cavities. The stability of each cavity impacts the precision of this measurement since it involves a relative motion between the two cavities. In this talk, we present proof of concept for a new method for heterodyne inertial sensing that enables absolute displacement measurement. Using an optical frequency comb beating separately with two optical cavities, we can eliminate common-mode noise from the reference oscillator, effectively forming a balanced inertial sensor. With this method, we reach a sensitivity of 700 fm/$\sqrt{\text{Hz}}$ at 1 Hz, close to the state-of-the-art of 260 fm/$\sqrt{\text{Hz}}$ [1], and 10 fm/$\sqrt{\text{Hz}}$ at 1 kHz.

A projected two-orders of magnitude improvement in sensitivity will be discussed along with its potential applications in gravitational waves detectors.

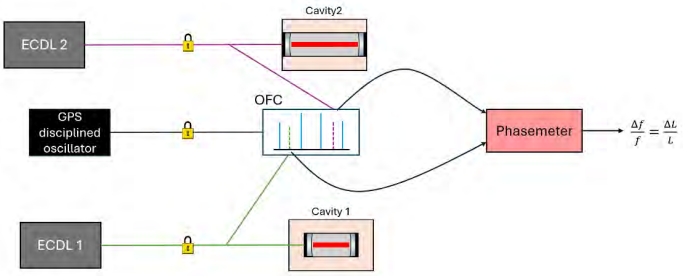

Figure 1: Scheme for the experimental setup. ECDL: External Cavity Diode Laser, OFC: Optical Frequency Comb.

[1] Chalathadka Subrahmanya S, Darsow-Fromm C and Gerberding O 2025 *Opt. Express* 33 4044
[2] Gray M B, McClelland D E, Barton M and Kawamura S 1999 *Opt. Quantum Electron.* 31 571
[3] Zhao G, Ding B, Watchi J, Deraemaeker A and Collette C 2020 *Mech. Syst. Signal Process.* 145 106959

Cavity Solitons as a Nonlinear Substrate for Photonic Neuromorphic Computing

Amir Arsalan Arabieh[1,2], Alessandro Lupo[1,2], Simon-Pierre Gorza[2], Serge Massar[1]

[1]*Laboratoire d'Information Quantique, CP 224, ULB, 1050, Brussels, Belgium*
[2]*Service OPERA-Photonique, CP 194/5, ULB, 1050, Brussels, Belgium*

Abstract. We demonstrate that cavity solitons sustained in a fiber optical cavity provide an optical platform for photonic reservoir computing. A key finding is that Kelly sidebands— radiative waves emitted during soliton reshaping—enrich the reservoir dynamics and significantly enhance computational performance.

Theoretical framework. Cavity solitons are optical pulses phase-locked to a coherent drive, sustained by a double balance: chromatic dispersion is compensated by self-phase modulation, while intrinsic cavity losses are offset b y c ontinuous d riving [1]. R eservoir c omputing is a recurrent neural-network paradigm in which fixed i nternal d ynamics p rovide a nonlinear mapping of the input into a high-dimensional state space, and only the readout weights are trained [2]. In this work, we define reservoir nodes as distinct spectral channels of the soliton spectrum: Kelly sidebands and their spectral interference with the soliton introduce rich, history-dependent dynamics that support the echo-state property required for reservoir computing [3].

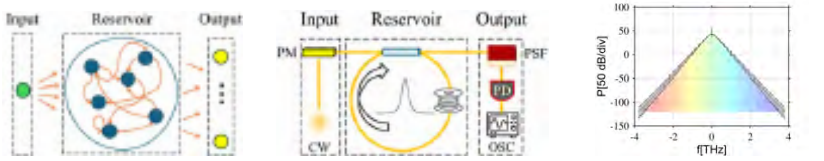

(a) Reservoir Computing **(b)** Photonic Implementation **(c)** Solitons as a physical substrate

Figure 1: Input layer: the phase of a continuous-wave (CW) laser is modulated with a phase modulator (PM). Reservoir layer: cavity solitons evolve inside the fiber cavity in response to the input modulation. Output layer: the time-dependent power in individual frequency channels is measured using a programmable spectral filter (PSF) and a photodiode (PD).

Results. With a 50-node reservoir, simulations yield a 32-step linear memory capacity, 90.5% accuracy for nonlinear channel equalization at SNR = 12 dB, and Mackey–Glass forecasting NRMSE of 0.01, 0.02, and 0.03 for 6-, 10-, and 15-step horizons. Overall, performance exceeds a linear reservoir and is competitive with state-of-the-art photonic reservoir implementations. Experimentally, intracavity gain compensates losses, giving an effective round-trip loss of $\Lambda \approx 3\%$ and a finesse of ~ 200. The XOR task reaches 100% accuracy for a 1-symbol delay, and Hénon map prediction achieves NRMSE = 0.30 versus 0.44 for a linear reservoir.

[1] N. Akhmediev and A. Ankiewicz, *Dissipative Solitons*, Springer, Berlin, 2005.

[2] H. Jaeger and H. Haas, "Harnessing nonlinearity: Predicting chaotic systems and saving energy in wireless communication," *Science*, **304**(5667), 78–80 (2004).

[3] A. A. Arabieh, A. Lupo, S.-P. Gorza, and S. Massar, "Cavity Solitons as a Nonlinear Substrate for Photonic Neuromorphic Computing," *arXiv:2602.18110*, 2026.

Coercivity-Size Map of Magnetic Nanoflowers: Elucidating the Hyperthermia Sweet Spot

E. M. Jefremovas[1,2], L. Calus[3], and **J. Leliaert**[3]

[1]*Department of Physics and Materials Science, University of Luxembourg, Luxembourg, L-1511, Luxembourg*
[2]*Institute of Advanced Studies, University of Luxembourg city, Esch-sur-Alzette, L-4365, Luxembourg*
[3]*Dept. of Solid State Sciences, Ghent University, Ghent, 9000, Belgium*

Iron-oxide nanoflowers (NFs) are one of the most efficient nanoheaters for magnetic hyperthermia therapy. However, the physics underlying the dynamic response of realistic nanoparticles, containing disorder, beyond the single-domain limit remains poorly understood.

Using large-scale micromagnetic simulations, the magnetization of biocompatible iron-oxide NFs (d = 10–400 nm) has been mapped, connecting their microstructure to their macroscopic magnetic response. Above the single-domain regime (d > 50 nm), the magnetization folds into a vortex state, within which the coercivity reaches a secondary maximum, not present for nondisordered nanoparticles. The dynamics of the vortex shows two distinct reversal modes: 1) a core-dominated one, with an increasing coercivity with diameter; 2) a flux-closure-domains dominated reversal mode, with a decreasing coercivity-size dependence. The coercivity maximum is located at the transition between both reversal modes and results from the combination of grain anisotropy and grain-boundary pinning.

Our results[1] provide the first description of spin textures in iron oxide NFs beyond the macrospin framework, revealing how particles with identical static magnetization exhibit fundamentally distinct dynamics, which result in different macroscopic behavior. By adjusting the grain size, the coercivity “sweet spot” can be tailored, offering a practical route to next-generation, high-efficiency nanoheaters.

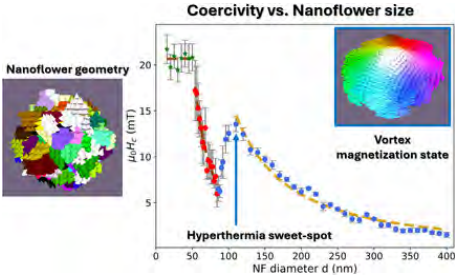

Figure 1: The simulated nanoflower geometry, its vortex magnetization state and the resulting magnetic coercivity as function of nanoflower size. The strongly nonlinear behaviour displays a secondary maximum corresponding to optimal performance in the cancer therapy magnetic particly hyperthermia.

[1] E. M. Jefremovas, L. Calus, J. Leliaert 2026 *Small Science,* **6**, e202500490

O10

DFT modeling of strained group-IV color centers in diamond

T.G.I. van Wijk[1,2], E.A. Melan[1,2,3], R. Mary Joy[2,4], E.Y. Guillaume[1,3], P. Pobedinskas[2,4], K. Haenen[2,4], and **D.E.P. Vanpoucke[1,2]**

[1]*UHasselt, IUMAT, QuATOMs group, 3500 Hasselt, Belgium*
[2]*imec, IUMAT, 3590 Diepenbeek, Belgium*
[3]*University of Namur, NISM, 5000 Namur, Belgium*
[4]*UHasselt, IUMAT, WBGM group, 3500 Hasselt, Belgium*

Diamond color centers are considered as viable candidates for solid state qubits and single photon sources for quantum technological applications ranging from quantum sensing to quantum information processing [1]. Color centers are created through ion beam implantation or incorporation during chemical vapor deposition. This way most elements of the periodic table have been considered at some point in the past, even lanthanides like Eu, due to their sharp spectral properties [2]. However, in recent years, group-IV color centers have been gaining attention due to their excellent Debye–Waller factor, making them very suitable for optically based quantum applications. In such applications, a sharp and robust zero-phonon line (ZPL) are prime qualities sought after. Unfortunately, practical diamond based devices contain several sources of strain, originating from the ion beam implantation and annealing during device fabrication. This strain results in a shifting of the ZPL depending on the type of strain and magnitude experienced by the color center [3,4,5].

Using density functional theory (DFT) calculations, the impact of isotropic and anisotropic strain on the GeV and SnV centers in diamond is investigated, with the aim of understanding the experimentally observed distributions of ZPL positions. By using defect concentrations of 1.5% down to 0.1% (64–1000 atom conventional cells) we show that it is possible to extrapolate to experimentally relevant concentrations [3,4,5]. The calculated ZPL position and strain-induced shifts are presented for both neutral and negatively charged color centers. For the GeV^0 color center, both red and blue shifts are obtained for isotropic strain, while anisotropic strain only gives rise to a redshift. In case of the latter, the absolute magnitude of the shift is also significantly larger [3]. In case of the SnV^0 and SnV^-, the position of the ZPL shows a smaller dependence on the color center concentration. In contrast, the ZPL shift for SnV centers is larger than the one obtained for the GeV^0 color center [4,5]. We also note that the impact of the charge state is rather non-trivial. The calculated results are discussed within the context of the experimental observation of distributions of ZPL positions for the SnV and GeV centers [3,4]. We highlight some of the pitfalls when comparing calculated and experimental results, and indicate how further experimental-theoretical studies can provide insights into the black box of experimentally doped samples [4,5].

[1] E.Y. Guillaume, *et al.* 2025 in *Nanophotonics with Diamond and Silicon Carbide for Quantum Technologies* **Chap. 5** ISBN: 978-0-443-13717-4
[2] D.E.P. Vanpoucke, *et al.* 2019 *Diam. Relat. Mater.* **94**, 233-241
[3] T.G.I. van Wijk, *et al.* 2025 *Carbon* **234**, 119928
[4] R. Mary Joy, *et al.* 2026 *ACS Mater. Lett.* 8(1), 137-144
[5] D.E.P. Vanpoucke 2026 *Diam. Relat. Mater.* "Modeling the Zero-Phonon Line of strained SnV centers in diamond" (Under revision)

O11

Ultrafast dynamics of strongly-coupled plasmonic metasurfaces

The Linh Pham[1], Amirmostafa Amirjani[1], Kacper Pilarczyk[1], Fei Han[1], Nils Deßmann[2], Joris Van de Vondel[1], Thanh Tung Nguyen[3], Ewald Janssens[1]

[1]*Quantum Solid State Physics, KU Leuven, 3001 Leuven, Belgium;* thelinh.pham@kuleuven.be
[2]*Institute for Molecules and Materials, FELIX Laboratory, Radboud University, 6525 ED, Nijmegen, Netherlands*
[3]*Institute of Materials Science, Vietnam Academy of Science and Technology, Hanoi, Vietnam*

The field of metasurfaces is rapidly advancing from fundamental science to real technologies. Thanks to the ability to tailor light–matter interactions through artificial structuring of metasurfaces, advanced optoelectronic devices are within reach [1]. To fully harness this potential, coupling between resonant elements is essential, as it introduces a higher level of control over optical functionality. Yet the ultrafast response of strongly coupled metasurfaces, especially under intense optical excitation, remains largely unexplored [2].

Here, we investigate the transient dynamics of strongly coupled plasmonic metasurfaces composed of nanometrically spaced gold dipole and quadrupole resonators on a silicon support, using time-resolved mid-infrared pump–probe spectroscopy [3]. Their near-field interaction gives rise to destructive interference and a pronounced plasmon-induced transparency (PIT) resonance, making this system an ideal platform for studying ultrafast coupling physics. Aside from a transmission increase lasting several tens of picoseconds due to impact ionization in silicon, we observe an unexpected subpicosecond transmission spike. We attribute this feature to a direct field-driven interaction unique to the strongly coupled regime, where hybrid modes are coherently excited and rapidly exchange energy, a pathway absent in isolated or weakly coupled structures. Remarkably, despite the intense excitation and rapid dynamics, the PIT resonance remains spectrally robust, evidencing persistent near-field coupling. Numerical modeling captures the temporal evolution of the bright- and dark-mode damping rates and the inter-resonator coupling strength, providing a clear physical picture. These findings uncover a previously hidden ultrafast dynamics in strongly coupled plasmonic metasurfaces and open a route toward sub-picosecond mid-infrared all-optical modulation, which holds great promise for free-space communication.

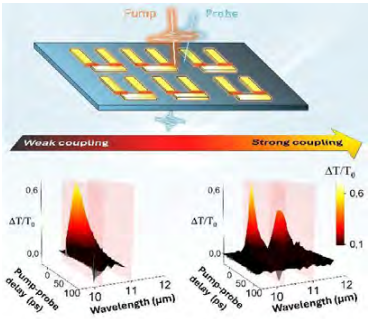

[1] Cui TJ, Zhang S, Alù A, Wegener M, et al. 2024 *JPhys Photonics* **6** 032502
[2] Maiuri M, Schirato A, Cerullo G, Della Valle G 2024 *ACS Photonics* **11** 2888–905
[3] Pham TL, Amirjani A, Pilarczyk K, et al. 2026 *Laser Photon Rev* e03113.

O12

Analytical approaches to lattice polarons in finite-width conduction bands

S. N. Klimin[1], J. Tempere[1], M. Houtput[1], I. Zappacosta[1], S. Ragni[2], T. Hahn[3], L. Celiberti[3], C. Franchini[3] and A. C. Mishchenko[2]

[1]*TQC, Universiteit Antwerpen, Antwerpen, 2610, Belgium*
[2]*Institute of Physics, Zagreb, Croatia*
[3]*Computational Materials Physics, University of Vienna, Austria*

We develop and compare analytical approaches for the polaron problem in finite-width, non-parabolic conduction bands [1, 2]. Our main result is an extension of the Feynman variational method to tight-binding lattices [1], where the effective-mass approximation breaks down. We also revisit analytical methods originally formulated for continuum polarons, including canonical transformations and improved self-consistent Wigner–Brillouin approximations, and generalize them to lattice systems. In a finite-bandwidth lattice, these approaches exhibit qualitative features absent in the continuum case, such as a nontrivial connection between weak- and strong-coupling limits. An improved Wigner–Brillouin scheme yields a momentum-dependent polaron self-energy free of resonances and consistent with perturbation theory at zero momentum.

The methods are applied to the Holstein model and benchmarked against numerically exact calculations, including Diagrammatic Monte Carlo, exact diagonalization, and density-matrix renormalization-group results, and are further extended to polarons with Rashba spin–orbit coupling.

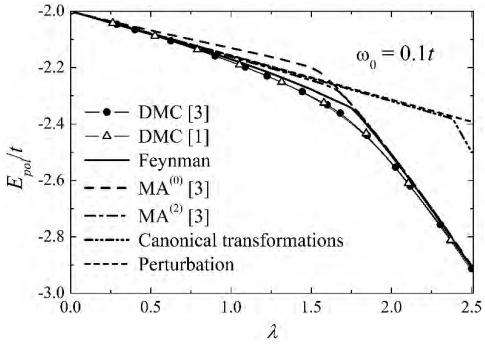

Figure 1: ground-state energy of a Holstein polaron calculated within the Feynman variational method compared with results of Diagrammatic Monte Carlo (DMC), method of canonical transformations and Momentum Average Approximation (MA) [3]

The figure shows the ground-state energy of a Holstein polaron versus coupling strength, demonstrating close agreement between the modified Feynman variational method and numerically exact results.

[1] S. N. Klimin, J. Tempere, M. Houtput, I. Zappacosta, S. Ragni, T. Hahn, L. Celiberti, C. Franchini and A. S. Mishchenko, *arXiv:2603.09609* (2026)
[2] S. N. Klimin, J. Tempere, M. Houtput, S. Ragni, T. Hahn, C. Franchini and A. S. Mishchenko, Phys. Rev. B **110**, 075107 (2024).
[3] G. L. Goodvin, M. Berciu, and G. A. Sawatzky, Phys. Rev. B **74**, 245104 (2006).

O13

Substitutional Mn dimers in graphene created by ultralow-energy cluster implantation

Chen He[1], Karina Landivar[2], Simona Achilli[2], Ewald Janssens[1], and Lino da Costa Pereira[1]

[1]*Quantum Solid-State Physics, Department of Physics and Astronomy, KU Leuven, Leuven, 3001, Belgium*
[2]*ETSF and Dipartimento di Fisica "Aldo Pontremoli", Università degli Studi di Milano, Milano, I-20133, Italy*

The deliberate introduction of atomic defects or dopants can tailor graphene's electronic, magnetic, and chemical properties. Transition-metal dopants are of particular interest because their partially filled *d* orbitals can modify spin moments, spin-orbital coupling, and electron localization. However, because metal atoms are thermodynamically unfavorable in graphene, it is difficult to introduce them through equilibrium methods. Ion implantation can be used to create out-of-equilibrium structures. However, conventional implantation with keV energies destroys the graphene lattice. Ultralow-energy (ULE) ion implantation with implantation energies in the tens-of-eV range, provides a promising strategy to overcome this problem. [1] Despite advances in single-metal-atom doping by utilizing ULE ion implantation, [2, 3] the controlled creation of multi-atom defects in two-dimensional materials remain challenging. Compared with single atoms, multi-atom transition-metal dopant complexes are expected to produce more pronounced lattice distortion and symmetry breaking, together with more strongly localized electronic states than isolated single dopants. [4, 5] Here, we show that ULE (82 eV) implantation of mass-selected Mn_2 cluster ions into monolayer graphene produces substitutional Mn dimers. Low-temperature scanning tunneling microscopy and spectroscopy, together with density-functional theory calculations, identify these Mn–Mn pairs by a characteristic four-lobe appearance and distinct spectroscopic signatures. Molecular dynamics simulations indicate that the implanted Mn_2 clusters fragment upon impact, displace carbon atoms, and subsequently recombine into substitutional dimers within the graphene lattice. Our results establish ULE cluster implantation as an effective route for engineering multi-atom defects in two-dimensional materials, extending ultralow-energy implantation beyond single-atom doping.

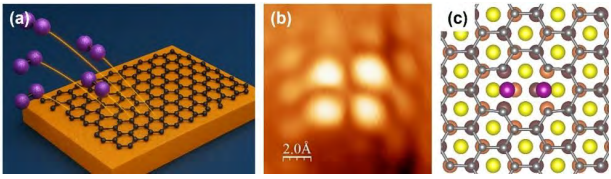

Figure 1: (a) Schematic of the ultralow-energy (ULE) cluster implantation into graphene/Cu(111). (b) Experimental STM topographies of a substitutional Mn_2 and (c) corresponding atomic structure. (purple: Mn; gray: C; yellow: first layer of Cu; orange: second layer of Cu; brown: third layer of Cu).

[1] Bangert Ursel *et al* 2013 *Nano Lett.* **13** 4902.
[2] Lin Pin-Cheng *et al* 2021 *ACS nano* **15** 5449.
[3] Villarreal Renan *et al* 2025 *ACS Nano* **18** 17815.
[4] Lv Ruitao *et al* 2012 *Sci. Rep.* ***2*** 586.
[5] Tison Yann *et al* 2015 *ACS nano* **9** 670.

O14

Pole figure measurements in grazing-incidence configuration for characterizing thin film texture

Arno Depoorter[a], Eduardo Solano[b], Cristian Mocuta[c], Zhiwei Zhang[a], Jolien Dendooven[a], Christophe Detavernier[a] and Matthias Filez[a]

[a] *CoCooN research group, Department of Solid State Sciences, Ghent University, Belgium*
[b] *NCD-SWEET beamline, ALBA Synchrotron Light Source, Spain*
[c] *DiffAbs beamline, Synchrotron SOLEIL, France*

Characterizing crystalline texture, or the distribution of crystal orientation is crucial for many applications in materials science. Crystalline texture is commonly studied using X-ray diffraction pole figures, which map the orientation of specific crystal planes. Conventional pole figure measurements use a symmetric θ-2θ geometry (Figure 1a), featuring deep X-ray penetration into the sample (Figure 1b). While effective for bulk materials, this approach is less sensitive to thin films and supported nanoparticles and is difficult to combine with *in-situ* experiments due to the necessary tilting of the sample.

In this work, we present grazing-incidence wide-angle X-ray scattering (GIWAXS) as an alternative method for measuring pole figures with enhanced sensitivity to the near-surface region. By directing the X-ray beam onto the sample at a grazing incidence angle, the X-ray penetration depth is significantly reduced (Figure 1b), making the technique especially well-suited for thin films and supported nanoparticles. Pole figures are obtained by continuously rotating the sample in its own plane while collecting two-dimensional GIWAXS patterns, allowing pole figures for multiple lattice planes to be probed simultaneously.

Using Pt thin films and nanoparticles supported on MgO substrates, we demonstrate that adjusting the grazing-incidence angle provides control over the information depth. At incident angles below the critical angle of the substrate, the diffraction signal from Pt nanoparticles is strongly enhanced relative to the substrate background. In Figure 1c, peaks corresponding to a small subpopulation of misaligned Pt grains can be observed only in GIWAXS geometry, demonstrating the enhanced sensitivity of the pole figures measured using GIWAXS. For thin films, varying the incident angle enables depth-resolved texture analysis, which is not feasible using the conventional θ-2θ geometry.

Overall, grazing-incidence pole figure measurements combine higher sensitivity to the near-surface region, simpler experimental geometry, and depth profiling capabilities. These advantages make GIWAXS a powerful tool for future *ex-* and *in-situ* texture analysis of thin films and supported nanoparticles.

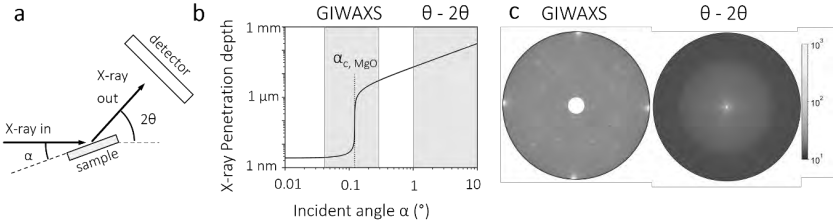

Figure 1: Benefits of GIWAXS geometry compared to state-of-the-art θ-2θ geometry. **a**: X-ray diffractometer setup. **b**: X-ray penetration depth versus incident angle for 18 keV X-rays on MgO. **c**: Pt 200 pole figures for Pt nanoparticles in GIWAXS (left) and θ-2θ (right) geometry.

Publication: Depoorter, A. et al. (2026). *Journal of Applied Crystallography*, *59*, 108–116.

O15

The last stages of the motion of eccentric binary systems

Guillaume Lhost[1]

[1]*Physics of the Universe, Fields and Gravitation, Université de Mons*

Eccentric binary systems can be modelled up to the separatrix crossing within the self-force framework by using first principles. At this stage, the timescale of the dynamics changes, and the prescription of post-adiabatic expansion ceases to be applicable. In the quasi-circular case, the development of a transition-to-plunge model, together with a post-geodesic expansion makes it possible to calculate full trajectories and waveforms from the inspiral to the plunge.
In this presentation, we introduce a model that addresses the transition to plunge for eccentric binary systems. Starting at the separatrix crossing, the secondary is expected to evolve along a perturbed homoclinic orbit before it transits to the merger phase. We present different phases of the motion with different expansions in the mass ratio, and compute waveforms on these trajectories.

O16

Holography as a tool for strongly coupled dynamics

Paul Hynek[1]

[1]*Instituut voor Theoretische Fysica, KU Leuven*

The AdS/CFT correspondence is a precise mathematical framework which relates a theory of gravity in anti-de-Sitter space (AdS) to a non-gravitational conformal field theory (CFT) in one dimension lower. I will review the basic aspects of this holographic duality, and explain how one can access the strongly coupled regime in a wide class of CFTs. Holography thus provides a powerful tool to study theories in a regime where usual perturbative methods break down.

In the second part of my talk, I will describe how this approach allows us to study the dynamics of d-dimensional maximally supersymmetric Yang-Mills theories in the planar limit. When $d \neq 4$, these theories are non-conformal and therefore beyond the traditional AdS/CFT paradigm. Nevertheless, holography offers a precise framework to calculate correlation functions in these setups. I will discuss novel analytic results for 2pt- and 3pt-functions of scalar BPS operators, which could be tested using lattice QFT methods.

O17

The emergence of activity

A. Beyen[1], C. Maes[1], and J.-H. Pei[2]

[1]*Department of Physics and Astronomy, KU Leuven, B-3001 Leuven, Belgium*
[2]*School of Physics, Peking University, Beijing, 100871, China*

Can **activity be transmitted** from smaller to larger scales [1]? Which characteristics are transferred, and what new phenomena appear? These questions are especially important in the Physics of Life, where small, active constituents (e.g., molecular motors and driven ions) are coupled to macroscopic objects (e.g., cell membranes and tissues). In [2], we observe the exchange and emergence of activity and persistence in the reduced dynamics of an elastic membrane or polymer chain in contact with an active bath.

Specifically, as illustrated in Fig. 1, we consider a heavy elastic string with Klein-Gordon dynamics coupled to a **bath of run-and-tumble particles**. The string represents a one-dimensional membrane and is "slower" compared to the swiftness of the active particles. In other words, we treat the string as the analogue of a Brownian particle bombarded with fast active particles. We derive the induced Langevin-Klein-Gordon string dynamics with explicit expressions for the mean force, friction coefficient, and noise variance. The induced friction consists of two terms: one entropic, proportional to the noise variance, as in the Einstein relation for a thermal equilibrium bath, and a frenetic contribution that can take both signs. The frenetic part wins for higher bath persistence, which makes the **total friction negative** and creates a **wave instability** akin to inverse Landau damping. Detailed simulations confirm the initial growth driven by this anti-damping and exhibit a **rich steady-state behavior** (e.g., multimodal distributions, synchronized spatial correlations) depending on the chain strength, probe mass, and nonequilibrium condition. Based on these numerical results, we conjecture which corrections to the induced Langevin equation are needed beyond time-scale separation.

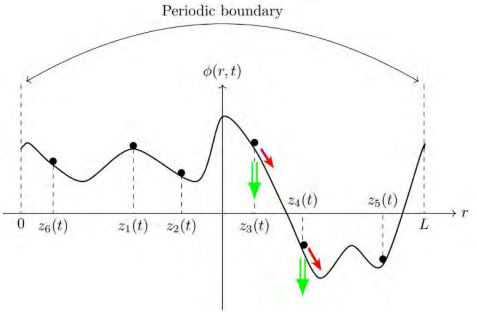

Figure 1: A configuration of active particles $z_i(t)$ coupled to the displacement field $\phi(r,t)$ on a circle. The particles push the field downwards (green arrow), while performing a gradient descent along ϕ (red arrow).

[1] C. Maes and J.-H., Transfer of active motion from medium to probe via the induced friction and noise. *Phys. Rev. Letters* **136**, 038301 (2026).
[2] A. Beyen, C. Maes, and J.-H. Pei, Coupling an elastic string to an active bath: the emergence of inverse damping. *Phys. Rev. E* **112**, L042103 (2025).

O18

Scrambling signature of scars

Thomas Michel[1], Mathias Steinhuber[2], Juan Diego Urbina[2], and Peter Schlagheck[1]

[1]*Université de Liège, Liège, Belgique*
[2]*Universität Regensburg, Regensburg, Germany*

We study signatures of scrambling, such as out-of-time-ordered correlators, that are associated with weakly unstable periodic orbits in a mixed or chaotic classical phase space, fulfilling Heller's criterion [1] for the existence of scars. As verified within generic dynamical systems like the kicked rotor and the driven pendulum, evaluating scrambling observables for coherent states centred in phase space about such periodic orbits gives rise to characteristic scar features both in the short and long time regimes, the latter amounting to a significant amendment of the characteristic growth exponent with respect to the generic semiclassical prediction [2,3]. Extensions to many-body scars in Bose-Hubbard rings [4] are discussed.

[1] J. Heller, 184 *Phys. Rev. Lett*. **53**, 1515
[2] J. Rammensee, J.-D. Urbina, and K. Richter, 2018 *Phys. Rev. Lett*. **121**, 124101
[3] T. R. Michel, J. Diego Urbina, and P. Schlagheck, 2025 J. *Phys. A: Math. Theor*. **58**, 275303
[4] Q. Hummel, K. Richter, and P. Schlagheck, 2023 *Phys. Rev. Lett*. **130**, 250402

Optimizing Range Shifter se to Lower Intrauterine Doses in Pencil Beam Scanning Proton Therapy during Pregnancy

J. Hohmann[1], A. Goedgebeur[2], M. De Saint-Hubert[3], D. Colson[2], F. Amant[4,5], M. Lambrecht[1,2], T. Depuydt[1,2]

[1]*Laboratory of Experimental Radiotherapy, KU Leuven, Leuven, Belgium*
[2]*Department of Radiation Oncology, UZ Leuven, Leuven, Belgium*
[3]*Belgian Nuclear Research Centre, SCK CEN, Mol, Belgium*
[4]*Department of Obstetrics and Gynaecology, UZ Leuven, Leuven, Belgium*
[5]*Department of Oncology - Gynaecological Oncology, KU Leuven, Leuven, Belgium*

Background and purpose: In radiotherapy during pregnancy, out-of-field (OOF) doses should be as low as reasonably achievable, with fetal exposure below 100 mSv to prevent deterministic effects and ideally near public dose limits to minimize stochastic risk. Proton therapy with pencil beam scanning (PBS) supports these objectives by delivering lower OOF dose than photon radiotherapy [1]. However, OOF dose increases when a range shifter (RS) is used, on which many PBS systems rely for superficial targets. This study evaluates planning strategies that optimize RS use in PBS to further minimize intrauterine dose while maintaining target coverage and plan quality, using breast cancer as an example case.

Materials and methods: Nine PBS breast treatment plans were created in RayStation 12A to deliver 42.30 Gy(RBE) to the breast and regional nodes with a 52.20 Gy(RBE) boost, using a 20-week computational pregnant phantom from the University of Florida [2]. Superficial target coverage was achieved using three RS configurations: (i) a conventional 3.5 cm Lexan RS with varying air gaps; (ii) beam splitting (BS) with varying air gaps, a technique in which the RS was removed for deeper energy layers (affecting 52% of MU); and (iii) replacement of the RS with a 3D-bolus (3 cm water-equivalent).

Plans were exported to TOPAS/GEANT4 for Monte Carlo simulation using a PBS beam model [3], previously validated for OOF dose in pregnant breast irradiation. For each plan simulation, the mean intrauterine dose equivalent was calculated by summing neutron and gamma components and scaling to the full treatment course.

Results: Across all treatment plans, the simulated combined neutron and gamma dose equivalent averaged within the uterus remained below 5.0 mSv. Smaller air gaps consistently resulted in lower dose. BS provided a further reduction, with doses of 2.3-2.6 mSv depending on the air gap. Replacing the RS with a 3D-bolus reduced the dose to 2.0 mSv. Overall, the lowest combined doses were obtained with the 3D-bolus and with BS at a 5 cm air gap, reducing the combined dose by 60% and 54%, respectively, relative to the conventional RS configuration with a 25 cm air gap.

Conclusion: For PBS breast irradiation during pregnancy, fetal doses were already well below the threshold of 100 mSv. Further reduction towards public dose limits was achieved by optimizing the use of the RS. The largest reductions were obtained by replacing the RS with a 3D-bolus, or by applying BS with small air gaps, which approximately halved the intrauterine dose.

[1] Blommaert J *et al* 2023 *Acta Obstet. Gynecol. Scand.:* **103** 767–74
[2] Maynard M R *et al* 2014 *Phys. Med. Biol.:* **59** 4325–43
[3] Colson D *et al* 2023 *Phys. Med. Biol.:* **68** 21NT02

A linear decomposition of total correlation in non-negative order-k contributions

Niels Van Santen[1]

[1]*Ghent University, Ghent, 9000, Belgium*

For a multivariate random variable the total correlation (TC) or multi-information [1] is an extension of mutual information that measures the degree to which the whole system differs from independence. Alternatively, it can be understood as a measure of the collective constraints in the system [2], or how much the variables in the system collectively know about each other. TC results in a single number representing these collective constraints, and does not give us any information about the scale at which these dependencies live. For an n-variable group the dependencies that make up the full TC could be present at the scale of pairs ($k = 2$), triplets ($k = 3$), all the way up to multiplets of order $k = n$.

There exists different ways to decompose TC in terms representing contributions at different orders k. Most notably via connected information [3], where through the construction of maximum entropy distributions at each order, connected information at order k measures the decrease in maximum entropy when going from knowing only the marginals at order $k-1$ to knowing also the marginals at order k. This is a complete and non-negative decomposition but computing multiple maximum entropy distributions is computationally expensive. On the other hand, looking at TC from a poset mereology point of view [4], it can be expressed in terms of increasing orders of interaction information. This decomposition is simpler to calculate, but suffers from the fact that the terms can be negative and that interaction information is not straightforward to interpret at orders $k > 3$. This motivates the search for practical and interpretable ways to decompose the higher-order interdependence in complex systems and capture the scale of the underlying order.

Here we suggest a way that uses the poset mereological approach on which we define a linear program with the specific constraints of completeness and non-negativity that we look for. We solve the linear program, ensuring that we give appropriate weight to the smallest subsets that explain the observed constraints. This way, e.g., triplets will get zero weight when pairwise constraints suffice to explain the full TC. This approach results in a computationally less expensive, non-negatiove, and complete decomposition which is straightforward to interpret in terms of dependencies at each scale.

We show, in direct comparison with connected information, results on common logic gates XOR, OR, and AND. XOR gates show a pure order-3 dependency, while AND and OR gates have contributions at both orders 2 and 3. As a proof of concept, we show that for systems of any size that consist of copies of the same variable, there is nothing beyond order 2 dependencies, and we apply the decomposition on an interacting spin system to identify the ceiling of interaction order present in the statistics. With this decomposition, we suggest a practical way in which we can distinguish how much information is redundant ($k = 2$) or synergistic ($k \geq 3$) and suggest a dimension of complexity of the data, i.e. the highest non-negative order.

[1] S. Watanabe. 1960 *IBM Journal of Research and Development*, **4**(1), 66–82
[2] F.E. Rosas, P.AM. Mediano, M. Gastpar, and H.J. Jensen. 2019 *Phys. Rev. E*, **100**(3), 032305
[3] E. Schneidman, S. Still, M.J. Berry, and W. Bialek. 2003 *Phys. Rev. Lett.* **91**(23), 238701
[4] Abel Jansma. 2025 *Phys. Rev. Research* **7**(2), 023016

O21

Mechanistic Control via High-Order Informational Gradients: Identifying Synergistic Drivers for Targeted Intervention

D. Marinazzo[1], T. Scagliarini[2], S. Stramaglia[2]

[1]*Department of Data Analysis, Ghent University, Ghent, Belgium*
[2]*Department of Physics, University of Bari, Italy*

While behavioral patterns in complex systems impose essential constraints on potential interaction rules, traditional control strategies often fail to identify the specific mechanistic drivers necessary for reliable intervention. This is largely because observable behaviors, typically captured via pairwise correlations, often treat disparate underlying **mechanisms** as identical. We address this by utilizing **Gradients of O-information (GOI)**, which act as loworder descriptors of high-order dependencies, providing a bridge between observed statistical patterns and the generative mechanisms of a system. The GOI score of a variable, calculated as the change in the overall O-information when that variable is added, serves to **refine the selection of generative rules**. In high-dimensional datasets, multiple mechanisms (e.g., loops, colliders, or mediators) can produce similar second-order statistics. However, high GOI scores disambiguate these roles: a significantly **negative gradient** identifies "synergistic drivers" (typically mechanistically associated with colliders), while a **positive gradient** identifies "redundant carriers" (mediators or confounders). This allows us to select generative models that match the system's true informational profile rather than just its output. Drawing on the 2D Ising model, we demonstrate that **statistical synergy** acts as a robust precursor to phase transitions, peaking in the disordered phase. By localizing these high-order effects to specific elements, such as the central spin in a frustrated system, we identify the primary targets for control. By shifting from a behavior-led to a mechanism-led paradigm, we enable the design of precise perturbations to steer systems toward or away from critical regime shifts, providing a new framework for the targeted control of high-dimensional dynamics.

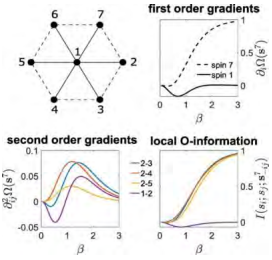

Figure 1: Top left: The hexagonal geometry of the Ising model, where continuous and dashed lines indicate ferromagnetic and antiferromagnetic interactions, respectively. Top right: The gradients with respect to single spins $\partial_i\Omega(\boldsymbol{s}^7)$ are plotted versus the inverse temperature β. Due to symmetry, the curves of peripheral spins 2–7 are equal. Bottom left: The second-order gradients $\partial_{ij}{}^2\Omega(\boldsymbol{s}^7)$ are plotted versus β. Due to symmetry, only four nonequivalent curves are plotted. Bottom right: The local Oinformation $I(s_i;s_j;\boldsymbol{s}^7{}_{-ij})$ is plotted for the same pairs of spins.

[1] Scagliarini, T., Nuzzi, D., Antonacci, Y., Faes, L., Rosas, F. E., Marinazzo, D., & Stramaglia, S. (2023). Gradients of O-information: Low-order descriptors of high-order dependencies. *Physical Review Research*, *5*(1), 013025.

O22

Analytical model for the strain-mismatch interaction in DNA

T. Mangelschots[1], E. Carlon [2], and J. Hooyberghs [1]

[1] *Hasselt University, Data Science Institute, Theory Lab, Agoralaan, 3590 Diepenbeek, Belgium*
[2]*Soft matter and Biophysics, KU Leuven, Celestijnenlaan 200D, 3001 Leuven, Belgium*

DNA-Hybridisation-based biosensing stands at the forefront of the development of liquid biopsies and, consequently, the next generation of non-invasive tumour detection. The thermodynamic difficulty of discriminating traces of Single Nucleotide Variants (SNVs) from the large excess of wild-type DNA background fundamentally limits them. Recent advances indicate that incorporating structural constraints in the design of molecular beacon-based sensors can significantly enhance their selectivity [1]. However, the underlying mechanism behind these constraints remains speculative. In this work, we test the hypothesis that these constraints induce torsional strain within these probes and seek to optimise their working regime by developing an analytically solvable coarse-grained model.

The sensor is modelled as a one-dimensional lattice system in which nodes are coupled via harmonic interactions of exponentially decaying (Kac-Baker-like) strength. Through the Schur complement of the twist interaction, the model effectively accounts for the higher-dimensional degrees of freedom in the DNA duplex. In a general framework, we aim to identify the non-additive free-energy interaction term that arises between two perturbations in the system, and then analyse its application to the presence of an SNV and the global frustration in the system. This approach allows us to analyse regimes in which a single-base mismatch destabilises the duplex. Specifically, we demonstrate that such a destabilising regime exists for any physical mismatch.

To validate the hypothesis that these constraints induce torsional frustration in the sensor, we perform coarse-grained simulations using oxDNA [2]. We construct a closed-loop sensor and vary the helical periodicity by comparing a 9-base-pair closing, which imposes a significant structural constraint, with its 10-base-pair counterpart. Using 3DNA analysis [3], we can extract physical degrees of freedom from the simulated duplexes and check whether twist is indeed the primary source of destabilisation in the system.

[1] Karadeema, R. J., Stancescu, M., Steidl, T. P., Bertot, S. C., & Kolpashchikov, D. M. (2018). The owl sensor: a ‘fragile’ DNA nanostructure for the analysis of single nucleotide variations. *Nanoscale*, *10*(21), 10116–10122. https://doi.org/10.1039/c8nr01107a

[2] P. Šulc, F. Romano, T. E. Ouldridge, L. Rovigatti, J. P. K. Doye, A. A. Louis, *J. Chem. Phys.* 137, 135101 (2012)

[3] Lu, Xiang-Jun, and Wilma K. Olson. "3DNA: A software package for the analysis, rebuilding and visualization of three-dimensional nucleic acid structures" *Nucleic Acids Research* 31.17 (2003): 5108-5121.

O23

Characterizing Biomolecular Kinetics through Out-of-Equilibrium Periodic Temperature Perturbations

R. Van Haverbeke[1], L-P. Jorissen[2,3], L. Jorissen[2], J. Vandevenne[2], Y. Stulens[1], J. Hendrix[3], R. Thoelen[2] and J. Hooyberghs[1]

[1]*UHasselt, Data Science Institute, Theory Lab, 3590, Diepenbeek, Belgium*
[2]*UHasselt, Instituut Voor Materiaalonderzoek, 3590, Diepenbeek, Belgium*
[3]*UHasselt, Biomedisch Onderzoeksinstituut, 3590, Diepenbeek, Belgium*

Characterizing biomolecular kinetics is essential in multiple domains, including molecular diagnostics and biotechnology. A prime example is found in protein folding, where a single molecule can navigate various structural states, each exhibiting a unique biological function. When kinetic pathways deviate, the resulting misfolding can lead to severe pathologies, as seen in neurodegenerative diseases such as Alzheimer's and Parkinson's. To understand why, and how these diseases occur, it is crucial to understand their underlying biomolecular mechanics and energy landscapes.

While protein folding remains the most well-known example of these dynamics, DNA nanostructures have emerged as a clinically relevant and highly programmable system for studying biomolecular transitions. By quantifying the kinetics of DNA, we can gain fundamental insight into the principles of molecular transitions in a controlled environment. However, characterizing these DNA transitions poses a significant challenge. Most current methodologies rely on steady-state, equilibrium techniques. These allow for the determination of the system's thermodynamic parameters (Gibbs free energy, Enthalpy, Entropy), but fail to quantify the transition rates between all states.

To overcome this, our research utilizes rapid temperature perturbations to push these DNA systems out of equilibrium. By sweeping the perturbation frequency and environmental conditions (such as DNA concentration), individual transition rates between states can be determined from ensemble measurements. In this presentation, I will demonstrate the physics underlying this methodology and show empirical validation for a two-state DNA system, where transition rate values were found to be consistent with results from established, single-molecule methods. Furthermore, the theoretical framework is designed to be extensible to more complex systems. By analyzing the system's response to the applied perturbation, we can characterize the underlying kinetics and transition rates, providing a scalable strategy to decode the intricate folding landscapes of diverse biomolecular systems.

Exploring α- and β-decay induced quenching of the radiative decay of the ^{229}Th nuclear-clock isomer in solid-state hosts

Yens Elskens[1]

[1]*Nuclear and Radiation Physics, Department of Physics and Astronomy, KU Leuven*

Due to its low excitation energy around 8.4 eV, the unique ^{229}Th isomer is the ideal candidate for developing a nuclear clock, which would be particularly suited for fundamental physics studies [1]. In the past, determining the precise energy value and measuring the isomer's radiative decay from a large-bandgap crystal doped with ^{229}Th, has proven difficult: the commonly used population of the isomer via the ^{233}U α-decay has a limited branching ratio towards the isomer and creates a high-radioluminescence background [2, 3]. However, recently, a new approach to populate the isomer through the β-decay of ^{229}Ac was proposed [2]. Using radioactive ^{229}Ra/^{229}Ac beams from ISOLDE (CERN) allowed to observe, for the first time, the radiative decay of the ^{229}Th isomer with vacuum-ultraviolet (VUV) spectroscopy, and allowed to successfully determine the resulting photon's wavelength with a relative uncertainty of O(10^{-3}) [4, 5]. Based on this work, narrowband laser excitation of the nuclear isomer embedded in CaF_2 was achieved using four-wave mixing [6], and, not much later, with a frequency comb, determining the energy to O(10^{-12}) precision [7]. This quick succession of successful experimental results boosted the development of a nuclear clock based on the ion trap and solid-state approach.

Using the methodology of [2, 4, 8], different large-bandgap crystals were investigated (among them MgF_2, $LiSrAlF_6$, and different types of CaF_2), focusing on the time behaviour of the radiative decay of ^{229m}Th, embedded in different crystal materials. These studies revealed a crystal-material-sensitive, time-dependent suppression of the observed radiative-decay rate. This so-called 'quenching of the radiative decay' can be linked to opening up the otherwise forbidden internal-conversion channel, and can be induced by both α and β decay. A relative effect of up to 40% could be quantified. The data further revealed a dependence of the quenching probability on implantation site and temperature.

The results of these studies will be presented and linked to the laser- and X-ray-induced quenching as recently reported in [9, 10, 11, 12].

[1] E Peik et al. 2021 *Quantum Science and Technology* **6.3**, p. 034002
[2] M. Verlinde et al. 2019 *Phys. Rev. C* **100**, p. 024315
[3] K. Beeks and T. Schumm. 2022 eng. PhD thesis. TU Wien
[4] S. Kraemer and J. Moens et al. 2023 *Nature* **617**(7962), pp. 706–710
[5] S. Kraemer and P. Van Duppen. 2022 PhD thesis. KU Leuven
[6] J. Tiedau et al. 2024 *Phys. Rev. Lett.* **13**, p. 182501
[7] Chuankun Zhang et al. 2024 *Nature* **633**(8028), pp. 63–70
[8] S. V. Pineda et al. 2025 *Phys. Rev. Res.* **7**, p. 013052
[9] F. Schaden et al. 2025 *Phys. Rev. Res.* **7**, p. L022036
[10] J. E. S. Terhune et al. 2025 *Phys. Rev. Res.* **7**, p. L022062
[11] Takahiro Hiraki et al. 2025. *arXiv:* 2509.00041 [nucl-ex]
[12] Ming Guan et al. 2026 *Phys. Rev. Lett.* **136**, p. 013203.

Determination of half-lives, alpha-beta branching and hindrance factors of ^{219,220}Po; implications on nuclear shape

J. Shaw[1], J.W. Wessolek[2, 3], B. Andel[4], A. N. Andreyev[5], S. Antalic[4], M. Au[3], S. Bara[1], A. E. Barzakh*, C. Bernard[3], S. Christophe[6], K. Chrysalidis[3], T. E. Cocolios[1], J. G. Cubiss[7], P. Das[8], U. Datta[8], F. Donaire[9], Z. Favier[3], V. N. Fedosseev[3], K. T. Flanagan[3], R. P. de Groote[1], D. Hanstorp[10], R. Heinke[3], A. A. H. Jaradat[3], J. Johnson[1, 3], U. Köster[11], A. Koszorus[1], L. Lalanne[1, 3], D. Leimbach[10], R. Lica[6], R. Mancheva[3], B. A. Marsh[3], J. Mišt[4], G. Neyens[1], M. Nichols[10], C. Nita[6], B. Olaizola[3], C. Page[5, 3], J. Pakarinen[12], Z. Podolyak[13], K. Rijpstra[14], R. Rossel[3], K. Wendt[15], X. F. Yang[16, 17], and Z. Yue[5, 3]

[1]*KU Leuven, B-3001 Leuven, Belgium*
[2]*The University of Manchester, Manchester M13 9PL, United Kingdom*
[3]*CERN, CH-1211 Geneva 23, Switzerland*
[4]*Comenius University in Bratislava, Šafárikovo námestie 6, 814 99 Bratislava, Slovakia*
[5]*University of York, York YO10 5DD, United Kingdom*
[6]*Horia Hulubei National Institute of Physics and Nuclear Engineering, R-077125 Bucharest, Romania*
[7]*The University of Edinburgh, EH9 3FD Edinburgh, United Kingdom*
[8]*Saha Institute of Nuclear Physics, Bidhannagar, Kolkata, West Bengal 700064, India*
[9]*Denmark Technical University, 2800 Kongens Lyngby, Denmark*
[10]*University of Gothenburg, SE-412 96 Gothenburg, Sweden*
[11]*Institut Laue-Langevin, F-38042 Grenoble, France*
[12]*University of Jyväskylä, P.O. Box 35, FI-40014 Jyväskylä, Finland*
[13]*University of Surrey, Guildford GU2 7XH, United Kingdom*
[14]*SCK CEN, Boeretang 200, 2400 Mol*
[15]*Johannes Gutenberg-Universität, Saarstr. 21, 55099 Mainz, Germany*
[16]*Peking University, Beijing 100871, China*
[17]*RIKEN Nishina Center, 2-1 Hirosawa, Wako, Saitama 351-0198, Japan*
[*] *Affiliated with an institute covered by a cooperation agreement with CERN at the time of the experiment.*

Octupole deformed nuclei are predicted to be found in the region $130 \leq N \leq 140$ and $85 \leq Z \leq 92$ [1]. Nuclei that exhibit octupole deformations are of interest for ongoing searches for permanent atomic electric-dipole-moments and beyond Standard Model physics. Recent studies suggest the region of octupole collectivity 'north-east' of ^{208}Pb extends down to At ($Z = 85$) [2]. However, no evidence for octupole deformation has been observed in the Po ($Z = 84$) isotopes up to $N = 135$ [3].

To investigate the lower boundary of the octupole deformed region 'north-east' of ^{208}Pb, decay spectroscopy studies of ^{219,220}Po were performed at CERN ISOLDE with the ISOLDE Decay Station (IDS). In this work, we present improved values for the half-life and $\alpha - \beta$ branching ratio of ^{219}Po ($N = 135$). Additionally, we present the first value for the half-life of ^{220}Po, and discuss the implications of these results on the limits of octupole deformation in this region.

[1] Y. Cao *et al* 'Landscape of pear-shaped even-even nuclei' 2020 *Phys. Rev. C*, vol. 102, no. 2, p. 024311, doi: 10.1103/PhysRevC.102.024311.
[2] A. E. Barzakh *et al.* 'Inverse odd-even staggering in nuclear charge radii and possible octupole collectivity in ^{217,218,219}At revealed by in-source laser spectroscopy' 2019 *Phys. Rev. C*, vol. 99, no. 5, p. 054317, doi: 10.1103/PhysRevC.99.054317.
[3] D. A. Fink *et al.* 'In-Source Laser Spectroscopy with the Laser Ion Source and Trap: First Direct Study of the Ground-State Properties of Po 217,219', 2015 *Phys. Rev. X*, vol. 5, no. 1, p. 011018, doi: 10.1103/PhysRevX.5.011018.

O26

Investigating anomalous air showers with the SKA-Low

V. De Henau[1]

[1] *Inter-University Institute For High Energies (IIHE), Vrije Universiteit Brussel (VUB), Brussels, 1050, Belgium*

Cosmic rays are particles travelling in outer space at near light speeds. The origins of cosmic rays are still unknown, with large uncertainties in the transition region between Galactic and extragalactic sources (10^16 - 10^18 eV) [1]. When one of these high-energy particles collides with Earth's atmosphere, it causes an extensive air shower (EAS). However, the exact mechanism describing these collisions still has large uncertainties because the hadronic interaction models at EAS energies are beyond particle collider energies [2]. Most EAS exhibit a characteristic "universal" longitudinal profile (the particle amount as a function of atmospheric depth), with a single peak. The depth at which this peak occurs gives a measurement of the cosmic ray particle mass [3]. Low-mass particles, on average, penetrate deeper into the atmosphere before interacting, producing a shower maximum closer to the ground. These EAS emit radio waves, and by measuring this, we can reconstruct the energy and particle type of the cosmic ray, but due to uncertainties in the hadronic models, this is limited in accuracy. However, a rare phenomenon known as the anomalous shower deviates significantly from this universal profile. These anomalies are caused by secondary particles with high energies compared to the primary particle, traveling a significant distance further in the atmosphere. This causes the longitudinal profile to become elongated, and hence we call these stretched showers. Looking at an even rarer phenomenon caused by an energetic secondary travel even further into the atmosphere, the sub-shower can be displaced significantly enough from the main shower to cause a second bump in the longitudinal profile. These showers are called a double bump shower. These anomalous showers can be used to measure the crosssection of the hadronic interactions, and they hold additional information about the primary cosmic ray. Current cosmic ray experiments lack the resolution to distinguish between these different types of showers. Simulations have shown that the upcoming SKA-Low radio telescope will possess the sensitivity and resolution necessary to detect and reconstruct anomalous showers and thus be the first ever experiment capable of doing so [4].

[1] J. Bluemer, R. Engel, J. R. Hoerandel, (2009), doi:10.1016/j.ppnp.2009.05.002.
[2] D. Maurin *et al.*, (2025), doi:10.1016/j.physrep.2025.11.002.
[3] P. Lipari, (2008), doi:10.1103/PhysRevD.79.063001.
[4] V. De Henau *et al.*, (2025), doi:10.22323/1.501.0236.

Pre-commissioning for the Phase-2 upgrade of the CMS outer tracker with cosmic muons and R&D of new silicon sensors

M. Beghuin[1,2], M. Delcourt[2], S. Lowette[2], and P. Vanlaer[1] on behalf of the CMS Tracker Group
[1]*Université Libre de Bruxelles, Ixelles, 1050, Belgium*
[2]*Vrije Universiteit Brussel, Ixelles, 1050, Belgium*

The silicon tracker of the Compact Muon Solenoid (CMS) will be upgraded in the coming years as part of the High-Luminosity Large Hadron Collider (HL-LHC) program at CERN, designed to operate at peak luminosities of up to 7.5 x 10^{34} $cm^{-2}s^{-1}$ [1]. The outer-most layers of the tracker will be composed of 2S modules, consisting of two silicon strip sensors enabling a coarse estimation of the transverse momentum (p_T) of charged particles and allowing the tracker to contribute to the Level-1 trigger. Thanks to this system, event selection can be performed by exploiting tracking information at 40MHz, the bunch crossing frequency.

Belgium has taken a major responsibility by committing to assemble more than 1500 2S modules at the Inter-University Institute for High Energies (IIHE - ULB/VUB) in Brussels, and to integrate them at UCLouvain in Louvain-la-Neuve. Testing of the read-out electronics at different stages of the assembly process is a key feature for quality evaluation of the modules and for the identification of sources of noise or performance degradation.

As has been proven in the past during the commissioning and operation of the current silicon strip tracker, cosmic rays are a valuable resource for the integration of modules with the CMS data acquisition, the development of track reconstruction tools, as well as the development of calibration and alignment procedures. These are critical milestones that must be prepared before operation begins [2, 3].

To this end, a small-scale cosmic rack, comprising up to 5 vertically stacked 2S modules, will constitute a useful tool to investigate how to best exploit cosmic triggers, which are not synchronous with the LHC clock. I am deploying such a rack at IIHE, where the acquisition system is based on the readout system used at the test station at the assembly facility. I plan to interface the cosmic data within the CMS track reconstruction software, for which the local reconstruction, alignment, and calibration code will be specifically developed for the 2S modules in the cosmic-ray data taking conditions.

The inner part of the tracker, composed of pixelated sensors, will be exposed to high radiation levels, leading to its replacement midway through the HL-LHC run. Ongoing research focuses on the development of new position-sensitive silicon sensors targeting a 50 ps accuracy in particle crossing time measurement, enabling an additional coordinate in particle tracking (4D tracking). The Trench-Isolated Low-Gain Avalanche Diodes (TI-LGADs) are candidates for this Phase-3 upgrade of the tracker [4]. To characterize such sensors, I plan to set up a laser-based Transient Current Technique (TCT) system at IIHE, subject to funding availability.

[1] The CMS Collaboration 2017 CERN-LHCC-2017-009 CMS-TDR-014
[2] The CMS Collaboration 2010 *J. Instrum.* **5** T03009
[3] The CMS Collaboration 2014 *J. Instrum.* **9** P06009
[4] Giacomini G 2023 *Sensors* **23** 2132

milliQan: Search for Millicharged Particles in Proton-Proton Collisions at $\sqrt{s}$ = 13.6 TeV

S. Alcott,[1] Z. Bhatti,[2] J. Brooke,[3] C. Campagnari,[1] M. Carrigan,[4] M. Citron,[5] R. De Los Santos,[4] A. De Roeck,[6] C. Dorofeev,[7] T. Du,[8] M. Gastal,[6] J. Goldstein,[3] F. Golf,[9] N. Gonzalez,[5,10] A. Haas,[2] J. Heymann,[8] C. S. Hill ,[4] D. Imani,[1] M. Joyce,[4] K. Larina,[1] R. Loos,[6] S. Lowette,[11] H. Mei,[12] D. W. Miller,[8] B. Peng,[4] S. N. Santpur,[1] I. Reed,[9] E. Schaffer,[1] R. Schmitz,[1] J. Steenis,[5] D. Stuart,[1] J. S. Tafoya Vargas,[5] D. Vannerom,[11] **T. Wybouw,**[11] Z. Xiao,[4] H. Zaraket,[13] G. Zecchinelli,[9] and C. Zheng [4]

[1]*University of California, Santa Barbara, California 93106, USA*
[2]*New York University, New York, New York 10012, USA*
[3]*University of Bristol, Bristol, BS8 1TH, United Kingdom*
[4]*The Ohio State University, Columbus, Ohio 43210, USA*
[5]*University of California, Davis, California 95616, USA*
[6]*CERN, Geneva 1211, Switzerland*
[7]*University of Oregon, Eugene Oregon, 97403, US*
[8]*University of Chicago, Chicago, Illinois 60637, USA*
[9]*Boston University, Boston, Massachusetts 02215, USA*
[10]*University of California, Santa Cruz, California 95064, USA*
[11]*Vrije Universiteit Brussel, Brussel 1050, Belgium*
[12]*Shanghai Jiao Tong University, Shanghai China*
[13]*Lebanese University, Hadeth-Beirut, Lebanon*

We will report the status of the milliQan experiment at CERN. The milliQan "bar" detector was completed in June 2023 and has been taking physics data since then. The milliQan "slab" detector was completed in Fall of 2024 and is being commissioned. We will give an update on the readiness of the slab detector for physics data taking. Finally, we will present first physics results on the search for millicharged particles in 127 fb^{-1} pp collision data recorded by the bar detector during LHC Run 3, as published in [1].

[1] Alcott et al 2025 *Phys. Rev. Lett.* **135**, 121802

Search for Atmospheric Millicharged Particles with the IceCube Upgrade

L. Lallement Arnaud[1] and J.A. Aguilar Sánchez[1]

[1]*Université libre de Bruxelles, Brussels, 1050, Belgium*

Millicharged particles—hypothetical particles carrying a small fraction of the elementary electric charge—naturally arise in extensions of the Standard Model, and can be probed through their weak electromagnetic interactions in large-volume detectors. The IceCube Upgrade, as a low-energy extension of the IceCube Neutrino Observatory, is particularly well suited to detect the suppressed light yield expected from these particles.

In this work, we present one of the first combined calculations of atmospheric millicharged particle fluxes, including both meson decay and proton bremsstrahlung [1, 2]. While meson decay has traditionally been the primary production channel, proton bremsstrahlung remains subject to significant theoretical uncertainties; we compare two treatments and assess their impact. We then build a simulation framework for the IceCube Upgrade that propagates millicharged particles through the Earth, consistently accounting for attenuation effects.

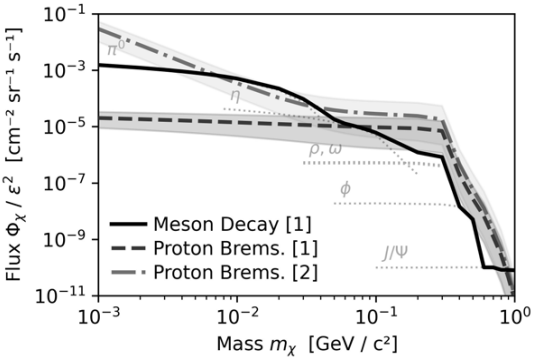

Figure 1: Fluxes of millicharged particles at the Earth's surface as a function of the mass, from meson decay and proton bremsstrahlung in the atmosphere.

We confirm that atmospheric production provides a relevant source of sub-GeV millicharged particles for the IceCube Upgrade, with proton bremsstrahlung significantly enhancing the flux at higher masses. These results lay the groundwork for the first dedicated search for atmospheric millicharged particles with the IceCube Upgrade, and one of the first such searches with a large-volume detector.

[1] Du M, Fang R and Liu Z 2024 *J. High Energy Phys.* 2024 174
[2] Bailloeul L *et al* 2025 arXiv:2512.11027

PHYWE – From Göttingen to the World

Meike Bremenkamp[1]

[1]*PHYWE Systeme GmbH & Co. KG, 37079 Göttingen, Germany*

This presentation offers an insight into PHYWE's legacy as a global provider of scientific education tools. We'll begin with a brief journey through the company's history, highlighting key milestones.

Next, we'll explore the scientific heritage of Göttingen — a city renowned for its remarkable contributions to physics, particularly in quantum theory, and its connection to numerous Nobel Prize laureates. Building on this, we will look at PHYWE's Nobel Prize experiment kits, which allow students to engage directly with the physics behind some of the most groundbreaking discoveries in science history.

We'll then introduce two live experiments featured at the fair: an X-ray device, and a renewable energy system that demonstrates the use of light to split water, store hydrogen and oxygen, and later convert them back into electricity via a fuel cell. These experiments connect directly to the fair's themes of quantum physics and sustainability.

To conclude, we'll reflect on the vital role of education in shaping the future of science — not only by preserving its past but by inspiring the next generation of innovators.

How this all comes together in practice will be shown in the following slides, which outline the structure and flow of the full presentation. These may be altered depending on the time span of the presentation.

Asteroseismology & Exoplanets in the Milky Way: A Research-Based STEM Module for Secondary Education

R. Stanley[1], C. Aerts[1], K. Hakim[1] and M. De Cock[2]

[1]*Institute of Astronomy, KU Leuven, Celestijnenlaan 200D, 3001 Leuven, Belgium*
[2]*KU Leuven, Department of Physics and Astronomy and LESEC, Celestijnenlaan 200C, 3001 Leuven, Belgium*

The challenge of engaging secondary school students with cutting edge physics research demands teaching materials that are both scientifically authentic and accessible to students. We present *Asteroseismology & Exoplanets in the Milky Way*, a Junior College STEM module developed at KU Leuven that brings active research directly into the classroom for 14-18 year olds.

Asteroseismology, the study of stellar oscillations, or starquakes, enables the determination of stellar masses, radii, and ages with unprecedented precision, and underpins our ability to characterise the host stars of exoplanets. The module introduces these concepts through an integrated STEM framework, interweaving mathematics, physics, chemistry, and data science in a way characteristic of modern astronomical research.

The centrepiece of the module is a student project, *Let's Make You a Real Asteroseismologist!*, in which each student is assigned their own star from the NASA Kepler mission. Using the star's power density spectrum, students identify oscillation modes, measure frequency separations, and determine the star's physical properties. Through this project they work with the same observational data as professional researchers; the solutions are taken from the peer-reviewed Kepler seismic LEGACY sample [1].

The module requires no prior knowledge of astronomy from teachers or students, and has been designed for use by physics, mathematics, and general science teachers. A structured teacher training programme accompanies the materials, equipping secondary school teachers with the subject confidence and practical guidance needed to deliver the full module. We discuss the design principles behind the module and its potential to support physics education at the secondary level.

[1] Lund, M. N., “Standing on the Shoulders of Dwarfs: the Kepler Asteroseismic LEGACY Sample. I. Oscillation Mode Parameters”, *The Astrophysical Journal*, vol. 835, no. 2, Art. no. 172, IOP, 2017. doi:10.3847/1538-4357/835/2/172.

Impact of Scale Comprehension on High School Students' Conceptual Understanding of Astronomical Phenomena

W. Keppens[1,4,5], M. De Cock[1,4,5], W. Van Dooren[2,4], H. Van Winckel[1] and J. Sermeus[1,2,3,4,5]

[1]*Department of Physics and Astronomy, KU Leuven, Celestijnenlaan 200C, 3001 Leuven, Belgium*
[2]*Faculty of Psychology and Educational Sciences, KU Leuven, Dekenstraat 2, 3000 Leuven, Belgium*
[3]*Royal Observatory of Belgium, Planetarium, Bouchoutlaan 10, 1020 Brussels, Belgium*
[4]*Leuven Educational Research Institute (LIVO)*
[5]*Leuven Engineering & Science Education Center (LESEC)*

The field of astronomy presents students with spatial scales that are difficult to grasp. Teaching these scales is especially challenging due to students' (and in general, people's) limited comprehension of large numbers and the abundance of schematic (but scale-inaccurate) depictions in astronomy textbooks [1, 2]. As a result, most students drastically underestimate the sizes and distances in our Solar System and beyond [3]. Nonetheless, it has been long suggested that a thorough understanding of the involved spatial scales is essential to reach a deeper understanding of a wide range of astronomical topics [4].

In this project, we investigate the impact of scale comprehension on students' explanations for basic astronomical phenomena. Their scale estimates were assessed through an interactive online survey. Based on their survey answers, specific students were selected for individual, semi-structured interviews addressing the (variation in the) apparent sizes of the Moon and Sun, solar (total and annular) eclipses and Moon phases.

During a first round of interviews, we selected N = 25 students who drastically underestimated most to all sizes and distances probed in the survey. We documented how such skewed scale assumptions influenced their reasoning on the discussed astronomical phenomena. For instance, when students placed the Moon very close to Earth, they reasoned that the Moon should look smaller when seen low above the horizon than highly elevated, as in the former case it is physically further from the observer. Likewise, they reasoned that multiple observers on Earth can simultaneously see (very) different Moon phases, as their perspectives on the Moon differ.

In a second round of interviews, N = 17 students with a (rather) accurate idea of the spatial scales in the Earth-Moon-Sun system were interviewed. We noted how these students often refrained from making the same scale-related erroneous reasonings as their peers with poor scale comprehension. However, they were not flawless in their explanations either – for instance, multiple students still explained Moon phases in terms of the Earth's shadow.

Based on our results, we argue that spatial scale comprehension is a necessary but not sufficient condition for astronomical conceptual understanding. We suggest other conditions to include a solid factual content knowledge base, 3D spatial thinking skills and an understanding of the mechanisms of light propagation and shadow formation. The implications of these findings are discussed in the presentation.

[1] Brass, A. and Harkness, S.S. 2017 *Cognitive Science* **9**(2):53-68.
[2] Taylor, R.S. and Grundstrom, E.D. 2011 *Astronomy Education Review* **19** 010104
[3] Keppens, W. *et al* 2025 *Phys. Rev. Phys. Educ. Res.* **21** 010159
[4] Salimpour, S., Fitzgerals, M. And Eriksson, U. 2024 *Astronomy Education Journal* **4**(1)

Improved effectiveness of nuclear physics lessons through targeted development of didactic materials

P. Vandevorst[1], J. Luyten[2], M Coeck[2] and J. Rock[1]

[1]*Antwerp School of Education, University of Antwerp, Antwerp, 2000, Belgium*
[2]*Belgian Nuclear Research Centre SCK CEN, Mol, 2400, Belgium*

A clear understanding of radioactivity and ionising radiation is essential for everyone in modern society, given their wide-ranging applications in nuclear energy, medical diagnosis and treatment, and various other non-power uses. Furthermore, the nuclear sector is growing. In the (near) future, Belgium and by extension Europe, will need more well-trained workers across the nuclear sector. The foundations for the careers of these employees who will fill key roles in the sector are laid as early as secondary school. Despite its societal importance and the prospect of sustainable, challenging jobs, research shows that many students hold misconceptions about the nuclear sector. In addition, nuclear physics is perceived as a challenging subject for pupils in the upper levels of secondary education due to its abstract concepts, their limited prior knowledge of physics and chemistry, the lack of realistic experiments, and the complex social context surrounding nuclear technology and its applications. Furthermore, this topic is also challenging for teachers because they often do not have access to the most up-to-date information from the R&D and industrial community, and because not every teacher has a background in physics. [1, 2]

The Antwerp School of Education and the Belgian Nuclear Research Centre (SCK CEN) collaborated on a survey that was conducted among 109 high-school teachers who teach about radioactivity and ionising radiation. The survey covers teachers' professional background; the perceived difficulty of preparing and teaching lessons on radioactivity and ionising radiation in comparison with other topics; the use and quality of available didactic materials; and teachers' instructional needs, including additional didactic materials.

The results of this survey show that less experienced teachers have a strong need for up-to-date information on the topic of radioactivity and ionising radiation. In addition, 49% of respondents reported difficulties when teaching about these topics, specifically due to the higher level of abstraction compared to other topics in the curriculum. Respondents additionally perceive that their students are primarily interested in the applications of this topic and in its health effects.

Driven by these results new didactic material was developed that focuses on active learning and the use of simulations. The effectiveness was evaluated through a comparative classroom study involving two groups of high-school students enrolled in human sciences, economics–modern languages, and Latin–modern languages. One group followed a traditional lecture-based approach (control group), while the other received interactive instruction (experimental group). The effectiveness will be studied based on the achievement of the learning outcomes comparing pre- and post-tests results of the control and experimental group. Although the study is still in progress, its completion is ensured before the conference, at which the results can be presented.

By combining state-of-the-art information from R&D, teacher perspectives and classroom-based evaluations, this research seeks to facilitate future instructional design and professional support in radiation-related topics.

[1] Rego F and Peralta L 2006 *Phys. Educ*. **41** 259
[2] Morales López A and Tuzón P 2022 *Sci & Educ* **31** 405

Poster Presentations

P1

A simplex based conservative discretization of the Lorentz force for liquid metal flows

R. Alliet[1], M. Bernard[2], G. Lartigue[3], and B. Knaepen[1]

[1] *Physique des Systèmes Dynamiques, Faculté des Sciences, Université Libre de Bruxelles, Ixelles, 1050, Belgium*
[2] *LEGI, Université Grenoble Alpes, CNRS, Gières, 38610, France*
[3] *CORIA CNRS UMR6614, Saint-Etienne-du-Rouvray, 76800, France*

Numerical simulations of liquid metal flows under the influence of strong magnetic fields are of great importance for the design of liquid metal blankets in fusion reactors. For intense magnetic fields, the flow within the blankets is notoriously challenging to compute numerically due to extremely thin boundary layers, requiring very fine meshes in some parts of the computational domain. As of today, no CFD code can provide complete and accurate solutions to tackle the full complexity of blanket systems like that foreseen in ITER, although significant progress has been made in recent years.

In this work we examine a novel, conservative, discretization of the Lorentz force. This formulation is tailored to solvers using median dual grids built from simplicial elements in a vertex-centred way. Using the quasi-static approximation, the Lorentz force is expressed as,

$$\boldsymbol{f}_L = \boldsymbol{j} \times \boldsymbol{B} = \sigma(-\nabla\phi + \boldsymbol{u} \times \boldsymbol{B}) \times \boldsymbol{B}, \tag{1}$$

To determine the Lorentz force in a conservative way we make use of the divergence-free nature of $\boldsymbol{j}$,

$$\boldsymbol{j} = \nabla \cdot (\boldsymbol{j}\boldsymbol{x}) \tag{2}$$

as in the pioneering work of Ni et al. [1]. In our new formulation, the volume averaged Lorentz force is then discretized based on the Laplacian operator proposed in [2] as,

$$\overline{\boldsymbol{f}_L}^{V_\alpha} = \frac{\sigma}{2V_\alpha}\boldsymbol{B} \times \sum_j \left\{ \left[\boldsymbol{x}_{J,b} \frac{\boldsymbol{S}_{J,j} \cdot \boldsymbol{S}_{J,i}}{2V_J} + \boldsymbol{x}_{K,b} \frac{\boldsymbol{S}_{K,j} \cdot \boldsymbol{S}_{K,i}}{2V_K} \right] (\phi_j - \phi_i) + \boldsymbol{x}_j (\boldsymbol{u}_j \times \boldsymbol{B}) \cdot \boldsymbol{S}_{pf,ij} \right\}, \tag{3}$$

This novel technique is compared to existing non-conservative methods in the YALES2 solver on highly skewed meshes. Results indicate that the simplicial scheme outperforms them in terms of accuracy, while retaining the same order of convergence. The conservative formulation further allows the accurate capture of high Hartmann number flows. For incompressible flows, the use conservative and consistent method can be extended to the pressure gradient.

[1] Ni, M.-J. et al 2007 *J. Comput. Phys.:* **227**, 205–228
[2] Specogna, R. and Trevisan, F 2011 *J. Comput. Phys.:* **230**, 1370–1381

Minimization of Ion Cyclotron Parasitic Edge Dissipation

S. Carli, D. Van Eester, P. Lamalle, V. Maquet, and M. Vergote

LPP-ERM/KMS, Brussels, 1000, Belgium

In this work we present the status and plans for the Minimization of Ion Cyclotron Parasitic Edge Dissipation (MinICPED) project. In magnetically confined nuclear fusion reactors, electromagnetic waves in the ion cyclotron range of frequencies (ICRF) are often employed as external heating source to initiate the fusion reactions. While ICRF has been successfully employed in current tokamak devices, and is planned for future reactors like ITER, its interaction with the plasma edge still requires. In particular, the wave-plasma coupling, hence the power delivered to the plasma, strongly depends on the plasma edge density profile in front of the antenna. Similarly, there is ample evidence of ICRF-induced plasma edge density modifications, through ponderomotive acceleration and sheath rectification, which in turn modify the wave-plasma coupling, dissipate wave energy in the edge, and enhanced impurity sputtering. Taking into account these nonlinear 3D effects into a consistent modeling picture is quite involved, and attempts have been limited so far. In [1,2] an integrated modeling was set up, coupling a plasma edge code with a wave and RF-sheath code. However, neither of the two studies self-consistently treated $E \times B$ drifts induced by RF-sheaths. In [3] instead, a simplified plasma model together with a wave model, self-consistently accounted for the ponderomotive drift in the plasma bulk, excluding RF sheaths.

In the MinICPED project we aim at improving the current state-of-the-art by building an integrated modeling framework which self-consistently accounts for RF-induced ponderomotive and sheath effects on the plasma edge behaviour and wave-plasma coupling. We base ourselves on [1,2,4] and couple the wave model implemented in NGSOLVE in [5], the state-of-the-art plasma edge code SOLPS-ITER [6], and the RF-sheath code SSWICH [7]. Compared to [1,2], we self-consistently evolve the plasma edge behaviour accounting for RF-induced ponderomotive drifts and RF sheath biasing. We are currently deriving and implementing the ponderomotive effect in SOLPS-ITER based on [3,8], and carrying on a verification step using the Method of Manufactured Solutions. The next step will be the co-simulation of SOLPS-ITER with the wave model in NGSOLVE, and later on also with SSWICH. Since SOLPS-ITER is at the moment limited to 2D geometries, we plan on replacing it with a 3D code such as SOLEDGE3X, Hermes3, or EMC3. With such an integrated modeling framework, we aim at improving the antenna design and operation, reducing wave losses and parasitic dissipation in the edge.

[1] Zhang W *et al* 2017 *Nucl. Fusion* **57** 116048
[2] Kumar A *et al* 2025 *Nucl. Fusion* **65** 076039
[3] Van Eester D *et al* 2023 *Physics* **5** 116
[4] Myra J R 2021 J. *Plasma Phys.* **87** 905870504
[5] Maquet V *et al* 2026 *EPJ Web Conf.* **346** 01020
[6] Wiesen S *et al* 2015 *J. Nucl. Mater.* **463** 480
[7] Colas L *et al* 2012 *Phys. Plasmas* **19** 092505
[8] Klima R 1698 *Czech. J. Phys. B* **18** 1280

P3

Creating NOON states with ultracold atoms using time crystals

Célia Delaive[1]

[1]*CESAM, Université de Liège*

NOON states are highly entangled states involving N bosons distributed over two modes and are of great interest for quantum metrology due to their sensitivity to external forces and light fields. Their realization remains challenging, in particular because of the slowness of the collective tunneling underlying their formation, as well as the requirement of perfect symmetry between the two modes. In this project, we propose to overcome the symmetry problem by introducing a periodic driving, such that the resulting NOON state forms a discrete time crystal. We also consider two protocols to accelerate its formation. The first relies on the same periodic driving, which induces chaotic dynamics in the system. The chaos will assist the tunneling process. The second relies on optimal control of the energy of an additional mode, combined with counterdiabatic driving.

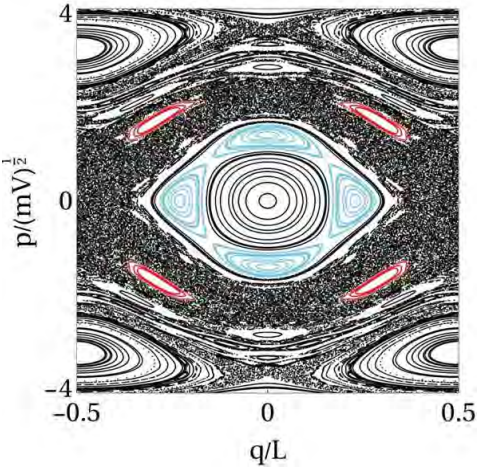

Figure: Example of a Poincaré section of the classical single-particle dynamics corresponding to the periodically driven Hamiltonien $H = \frac{p^2}{2m} - V\cos(q)\left(1 + \delta\cos(\omega t)\right)$. In red we have a 2:1 resonance, the islands are separated by a chaotic sea, making them a good candidate for the chasassited tunneling. In blue we have a 4:1 resonance. It constitutes a good candidate, in addition to the center of the phase-space, for the geodesic-counterdiabatic driving protocol.

P4

Computational Fluid Dynamics for Liquid Metal Flows subject to Magnetic fields

Gayina Louis[1], Bernard Knaepen[1], and Sven Van Loo[2]

[1]*ULB, Bruxelles, 1050, Belgium*
[2]*UGent, Gent, 9000, Belgium*

Simulating liquid metal blanket flows in fusion reactors is computationally demanding because strong magnetic fields create extremely thin boundary layers that require fine computational meshes. To overcome this, we adapted the MG code [2]—originally designed for compressible astrophysical flows—to simulate quasi-static, incompressible magnetohydrodynamic (MHD) conditions. By leveraging MG's hierarchical adaptive mesh refinement (AMR) to efficiently resolve steep gradients, we can simulate more complex cases. Finally, we validate this new implementation by comparing its predictions against analytical solutions for MHD flow in a square duct with both electrically insulating and conducting walls.

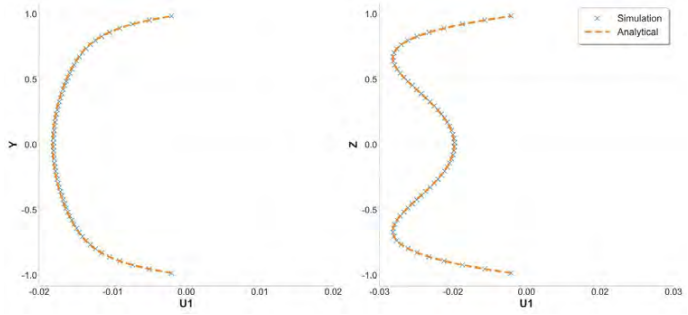

Figure 1: Validation of the quasi-static MHD implementation. The simulated IMG code velocity profiles (blue) demonstrate agreement with the exact analytical solution (orange) for the Hunt flow case [1].

While our initial numerical implementation employs second-order accurate finite volume methods, this work also details our current progress toward refining the discretization scheme with higher-order interpolations. To accommodate the diverse geometric configurations of fusion reactors—ranging from simple rectangular ducts to complex toroidal designs—the expanded code will support both Cartesian and cylindrical coordinate systems. Additionally, we outline future plans to incorporate critical physical phenomena, specifically thermal conduction, which is essential for the accurate modeling of liquid metal blankets.

[1] J.C.R. Hunt. Magnetohydrodynamic flow in rectangular ducts. 1965 *Journal of Fluid Mechanics* **21**(4), 577–590
[2] S. Van Loo, J.C. Tan, and S.A.E.G. Falle. Magnetic fields and galactic star formation rates. 2015 *The Astrophysical Journal Letters* **800**(1), L11

P5

Progress in the implementation of the integral dielectric kernel to model RF heating in toroidal plasmas

B.C.G. Reman[1], P.U. Lamalle[1], J. Zaleski[3], C. Slaby[2a], C. Geuzaine[3], V. Maquet[1], D. Van Eester[1], M. Campos Pinto[2b], Y. Güçlü[2b] and E. Moral Sánchez[2b]

[1]*Laboratory for Plasma Physics, Royal Military Academy, Brussels, Belgium*
[2]*Max-Planck-Institut für Plasmaphysik, 17491* [2a]*Greifswald and* [2b]*Garching, Germany*
[3]*Dept. of Electrical Engineering and Computer Science, University of Liège, Belgium*

As discussed in Ref. [1], recent theoretical and numerical treatments [2, 3] have sought to express the plasma radiofrequency (RF) response as a nonlocal integral operator formulated in configuration space. Analytical expressions of the integral kernels are available for Maxwellian particle species. This approach enables *(i)* direct use of the finite element method (FEM) to model wave propagation and absorption in hot inhomogeneous fusion plasmas, *(ii)* local mesh-refinement, *(iii)* provides RF field representations suited to address tokamak geometry, and *(iv)* allows to connect plasma model with antenna models. The present contribution focuses on the concrete application of this method. We are exploring physical and numerical aspects through the development of PLIKES, a new "in- house" FEM code. It solves Maxwell's equations in the frequency domain in the presence of the nonlocal kernel in 2.5D slab geometry to lowest order in finite Larmor radius as a first step, i. e. with focus on wave dispersion effects along the equilibrium magnetic field and the associated fundamental cyclotron and Landau dampings. This integro-differential formulation is untypical of FEM [4]. The present efforts are dedicated to enrich the description of the parallel dynamics, the perpendicular ones are further studied in Refs [5,6]. In particular we are considering a field aligned coordinate system to retain parallel magnetic field g radients. The envisaged conformal map between the FEM reference domain and the physical mesh will allow to single out the parallel magnetic field direction. This will then directly provide the direction of the nonlocal coupling in the implementation. In addition, the parallel component of the RF field $E_{\parallel}$, typically three decades smaller than $E_{\perp}$, will be extracted for adequate numerical treatment. Yet, this comes with challenges that include: a curl conforming transformation, the adaptation of the boundary conditions together with the expression of new kernels to cross resonances and tangential resonances. We also present preliminary results and describe the future developments using extension of advanced FEM libraries such as Psydac [7] and GmshFEM [8,9] to incorporate our new formulation.

[1] P.U. Lamalle *et. al.* (2025), 20th RF Power in Plasmas Conf., Hohenkammer, Germany
[2] P. U. Lamalle, *AIP Conference Proceedings*, **2254 1**, 100001 (2020).
[3] M. Machielsen *et al.*, *Fundamental Plasma Physics*, **3**, 100008 (2023).
[4] Shiraiwa, S., *et al.*, *Phys. Plasmas* **17**, 056119 (2010).
[5] D. Van Eester, *et al.* "Almost-off-the-shelf tools for ICRH modelling", *25th Topical Con-ference on Radio-Frequency Power in Plasmas* (2025).
[6] V. Maquet, *et al.* "Implementation of a fast 2D wave-solver using the BUDE method with NGSolve", *25th Topical Conference on Radio-Frequency Power in Plasmas* (2025).
[7] Güçlü, Y. *et al.*, "PSYDAC: A High-Performance IGA Library in Python" *CIMNE* (2022) https://doi.org/10.23967/eccomas.2022.227.
[8] Royer, A. *et al. 14th World Congress on Computational Mechanics (WCCM), ECCOMAS Congress 2020.* Scipedia, 2021.
[9] Zaleski, J. *et al.* "Finite Element Formulation with Integral Dielectric Kernel for ICRH Plasma Heating on Non-Field-Aligned Meshes", *WAVES* 2026, Montreal, Canada.

P6

Towards calibrating antenna orientations using the Galaxy with RNO-G

J. Stoffels[1]

[1]*Vrije Universiteit Brussel, Brussels, 1050, Belgium*

The Radio Neutrino Observatory in Greenland (RNO-G) aims to detect UHE neutrinos (E > 100 PeV) [1]. With an array of upward-facing near-surface antennas operating in the 80-700 MHz range, the RNO-G surface component is sensitive to broadband signals originating from many sources, such as background noise induced by the Milky Way. In this contribution, I use the measured Galactic noise to enhance/improve our understanding of the detector, particularly its application in calibrating the antenna orientation through cmparison with simulation [2,3].

[1] S. Agarwal et al. JINST 20.04 (2025), P04015. DOI: 10.1088/1748-0221/20/04/P04015.
[2] M. Büsken, T. Fodran, and T. Huege Astronomy & Astrophysics 679 (2023) A50.
[3] C. Glaser et al, The European Physical Journal C 80.2 (Jan. 2020). issn: 1434-6052.

P7

Underlying physics of a plasmonic metasurface-based Optical Solar Reflector: toward enhanced and lightweight thermal management

L. Viseur[1,*], A. Mayer[1], L. Henrard[1], and M. Lobet[1]

[1]*Department of Physics, University of Namur, rue de Bruxelles 61, 5000 Namur, Belgium*
**lucas.viseur@unamur.be*

Optical solar reflectors (OSRs) are key components for spacecraft thermal control, requiring low solar absorptance combined with high thermal infrared emissivity [1]. Incumbents glass tiles or polymers meet these requirements but often suffer either from fragility and rigidity [1] or UV degradation and a lack of sustainability [2], respectively. In this context, plasmonic metasurfaces provide a promising alternative towards lightweight spacecraft thermal control by enabling subwavelength control of absorption and emission through geometry and material design [3].

In our work, we investigate a plasmonic metasurface-based OSR composed of an aluminum back reflector, a SiO_2 dielectric spacer, and a nanostructured aluminum-doped zinc oxide (AZO) layer. This architecture forms a resonant system, in which multiple physical mechanisms jointly shape the spectral response. Localized surface plasmon resonances supported by the patterned AZO layer enhance emissivity in the thermal infrared, while Fabry– Pérot cavity effects introduced by the dielectric spacer generate additional spectral selectivity across both the solar and infrared ranges. The aluminum back reflector suppresses transmission and enforces reflection, further influencing the overall design response.

A detailed analysis of the underlying physical mechanisms reveals a complex interplay between plasmonic resonances, cavity interference, reflection and Reststrahlen bands. In particular, the geometrical and material parameters of the plasmonic layer involve an inherent trade-off between minimizing solar absorption and maximizing infrared emission. By taking advantage of this physics-based understanding, a systematic optimization strategy can be implemented.

The optimized design achieves a low solar absorptance of $\alpha = 0.16$ together with a high thermal emissivity of $\varepsilon = 0.83$. These results demonstrate the potential of plasmonic metasurface-based OSRs as compact, ultrathin, and high-performance thermal-control surfaces.

[1] N. Marshall and R. A. Breuch, “Optical solar reflector—A highly stable, low αs/ε spacecraft thermal control surface,” 1968 *Journal of Spacecraft and Rockets*, **5**, 9, pp. 1051–1056
[2] Putz, S. Wurster, T. E. J. Edwards, B. Volker, G. Milassin, D. M. Tobbens, and M. J. Cordill, “Mechanical and optical degradation of flexible optical solar reflectors during simulated low Earth orbit thermal cycling,” 2020 *Acta Astronautica*, **175**, pp. 277–289
[3] Sun, C. A. Riedel, Y. Wang, A. Urbani, M. Simeoni, S. Mengali, and O. L. Muskens, “Metasurface optical solar reflectors using AZO transparent conducting oxides for radiative cooling of spacecraft,” 2018 *ACS Photonics*, **5**, 2, pp. 495–501

P8

Simultaneous amplification of the angular and spatial Goos-Hänchen shifts by weak measurements

J. Bouchat[1], Y. Caudano[1]

[1]*Physics Department, Namur Institute for Complex Systems (naXys) and Namur Institute of Structured Matter (NISM), University of Namur, Rue de Bruxelles 61, 5000 Namur, Belgium*

Considering the reflection or the refraction of a laser beam between two media with different refractive indices leads to well-known deviations from the laws of geometrical optics called the Goos-Hänchen and the Imbert-Federov effects. These deviations appear as spatial and angular shifts of the beam's central axis, respectively within the plane of incidence and perpendicular to it [1]. More specifically, angular and spatial Goos-Hänchen shifts occur under partial and total reflection and are directly related to the variation of the modulus and phase of the Fresnel coefficients with respect to the incidence angle, evaluated for the central plane wave within the paraxial approximation. Importantly, for a non-absorbing isotropic medium, the angular Goos-Hänchen shift only appear in partial reflection, while the spatial Goos-Hänchen shifts only occur in total internal reflection.

However, detecting these displacements poses a challenging problem experimentally because the shifts are of the order of magnitude of the wavelength and are thus typically smaller than the resolution of a CCD camera. Emerging from the formalism of weak measurements in quantum mechanics, weak value amplification presents an elegant way to circumvent this limitation. Usually, weak measurements amplify these displacements by modifying the beam transverse profile in such a way that the relative shift between different polarisations increases at the cost of a very low intensity. To make this possible, a post-selected polarization state has to be nearly orthogonal to a pre-selected state that combines two eigen polarizations undergoing different shifts. This method measures only the relative amplified spatial or angular shifts, without the possibility to access to the individual amplified shifts [2].

In a uniaxial anisotropic medium, a plane wave will be split between an ordinary mode with an isotropic refractive index and an extraordinary mode with a refractive index varying with the angle between the direction of propagation and the optical axis [3]. When considering the transmitted medium as a uniaxial anisotropic medium with an optical axis in the plane of incidence, the two eigen polarizations states are preserved and do not mix at the interface upon reflection and refraction but they present two different critical angles. This results in a new regime where a single eigen polarization is totally reflected, generating a spatial shift in the plane of incidence, while the other is partially transmitted, generating an angular shift. In this context, weak value amplification enables digital imaging of the combined angular and spatial Goos-Hänchen shifts in a way that would give access to their absolute amplified value.

[1] Bliokh, K. Y., & Aiello, A. (2013). Goos–Hänchen and Imbert–Fedorov beam shifts: an overview. *Journal of Optics*, *15*(1), 014001.
[2] Prajapati, C., & Viswanathan, N. K. (2017). Simultaneous weak measurement of angular and spatial Goos–Hänchen and Imbert-Fedorov shifts. *Journal of Optics*, *19*(10), 105611.
[3] Lekner, J. (1991). Reflection and refraction by uniaxial crystals. *Journal of Physics: Condensed Matter*, *3*(32), 6121.

P9

Proposal for Production of Ca Heavy-Rydberg States by Electron Transfer From Ultra-Long-Range Rydberg Molecules

A. Bouillon[1], **R. Dartois**[1], and M. Génévriez[1]

[1]*UCLouvain, Institute of Condensed Matter and Nanosciences, Louvain-la-Neuve, BE-1348, Belgium*

Heavy-Rydberg (HR) ion-pair states are molecular states composed of a positive and a negative ion that interact Coulombically. Their vibrational wavefunctions and energies thus behave similarly to those of electronic states in the Hydrogen atom, as the electron of the latter is replaced by an anion in the former. In the $Ca^+(4s)$-$Ca^-(4p_j)$ case, because of the very small Ca electron affinity, the Coulomb potential of heavy-Rydberg states crosses the molecular potential energy curves of many ultra-long-range Rydberg molecules (ULRRM). These molecules result from the multiple scatterings of a Rydberg electron off a neutral perturbing atom. Their bond length is similar to the size of the Rydberg atom, and ranges from ~200 to ~450 a_0 for the principal quantum number n=10-15 of the Rydberg electron considered in this work. Their potential energy curves indeed cross the HR Coulomb one in a region where the electronic wavefunctions of the two molecular systems significantly overlap, yielding a non-vanishing electron-transfer-type interaction between them.

Exciting a HR state directly from a ground-state molecule is a very unlikely process due to the poor overlap between the vibrational wavefunctions of the two systems and has only been achieved via multi-photon excitation schemes. We suggest and theoretically demonstrate that the interaction between ULRRM and HR potential energy curves in Ca is of great interest, as it results in significant mixing between the two systems and consequently enables direct excitation of cold HR ion pairs via excitation of the ULRRM component of the mixed vibrational states. ULRRMs of different atomic species have indeed already been photoassociated [1]. This excitation scheme, besides leading to the formation of cold HR molecules, could be of great interest to study controlled electron transfer.

To investigate this proposal, we first determine the potential energy curves of the ULRRM by using the Fermi-Omont pseudopotential [1]. The electronic interaction between the two molecular systems is then calculated both numerically and analytically [2], employing the generalized local-frame transformation [3], for benchmark purposes. We then solve the Schrödinger equation by means of a discrete-variable-representation method with exterior complex scaling, enabling us to treat the dissociation channels and to find the vibrational wavefunctions, states and lifetimes, following a non-adiabatic description of the electron-transfer interaction. Finally, excitation efficiencies and lifetimes between diabatic and non-adiabatic vibronic states are compared. Preliminary results show that HR states can efficiently mix with ULRRM for n values between 10 and 13 and that this mixing substantially increases their direct excitation probability from a cold atomic gas, reaching values comparable to the pure ULRRM states. Ongoing calculations are considering other excitation schemes, relying on multi-step processes to increase the efficiency and range of n values that could be used to prepare HR states.

[1] Bendkowsky V *et al* 2009 *Nature* **458** 1005-1008
[2] Bouillon A and Génévriez M 2026 *Molecular Physics*
[3] Giannakeas P *et al* 2020 *Phys. Rev. A* **102** 033315

P10

Multimode solitons and soliton trains driven by space-time inputs to multimode fibers

J. Dechanxhe[1], S. W. Jolly[1], and P. Kockaert[1]

[1]*OPERA-Photonics, Université Libre de Bruxelles, 50 av. F.D. Roosevelt, CP194/5, B-1050 Bruxelles, Belgium*

Expanding nonlinear optics in optical fibers to multimode fibers has allowed for observing and learning about significantly more complex phenomena, while also enabling control over processes like beam self-cleaning, supercontinuum generation, and soliton formation [1]. Implicit in all of these investigations is the eventual development along nonlinear propagation of high-dimensional fields that are structured in space and time. In our work we consider the same physical system, i.e. a graded-index multimode fiber, but with input fields that already have their own space-time structure [2, 3]. In doing so we gain a much more explicit control over the highly nonlinear interactions, and can observe new effects such as multimode domain wall locking and especially a new form of multimode solitons, and trains of such solitons. We will discuss the formation and properties of these new nonlinear optical structures and the implications.

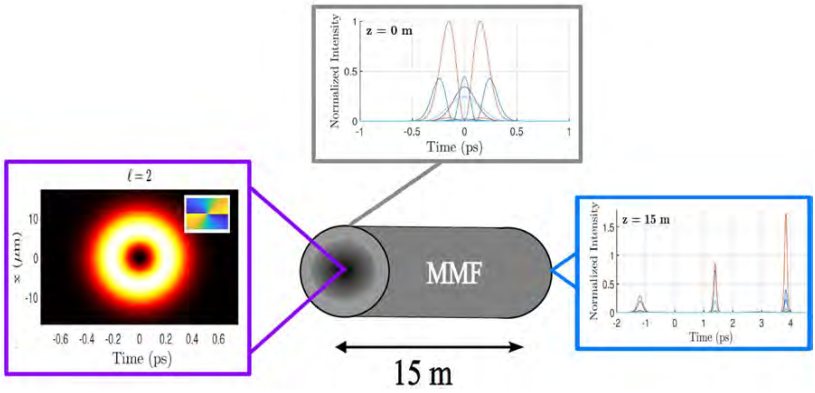

Figure 1: Illustration of multimode solitons train pumped by a single space-time object. The space-time input is a space-time optical vortex that excites several spatial modes of the multimode fiber (MMF). At the entry of the fiber, each mode has a distinct temporal profile. During propagation in the multimode fiber, the space-time optical vortex splits into several unique multimode solitons. Each soliton has a distinct modal composition, energy, and duration.

[1] K. Krupa et al. “Multimode Nonlinear Fibre Optics, a spatiotemporal avenue”. APL Photonics 4.110901 (2019).
[2] S. W. Jolly and P. Kockaert. “Coupling to multi-mode waveguides with space-time shaped free-space pulses”. Journal of Optics 25.5 (2023), p. 054002.
[3] A. Bekshaev. “Spatiotemporal optical vortices: Principles of description and basic properties”. APL Photonics 9.11 (2024), p. 110806.

P11

Near-Geometric Capture of Water by V_n^+ Clusters under Controlled Few-Collision Conditions

H. Jiang[1], B. Smeets[1], K. Hansen[1,2], Y. Zhang[1], P. Lievens[1], and E. Janssens[1]

[1]*Quantum Solid-state Physics, Department of Physics and Astronomy, KU Leuven, Leuven, 3001, Belgium*
[2]*Joint Centre for Quantum Studies and Department of Physics, School of Science, Tianjin University, Tianjin, 300072, P.R. China.*

Reactions of transition metal clusters with water are intensively studied as model systems for nanoscale oxidation chemistry and heterogeneous catalysis [1–4]. A key question in gas phase reaction is whether the reactivity is governed by long-range ion-molecule capture or short-range chemical dynamics.

Here we investigate the reaction of size-selected V_n^+ clusters (n = 7–40) with water vapor in a low-pressure collision cell as a function of the pressure. This approach enables a direct comparison between measured effective reaction cross sections and geometric capture limits.

Strikingly, effective reaction cross sections approach the geometric hard-sphere limit across the entire size range, indicating near-unity capture efficiency despite electronic complexity. This near-geometric capture represents a notable, non-trivial observation for water-metal cluster systems.

Studies with varied cluster source temperature reveal a non-monotonic trend in effective rate constants. Product distributions of oxygenated clusters ($V_nO_m^+$, m = 1–5), formed via dehydrogenation of water, indicate that internal cluster energy primarily modulates sequential oxidation rather than the initial capture step, consistent with capture-controlled association followed by temperature-dependent short-range dynamics.

These findings show that the critical stage determining the dehydrogenation rates is the dynamics after attachment. The temperature dependences show that these reactions proceed with very low, albeit non-zero activation energy.

[1] Heiz, U.; Landman, U., 2012 *Phys. Chem. Chem. Phys.*, **14**, 9255-9269.
[2] Luo, Z.; Castleman, A. W.; Khanna, S. N., 2016 *Chem. Rev.,* **116**, 14456-14492.
[3] Zhang, H., Wu, H., Jia, Y. et al., 2020 *Commun. Chem.*, **3**, 148.
[4] Hou, G.-L *et al* 2021 *Angew. Chem. Int. Ed.*, **60**, 27095-27101.

P12

Vacuum laser acceleration with aberrated ultrashort vector beams

S. W. Jolly[1], M. Lytova[2], F. Fillion-Gourdeau[2,3], and S. MacLean[2,3]

[1]*Service OPERA-Photonique, Université libre de Bruxelles (ULB), Brussels, Belgium*
[2]*Advanced Laser Light Source (ALLS) at INRS-EMT, 1650 blvd. Lionel-Boulet, Varennes, QC, J3X 1P7, Canada*
[3]*Infinite Potential Laboratories, 485 Wes Graham Way, Waterloo, ON, N2L 0A9, Canada*

The acceleration of electrons with tightly-focused high-power radially-polarized laser beams (RPLBs) is an interesting avenue to generate relativistic electron bunches with small emittance and femtosecond-level duration. This accelerating mechanism is highly sensitive to the exact spatio-temporal shape of the accelerating laser pulse. Owing to the tight-focusing and ultrashort nature of these pulses, their description is far from trivial. Simulations of electron trajectories have advanced to a very high level [1], but to describe the cutting-edge experiments [2,3,4] with realistic laser beams is an ongoing challenge. Because of these issues, a holistic approach to modeling arbitrarily aberrated ultrashort RPLBs is necessary (see Fig. 1).

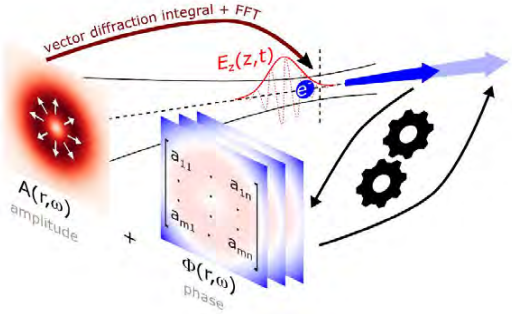

Figure 1: An arbitrary radially-polarized laser pulse can be represented as having a spatio-temporal amplitude $A(r,\omega)$ and a spatio-temporal phase $\Phi(r,\omega)$. The phase can be described by a large set of free parameters $a_{\{m,n\}}$, which we optimize over. This field develops a strong longitudinal electric field when tightly focused, which is responsible for electron acceleration.

We have already found a number of promising results for optimizing this process [6,7], and will continue to push this using more powerful computational models along with creative forms of aberrations and polarization gating. Our first new results show, for example, that simple spherical aberration can counter-intuitively increase the final electron energy.

[1] L. J. Wong, K.-H. Hong, et al., "Laser-induced linear-field particle acceleration in free space," Sci. Rep. **7**, 11159 (2017).
[2] S. Payeur, S. Fourmaux, et al., "Generation of a beam of fast electrons by tightly focusing a radially polarized ultrashort laser pulse," Appl. Phys. Lett. **101**, 041105 (2012).
[3] S. Carbajo, E. A. Nanni, et al., "Direct longitudinal laser acceleration of electrons in free space," Phys. Rev. Accel. Beams **19**, 021303 (2016).
[4] J. Powell, S. W. Jolly, at al., "Relativistic Electrons from Vacuum Laser Acceleration Using Tightly Focused Radially Polarized Beams," Phys. Rev. Lett. **133**, 155001 (2024).
[6] S. W. Jolly, "Influence of longitudinal chromatism on vacuum acceleration by intense radially polarized laser beams," Opt. Lett. **44**, 1833–1836 (2019).
[7] S. W. Jolly, "On the importance of frequency-dependent beam parameters for vacuum acceleration with few-cycle radially-polarized laser beams," Opt. Lett. **45**, 3865–3868 (2020).

Series of doubly excited states converging to the double-ionization threshold of Strontium atoms

***M. Jungers*[1]**, *M. Génévriez*[1]

[1]*UCLouvain, Louvain-la-Neuve, 1348, Belgium*

Atoms in highly doubly excited states (approximate principal quantum numbers of the inner and outer Rydberg electrons N and $n \gg 1$) are fascinating objects at the center of many physical phenomena such as electronic resonances, chaos and non-trivial correlation effects [1,2]. The excited electrons are nearly uncorrelated from the doubly charged ionic core and have their own two-electron wavefunction. Despite this apparent simplicity, one enters a domain in which correlation effects between the electrons are of great importance and reveal unique properties of the three-body quantum Coulomb problem [2].

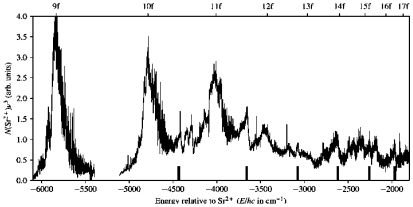

Figure 1. Experimental photoexcitation spectrum [2]. The vertical axis shows the number of Sr^{++} ions scaled by the cube of the wavenumber relative to the DI. The horizontal axis shows the wavenumber of the excitation laser relative to the DI threshold. The lines under consideration are marked by large bars.

Photo-excitation spectra of alkaline-earth atoms (Mg, Ca, Sr, Ba) serve as probes to study electronic correlation in highly doubly excited states. We focus here on Sr atoms and theoretically analyze an experimental spectrum recorded at the Max Born Institute. The experiment consists of photoexciting Sr atoms prepared in the $6d19l$ (l∼15) state to doubly excited states before converting the excited population to Sr^{++} ions via a combination of photo- and field-ionization [3]. Our goal is to explain the origin of a series of lines (Fig. 1) that appear right above each hydrogenic single-ionization threshold and, remarkably, converge up to the double-ionization (DI) threshold.

As we are only 0.5 eV below the DI threshold, the density of states is very large, and many eigenstates must be computed for an accurate reproduction of the spectrum. This requires diagonalizing large sections of the Hamiltonian via ab-initio configuration-interaction computations (e.g. N=7, …,10 and n→100) [2,3]. Using large-scale parallelization techniques, we can reproduce photo-excitation spectra for unprecedentedly high excitation energies. Our results are validated by direct comparison with the experimental spectrum, yielding good agreement. Theory reveals that only a handful of short-lived ($\tau \sim 0.1$ ps) resonances underlie each of the unassigned resonance series (large bars). The inner electron features an important s or d character, while the outer, highly excited electron exhibits a wavefunction that significantly departs from those of conventional Rydberg states. A careful analysis of the interactions responsible for these resonances and their marked appearance in the experimental spectra is under way.

[1] Jiang et al 2008 *Phys. Rev. A* **78**, 021401(R)
[2] M. Génévriez, M. Jungers et al 2025 *Phys. Rev. Lett.* **135**, 153002
[3] M. Génévriez et al 2021 *Phys. Rev. A* **104**, 012812

P14

Characterization of a Zeeman slower and a magnetooptical trap for ultracold Ca Rydberg physics

E. Marin-Bujedo[1], J. A. L. Grondin[1,2], T. Schiltz[1], T. Corbo[1], X. Urbain[1], and M. Génévriez[1]

[1] *Université Catholique de Louvain, Institute of Condensed Matter and Nanosciences, Chemin du Cyclotron 2, 1348 Louvain la Neuve, Belgium*

[2] *Katholieke Universiteit Leuven, Instituut voor Kern- en Stralingsfysica, Celestijnenlaan 200, 3001 Heverlee, Belgium*

Cold atoms are a cornerstone in any experimental atomic physics lab, since the low temperatures imply low motion of the atoms, or equivalently, higher control over them. Magneto-optical traps allow the routine preparation of samples of cold atoms for groundbreaking applications such as metrology[1], ultracold chemistry [2], the study of Bose-Einstein condensates [3], or quantum information [4].

The experimental sequence begins with a custom oven operating at approximately 500 °C, which evaporates solid calcium to emit a collimated atomic beam with a most probable velocity of 720 m/s. To bridge the gap between these high thermal speeds and the capture velocity of a magneto-optical trap (MOT), the beam is directed through a passive Zeeman slower. Utilizing a Halbach configuration of permanent magnets, this stage efficiently decelerates the atoms to 30 m/s without the need for external power or water cooling. These slowed atoms are then captured in the MOT, where they are cooled and trapped. Our results demonstrate state-of-the-art performance for a Ca MOT without repumping lasers, achieving a trapped population of 10^6 atoms with a density of 10^8 cm^{-3} , at a temperature of 1.0(3) mK, for a trapping lifetime of 16(2) ms.

To explore Rydberg physics within this cold sample, the setup employs a three-photon resonant excitation scheme: $4s^2\ {}^1S_0 \rightarrow 4s4p\ {}^1P_1 \rightarrow 4s4d\ {}^1D_2 \rightarrow 4sn\ell$. A segmented electrode stack is positioned at the center of the MOT chamber, and allows the application of precise continuous and pulsed electric fields. These electrodes enable the compensation of stray fields, the manipulation of states within the Stark manifold, and the pulsed-field ionization of the Rydberg atoms. The resulting ions are then guided toward a channel electron multiplier for high-sensitivity detection. The successful acquisition of calcium Rydberg spectra confirms the suitability of this platform for further research in ultracold Rydberg gases.

[1] R. Elvin, *et al*., "Cold-atom clock based on a diffractive optic", 2019 *Opt. Express* **27**, 38359-38366

[2] R. Brianna, *et al*., "Low-Temperature Kinetics and Dynamics with Coulomb Crystals". 2015 *Annual Review Physical Chemistry*, **66**, 475-495

[3] M. H. Anderson, *et al*. , "Observation of Bose-Einstein Condensation in a Dilute Atomic Vapor", 1995 *Science*, **269**, 198-201

[4] F. Schäfer, *et al.,* "Tools for quantum simulation with ultracold atoms in optical lattices", 2020 *Nat Rev Phys* **2**, 411–425

P15

Bio-inspired optimization of infrared absorbers

A. Marchand[1], K. Delmote[2], O. Deparis[2], and S. R. Mouchet[1,2,3,4]

[1]*Micro- and Nanophotonic Materials Group, Research Institute for Materials Science and Engineering, University of Mons, Mons, 7000, Belgium*
[2]*Department of Physics and Namur Institute of Structured Matter (NISM), University of Namur, Namur, 5000, Belgium*
[3]*Department of Physics and Astronomy, University of Exeter, Exeter, EX4 4Q, United Kingdom*
[4]*Institute of Life, Earth and Environment (ILEE), University of Namur, Namur, 5000, Belgium*

The control of thermal radiation is fundamental for the survival of many organisms, especially those lacking internal thermoregulatory systems. In this context, nature offers a wide array of elegant strategies for infrared management, shaped by millions of years of evolution that have led to highly specialized structures that optimize the absorption, emission, or reflection of thermal radiation [1, 2].

This research takes inspiration from species such as *Troides magellanus*, the Magellan Birdwing, which can regulate the absorption of infrared radiation through the structural design of its wings [3, 4]. In these cold-blooded animals, the link between wing morphology and optical properties results in highly efficient thermal radiation absorption.

Recent advances in bioinspired materials science have enabled the translation of natural strategies into engineered systems capable of efficiently optimizing infrared radiation absorption. By mimicking and adapting these naturally occurring architectures, it becomes possible to design advanced functional materials with radiative properties [2, 4]. This approach highlights the potential of natural systems as a source of design concepts for the development of innovative solutions in thermal management.

This contribution explores the interdisciplinary potential of bioinspired approaches linking biology, physics, and materials engineering. These concepts have applications across various sectors where the demand for thermal radiation management and absorption continues to grow. Overall, the study demonstrates how nature's innovation, when analyzed and adapted, can enable sustainable and high-performance solutions for modern engineering challenges.

[1] Mouchet SR, Deparis O 2021 Natural Photonics and Bioinspiration, Artech House: Boston, MA, USA; London, UK
[2] Mouchet SR 2025 *J. Roy. Soc. Interface* **22(223)** 20240284
[3] Herman A, Vandenbem C, Deparis O, Simonis P, Vigneron J-P 2011 *Proc. of SPIE* **8094** 80940H
[4] Delmote K, Marchand A, Deparis O, Mouchet SR 2026 *Proc. of SPIE* **14076** 14076-105

P16

Polonium-containing molecules in MYRRHA

J. Scheerlinck[1,2] and S. Cottenier[1,2]

[1]*Department of Electromechanical, Systems and Metal Engineering, Ghent University, Ghent, 9052, Belgium*

[2]*Center for Molecular Modeling, Ghent University, Ghent, 9052, Belgium*

MYRRHA, a next-generation nuclear fission reactor, produces the radiotoxic isotope ^{210}Po as a by-product of reactions involving Pb–Bi liquid metal coolant. Under reactor conditions, polonium may form volatile species such as (Bi)Po(Pb)O_xH_y, which pose a potential safety risk. The identification and characterization of these molecules remains experimentally challenging, motivating the use of advanced computational methods.

In this work, we combine multireference wavefunction methods (CASSCF/MS-CASPT2) with spin–orbit coupling via the SO-CASSI approach to investigate heavy-element systems relevant to MYRRHA. A key challenge in such calculations is the selection of an appropriate complete active space (CAS), which traditionally relies on chemical intuition and manual tuning. To address this, we implement and extend the automated active space selection tool *auto*CAS [1] for heavy-element applications. This required modifications to the underlying Serenity quantum chemistry code [2,3], including expanded basis infrastructure and numerical stabilization of intrinsic bond orbital localization for elements beyond $Z = 36$.

Initial benchmarks on the diatomic systems Po_2, Pb_2, and Te_2 demonstrate that the automated workflow reproduces experimental dissociation energies within 5–10 meV (computed D_e compared to experimental D_0, without ZPE correction). For TeO, the computed D_e of 4.50 eV overestimates the experimental reference of $\leq$3.90 eV by approximately 600 meV; this experimental value is an upper bound rather than a directly measured dissociation energy, so the true discrepancy may be larger. For PbO, the active space selection remains unreliable due to numerical instabilities, and results are preliminary.

Ongoing work focuses on improving the robustness of the active space selection across a broader class of heavy-element molecules and extending the pipeline to open-shell species. Ultimately, this will enable systematic computational screening of polonium-containing molecules, contributing to the design of targeted filtration strategies in MYRRHA.

[1] Stein C J and Reiher M 2017 *arXiv preprint* arXiv:1702.00450
[2] Unsleber J P, Dresselhaus T, Klahr K, Schnieders D, Böckers M, Barton D and Neugebauer J 2018 *J. Comput. Chem.* **39** 788
[3] Niemeyer N, Eschenbach P, Bensberg M, Tölle J, Hellmann L, Lampe L, Massolle A, Rikus A, Schnieders D, Unsleber J P and Neugebauer J 2023 *Wiley Interdiscip. Rev. Comput. Mol. Sci.* **13** e1647

Size-Dependent CO_2 Reduction by C_{60}-Supported Vanadium Cationic Clusters

B. J. B. Smeets[1], H. Jiang[1], Y. Zhang[1], G.-L. Hou[2], P. Lievens[1], and E. Janssens[1]

[1]*KU Leuven, Quantum Solid-State Physics, Dept. of Physics and Astronomy, Celestijnenlaan 200D box 2412, 3001 Leuven, Belgium*
[2] *School of Physics, Xi'an Jiaotong University, Xi'an, 710049 Shaanxi, People's Republic of China*

The conversion of CO_2 into useful fuels and chemicals represents an attractive strategy to mitigate emissions and lower our environmental footprint. Achieving this goal relies on the development of catalysts that feature high activity, selectivity and stability. Gas-phase experiments offer a unique environment that allows the investigation of these desired properties via isolated cluster model systems [1].

While isolated V^+ cations are known to form large $V(CO_2)_n^+$ clusters without undergoing reduction [2], the presence of a C_{60} fullerene support has previously been shown to have a critical role on V^+ single atom catalysts for water splitting [3]. Here, we investigate the influence of C_{60}, as a gas-phase model for a carbon support, on the CO_2 reduction capability of V_n^+ (n = 1–8) clusters. The $C_{60}V_n^+$ clusters were produced using a double-laser ablation source and their reactivity was probed by introducing controlled CO_2 pressures in a few-collisions reaction cell, followed by analysis using time-of-flight mass spectrometry.

The resulting pressure-dependent reaction profiles reveal pronounced size-dependent effects: CO_2 reduction is observed for $C_{60}V_1^+$ and $C_{60}V_3^+$ producing $C_{60}V_{1,3}O^+$, whereas the other cluster sizes show only CO_2 adsorption (Figure 1). Complementary measurements on bare $V_{1,3}^+$ clusters confirm that no reduction occurs in absence of the C_{60} support, demonstrating that C_{60} plays a crucial role in promoting CO_2 reduction and enhancing the reaction kinetics.

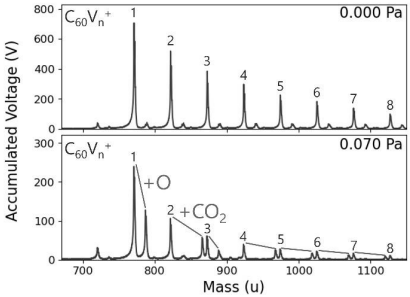

Figure 1: Two mass spectra of $C_{60}V_n^+$ clusters at 0.000 Pa and 0.070 Pa of CO_2-pressure in the collision cell. The difference between the two spectra indicate the products from the clusters reacting with CO_2, indicating a striking size-dependence between $C_{60}V_{1,3}^+$ and the other clusters.

[1] Vanbuel J., Ferrari P. and Janssens E. 2020 *Adv. Phys.:X.* **5**(1), 1754132
[2] Ricks A. M., Brathwaite A. D. and Duncan M. A. 2013 *J. Phys. Chem. A.* **117**(45), 11490– 11498
[3] Hou G.-L. et al. 2021 Angew. Chem. Int. Ed. **60**(52), 27095–27101

P18

Design and implementation of an experimental setup to measure complex weak values

Meetsinh Thakor[1], and Yves Caudano [1]

[1] *Physics Department, naXys and NISM, University of Namur, Rue de Bruxelles 61, 5000 Namur, Belgium*

The weak value was introduced in 1988 by Aharonov, Albert, and Vaidman [1] as a "New kind of value for a quantum variable" [2] that appears when averaging pre-selected and post-selected weak measurements. The weak value is a complex quantity. To determine the weak value in an optical experiment, we need to measure both the real and complex parts [3]. The setup confers precise control over the pre- and post-selected states, enabling the amplification of anomalous weak values in weak measurements. Such high-precision measurements have important applications in metrology, quantum sensing, and fundamental physics.

Using a specialized filtering technique, a clear Gaussian beam is generated from the collimated laser beam. The pre- and post-selected states are determined using polarizers, quarter-wave plates (QWPs), and half-wave plates (HWPs). Additionally, weak interaction is achieved using a birefringent material such as a quartz or calcite crystal. To measure the real and complex parts of a weak value, different setups of the optical lenses were used. A CCD image sensor serves as the detector.

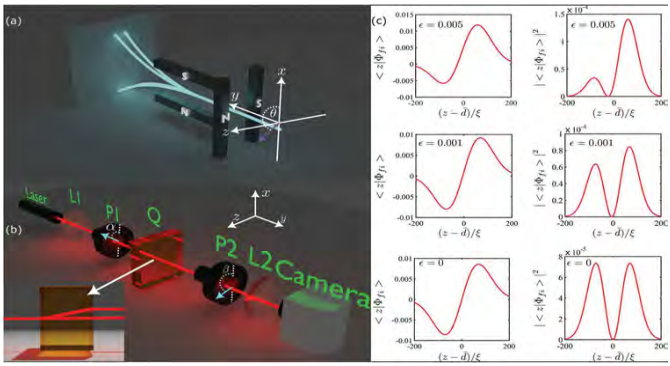

Figure 1: Understanding the post-selected weak measurement. a) A double Stern–Gerlach setup for implementing post-selected weak measurement. b) Optical setup with a weak birefringent crystal for realizing weak measurement. c) Post-selected field (probability amplitude) and intensity (probability) distribution in z-coordinate with changing post-selection parameter ϵ. The intensity profiles demonstrate centroid shifts of the post-selected meters. [**3**]

[1] Aharonov, Y., D. Z. Albert, L. Vaidman. (1988) Phys. Rev. Lett. 60, 1351–1354.
[2] Dressel, J *et al* (2014) Reviews of Modern Physics, 86(1), pp. 307–316.
[3] Dhara, R.*et al* (2025) Adv. Phys. Res. 2400136

P19

Strain effects on light-matter coupling and exciton trapping in monolayer TMDs

M. Van Hoorebeke[1], P. Manivannan[2], C. Sevik[2] and M. Wouters[1]

[1]*Theory of Quantum systems and Complex systems, Universiteit Antwerpen, Antwerp, 2610, Belgium*
[2]*Computational Materials Modeling for Nanoscience and Innovative Technologies, Universiteit Antwerpen, Antwerp, 2610, Belgium*

In recent years, 2D Transition metal dichalcogenides (TMD) have emerged as a promising platform to study strongly correlated excitonic physics and hybrid light-matter systems. These materials host strongly bound intralayer and interlayer excitons with advantageous properties like large exciton binding energy, long lifetime and strong oscillator strength, which can all be tuned by pressure (strain), electric fields and in the bilayer case by twisting the layers (moiré). Embedding such TMD materials in an optical microcavity allows for the formation of hybrid light-matter quasiparticles called exciton-polaritons, which inherit properties from both their excitonic and photonic components.

The effects of these tuning parameters are well-understood for excitons, but their hybridization with light in TMD materials has not been fully investigated yet. Here we examine the effects of tensile strain on the light-matter (Rabi) coupling in TMD monolayers and consider strain-induced nanobubbles as exciton trapping potentials [1]. To investigate the effect on the light-matter coupling, we employ the transfer matrix formalism to describe the optical properties of these 2D materials from Maxwell equations. Our approach combines a classical calculation of the transfer matrix, describing the dielectric structure of the microcavity, with quantum input from density functional theory (DFT) [2].

We show that the influence of strain on the light-matter coupling is limited, consistent with the binding energy showing little variation under strain. Our study of the effects of strain on exciton–polariton properties, such as light–matter coupling and exciton trapping, contributes to a systematic characterization of TMD tuning parameters in polariton microcavities, providing an overview of competing single-particle effects as a foundation for enhancing polariton interactions.

[1] Gastaldo M et al. 2023 *2D Mater. Appl.* ***7*** *71*
[2] Sevik C et al. M arXiv:2601.08585

P20

Fragmentation temperature of 1D and 3D quantum droplets in a BEC mixture

J. Van Loock[1], D. Ahmed-Braun[1], and J. Tempere[1]

[1]*TQC, Universiteit Antwerpen, Antwerpen, 2610, Belgium*

In a mixture of two Bose-Einstein condensates, the interactions can be tuned such that self-bound objects called quantum droplets appear [1, 2]. Whereas the ground states of such quantum droplets at finite temperature have been studied for three- and one-dimensional configurations, the possible fragmentation of these droplets has so far not been considered in these studies [3-6]. In this work we show that droplets can lower their free energy by splitting or fragmenting in a combination of multiple smaller droplets and/or a gas [7]. Three-dimensional droplets will split when the interspecies interaction strength is considerably stronger than the intraspecies interaction strength, and the number of atoms is of the same order as the minimum number of atoms necessary to form a droplet. One-dimensional droplets will fragment as long as the intraspecies and interspecies interactions strength do not vary too much in strength and the density is not to big compared with the scattering length. If the temperature rises, 1D droplets will split by expelling atoms, forming a gas of predominantly free atoms and pairs of atoms. These pairs remain present in the system up to considerably high temperatures compared to the transition temperature. Our results provide important insights on the stability of these droplets.

[1] Petrov, D. S. *Phys. Rev. Lett.* **115**, 155302 (2015)
[2] Petrov, D. S. & Astrakharchik, G. E. *Phys. Rev. Lett.* **117**, 100401 (2016)
[3] Guebli, N. & Boudjemâa, A. *Phys. Rev. A* **104**, 023310 (2021)
[4] Ota, M. & Astrakharchik, G. *SciPost Phys.* **9**, 020 (2020)
[5] Wang, J., Hu, H. & Liu, X.-J. New J. Phys. **22**, 103044 (2020)
[6] Boudjemâa, A. & Abbas, K. *New J. Phys.* **25**, 093052 (2023)
[7] Van Loock, J., Ahmed-Braun, D. & Tempere, J. *J Low Temp Phys* **222**, 73 (2026)

P21

Multi-laser stabilization system for ultracold-Rydberg-atom and precision-spectroscopy experiments

N. Vlekken[1], L. Janssens[1], V. Garzone[1], A. Lorvelec[1], M. Génévriez[1]

[1]*Université Catholique de Louvain, Louvain-la-Neuve, 1348, Belgium*

Ultracold-Rydberg-atom and precision-spectroscopy experiments often require multiple lasers that need to be frequency stabilized to reach the desired precision and efficiency of these types of experiments. The cost and complexity of the equipment needed for the different laser stabilization techniques in these multi-laser setups can ramp up quite fast. Multiple open-source FPGA development boards from Red Pitaya together with a modified open-source lockbox software package called PyRPL [1] are used to design a laser stabilization system based on Fabry-Pérot (FP) cavities that can implement different stabilization techniques in a compact, scalable and cost-efficient way.

I will describe the architecture of the system implemented in our lab to stabilize up to nine lasers simultaneously. The setup relies on the transfer of the stability of lasers locked to atomic references (Rb, Cs, Ca) to other lasers operated at different frequencies using FP cavities. This stability transfer is done with two techniques: scanning transfer cavity locking [2] and the Pound-Drever-Hall technique [3]. In each stabilization technique, the Red Pitaya plays a central role in the stabilization feedback loop: generating the error signals and modulation signals and driving the piezoelectric actuators of the FP cavities. Additionally, frequency-modulationbased laser locking is implemented using an acousto-optic modulator (AOM) for frequency modulation instead of the usual electro-optic modulators (EOMs) or modulation of the laser current/piezo voltage. The multi-laser stabilization system based on the open-source Red Pitaya boards can easily be adapted to match the specific needs of an experiment while being compact and cost-efficient.

[1] Neuhaus, L., Croquette, M., Metzdorff, R., Chua, S., Jacquet, P.-E., Journeaux, A., Heidmann, A., Briant, T., Jacqmin, T., Cohadon, P.-F., and Deléglise, S. (2024). Python Red Pitaya Lockbox (PyRPL): An open source software package for digital feedback control in quantum optics experiments. *Rev. Sci. Instrum.* **95**(3), 033003
[2] Pultinevicius, E., Rockenhäuser, M., Kogel, F., Groß, P., Garg, T., Prochnow, O. E., and Langen, T. (2023). A scalable scanning transfer cavity laser stabilization scheme based on the Red Pitaya STEMlab platform. *Rev. Sci. Instrum.* **94**(10), 103004
[3] Drever, R. W. P., Hall, J. L., Kowalski, F. V., Hough, J., Ford, G. M., Munley, A. J., and Ward, H. (1983). Laser phase and frequency stabilization using an optical resonator. *Appl. Phys. B – Photophys. Laser Chem.* **31**(2), 97–105

P22

From Symmetry to Stability: Structural and Electronic Transformation in Cs_2KInI_6

Mohammad Bakhsh,[1] Victor Trinquet,[1] Rogério Almeida Gouvêa,[1] Gian-Marco Rignanese,[1, 2] and Samuel Poncé[1, 2]

[1]*UCLouvain, Institute of Condensed Matter and Nanosciences (IMCN), Chemin des Étoiles 8, B-1348 Louvain-la-Neuve, Belgium.*

[2]*WEL Research Institute, avenue Pasteur 6, 1300 Wavre, Belgium.*

Cs_2KInI_6 is a promising lead-free halide double perovskite with a calculated direct band gap of 1.24 eV, ideal for solar cell applications. Our first-principles calculations reveal that its cubic phase ($Fm\bar{3}m$) is dynamically unstable. Using an accelerated machine learning approach, we identify 42 dynamically stable structures and further validate these findings using first-principles calculations on 11 of these. The most stable phase has $Cmc2_1$ symmetry with 20 atoms/unit cell. It lies 41.9 meV/atom below the cubic reference but lacks octahedral cation coordination. The most stable perovskite-like structure has $P\bar{3}$ symmetry with 10 atoms/unit cell and low octahedral connectivity. Structure-property trade-offs are highlighted, with calculated distortions generally widening the band gap, shifting it from direct to indirect, and flattening the band edges. This work showcases the synergy of genetic algorithms, machine-learned potentials, and first-principles validation for discovering stable materials.

P23

The Colour of Radiation: Developing a Photochromic Indicator for Dual-Mode UV Index Monitoring and Personal X-ray Dosimetry

E. Bossuyt[1], W. Hu[1], H. Vrielinck[1,*], and D. Poelman[1,*]

[1]*LumiLab, Department of Solid-State Science, Ghent University, 9000 Ghent, Belgium*

[*] Corresponding authors: Henk.Vrielinck@UGent.be, Dirk.Poelman@UGent.be

Photochromic rare-earth niobates offer a passive, visually readable approach to radiation dosimetry [1-3]. This work investigates photochromic $LaNbO_4:Pr^{3+},Er^{3+}$ (LNPE) and $GdNbO_4:Pr^{3+},Er^{3+}$ (GNPE) ceramics synthesised by solid-state sintering at 1350 to 1550°C. Upon irradiation, colour centres are populated that absorb across visible light, causing the pellets to darken visibly and their reflectivity to decrease, as shown in Fig. 1a. LNPE showed a modest UV response (~11.4% normalised reflectivity decrease) but a stronger X-ray response (~28.6%), while GNPE responded strongly to both UV (~37.8%) and X-ray (~39.1%) radiation. Both samples could be returned to their original state both optically as well as thermally. Particularly notable is the sensitive UV response of GNPE: its darkening kinetics yielded a half-saturation dose D_{50} of ~1.97 J/cm² and a threshold exposure of ~1.16 J/cm², equivalent to less than 4 minutes on a cloudy day (UVI 2) (Fig. 1b). Upconversion (UCL) and downconversion (DCL) luminescence were tracked as a function of accumulated dose, establishing a dual-mode readout that exploits both photochromic colouration and luminescence modulation from the same pellet[1]. Radiation-induced paramagnetic defects identified by Q-band and X-band EPR spectroscopy confirm the formation of hole and electron centres in both hosts. As a proof of concept, camera-based colour calculation software was developed, enabling practical dose estimation from a single smartphone photograph of the irradiated pellet. For this purpose, indicator cards were used, as shown in Fig. 1c.

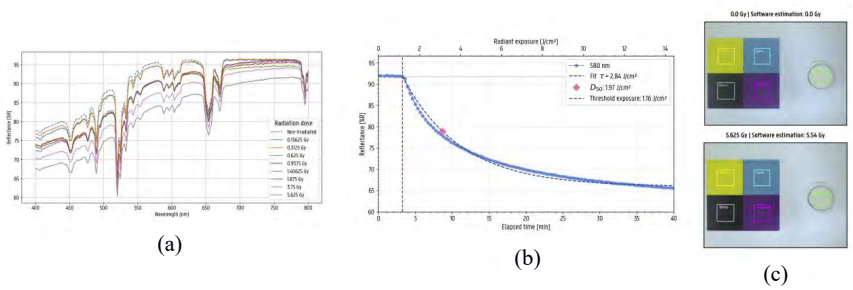

(a) (b) (c)

Figure 1: (a) Reflection spectra of GNPE upon X-ray radiation. (b) Darkening kinetics of GNPE upon UV radiation. (c) Indicator card with GNPE before (top) and after (bottom) X-ray radiation.

[1] R. Kuang, H. Lian, M. Gao, Y. Zhu, S. Gu, L. Shen, X. Lin, L. Huang, C.-G. Ma, A. Suchocki, Y. Zhydachevskyy, B.-M. Liu, and J. Wang, ACS Materials Letters, vol. 7, no. 3, pp. 820–828, 2025.
[2] P. Remya Mohan, E. Sreeja, A. Jose, T. Krishnapriya, C. Joseph, and P. R. Biju, Solid State Communications, vol. 401, p. 115937, 2025.
[3] Y. Suemune, Japanese Journal of Applied Physics, vol. 23, no. 2R, p. 253, feb 1984.

P24

Radio-photoluminescence in Eu activated $M_3(PO_4)_2$ (M = Sr, Ba)

E. Botterman[1,2], P. F. Smet[1], D. Van der Heggen[1], and H. Vrielinck[2]

[1] *Ghent University, Dept. Solid State Sciences, LumiLab, Gent, B-9000, Belgium*
[2] *Ghent University, Dept. Solid State Sciences, Defects in SemiConductors, Gent, B-9000, Belgium*

$Ba_3(PO_4)_2$ doped with Eu^{3+} undergoes a change in photoluminescence (PL) emission color from red to violet after irradiation with short-wavelength UV [1] or X-ray radiation [2]. This so-called radio-photoluminescence (RPL) effect is the result of stable electron trapping by part of the red-emitting Eu^{3+} ions, to form violet emitting Eu^{2+}. Consequently, $Ba_3(PO_4)_2$:Eu^{3+} can be used as a UV or X-ray radiation dosimeter, with the Eu^{2+}/Eu^{3+} PL intensity ratio as a self-calibrated dose response signal (see Figure 1). Even though the basic mechanism behind this RPL effect is easily understood, it still holds many mysteries. Only a fraction of the Eu^{3+} doped into the phosphor can undergo a stable photoreduction to Eu^{2+}. Although Eu^{3+} is present in multiple sites, stable electron trapping preferentially occurs at only one of the sites. The phosphor also exhibits intense, Eu^{2+}-related direct radioluminescence, that does not grow stronger with irradiation time, and even at radiation doses where hardly any stable Eu^{2+} formation has taken place, suggesting that Eu^{2+} also acts as a recombination center.

The aim of this study is to understand the limited RPL activity of Eu in this phosphor and to determine the sites in which Eu^{3+} and Eu^{2+} can be stabilized. To this end, Eu^{2+} and Eu^{3+} doped $Ba_3(PO_4)_2$ and structurally related $Sr_3(PO_4)_2$ were studied with PL, electron paramagnetic resonance (EPR) and scanning electron microscopy (SEM) coupled to energy dispersive X-ray spectroscopy (EDX) and cathodoluminescence (CL). Since Eu^{3+} is non-paramagnetic ($^7F_0$ ground state), we used Gd^{3+}, with the same electronic ground state as Eu^{2+} ($^8S_{7/2}$) and an ionic radius nearly identical to Eu^{3+} as a probe ion to study the structural diversity of the trivalent rare earth ion incorporation sites with EPR.

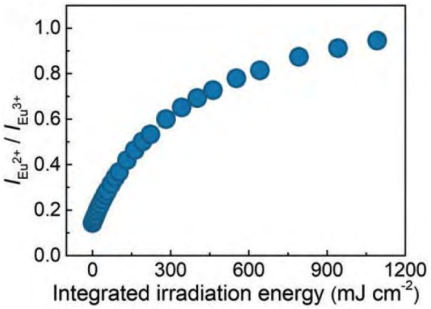

Figure 1: Eu^{2+}/Eu^{3+} PL intensity ratio of $Ba_{2.99}Eu_{0.01}(PO_4)_2$ under 365 nm LED excitation, as a function of UV irradiation dose (in mJ/cm^2) with a broadband UV light source (~250 – 350 nm) [1].

[1] Yang ZT *et al.* 2023 *Adv. Opt. Mater.* **11** 2300733
[2] Vrielinck H *et al.* 2026 *Molecules* **31** 1045

P25

Spectral and Polarization Control of Smith-Purcell Radiation via Chiral Dielectric Gratings

L. Cavenaile[1], T. Delplace[1], M. G. Abebe[1] and B. Maes[1]

[1]*Micro- and Nanophotonics Materials Group, Research Institute for Materials Science and Engineering, University of Mons, Place du Parc 20, 7000 Mons, Belgium*

The interaction between free electrons and periodic photonic structures enables the generation of tunable electromagnetic radiation, known as the Smith-Purcell (SP) effect [1]. This mechanism is fundamental for developing compact and novel light sources, e.g., in terahertz and X-Ray regimes. While initial designs relied on metallic gratings, recent advancements have shifted towards high-index dielectric structures. These offer lower losses and support resonances with high quality factors, allowing for maximal photon emission and optimized energy loss [2].

Current research focuses on tailoring these resonances to control the emission properties. Recent works have explored anomalous Doppler effects [3] and utilized geometric symmetry breaking, such as glide symmetry in coupled gratings, to direct radiation into specific halfspaces [4]. However, a persistent limitation in conventional two-dimensional (2D) SP devices is the polarization constraint: the electron beam naturally couples to Transverse Magnetic (TM) modes, leaving Transverse Electric (TE) modes largely inaccessible in standard 2D achiral models.

To overcome this limitation, we investigate the introduction of constitutive symmetry breaking via chirality [5]. Magneto-electric coupling in chiral (Pasteur) media is known to mix electric and magnetic dipoles, potentially allowing an electric source to excite TE modes [6]. In this work, we present both a theoretical framework and numerical demonstrations of a SP source combining a chiral layer (n = 1.4) with a silicon (Si) grating separated from a Si substrate. We develop a Coupled-Mode Theory (CMT) framework [7] to phenomenologically describe the mode hybridization and cross-polarization dynamics induced by the chiral environment. These analytical insights are corroborated by full-wave frequency-domain simulations. We demonstrate that the optical activity of the medium enables the excitation of a high-Q, TEpolarized resonance confined within the Si teeth, a mode strictly forbidden in standard achiral counterparts. By merging CMT models with rigorous numerical validation, this approach offers a robust new degree of freedom for wavelength and polarization shaping in free-electron photonics.

Acknowledgment: This work was supported by the FRS-FNRS.

[1] S. J. Smith and E. M. Purcell, “Visible Light from Localized Surface Charges Moving across a Grating”, 1953 *Phys Rev* **92**, 1069

[2] Y. Yang et al., “Maximal spontaneous photon emission and energy loss from free electrons”, 2018 *Nature Phys* **14** (9), 894

[3] X. Zhang et al., “Electron-beam-driven anomalous Doppler effects in Smith–Purcell radiation”, 2024 *Photonics Res* **12**(1), 78

[4] T. Delplace, I. Bouanati, G. Rosolen, and B. Maes, “Directional Smith-Purcell radiation via coupled high-index gratings”, 2026 *Optics Exp* **34**, 2450

[5] D. L. Jaggard, A. R. Mickelson, and C. H. Papas, “On electromagnetic waves in chiral media”, 1979 *Appl Phys* **18**(2), 211

[6] H.-Y. Wu and F. Vollmer, “Coherent multipolar amplification of chiroptical scattering and absorption from a magnetoelectric nanoparticle”, 2023 *Comm Phys* **6**, 251

[7] W. Suh, Z. Wang, and S. Fan, "Temporal coupled-mode theory and the presence of non-orthogonal modes in lossless multimode cavities", 2004 *IEEE J Quant Elec* **40**(10), 1511

P26

Advancing Solar Energy Conversion via 2D Heterostructures: Mechanistic Insights into Type-II and Z-scheme Charge Dynamics

Khawla Chaoui[1], Luc Henrard[1], Warda Elaggoune[2], Mohamed Achehboune[1,3]

[1]*Department of Physics, Institute of Structured Matter (NISM), University of Namur, Rue de Bruxelles 61, 5000, Namur, Belgium.*
[2]*Laboratoire de Physique des Matériaux (L2PM), Université 8 Mai 1945, BP 401, Guelma, Algeria.*
[3]*School of Applied and Engineering Physics, University Mohammed VI Polytechnic, Ben Guerir, 43150, Morocco*

The pursuit of high efficiency sustainable energy technologies has positioned two-dimensional (2D) heterostructures as frontline candidates for next-generation photovoltaics and photocatalytic water splitting. By exploiting their unique electronic coupling and large surface areas, these materials offer an unparalleled platform for optimizing solar-to-fuel and solar-to-electricity conversion.

This study systematically explores the mechanistic advantages of Type-II and Z-scheme band alignments in orchestrating carrier transport. While Type-II heterojunctions promote effective spatial separation of electrons and holes significantly reducing recombination rates and boost photovoltaic performance—the Z-scheme architecture provides a sophisticated route to emulate natural photosynthesis. This latter mechanism is particularly vital for maintaining the strong redox drive required for efficient hydrogen evolution.

Our analysis, supported by first-principles investigations, highlights two exemplary systems: the InN/PtSSe heterostructure, which leverages a third-generation Z-scheme for overall water splitting [1], and the BAs/GeC van der Waals heterostructure, where a Z-scheme configuration enables superior solar cell efficiency [2]. Collectively, these findings provide a theoretical roadmap for the rational design of 2D-based energy systems, emphasizing how band-edge engineering can overcome the kinetic bottlenecks of charge recombination.

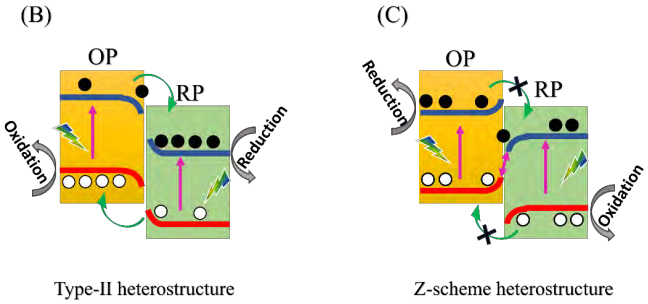

Figure 1: Comparative band alignment and carrier dynamics: Conventional Type-II vs. Z-scheme for water splitting and photovoltaics.

[1] Chaoui, K., Hamidani, A., & Zanat, K. (2025). International Journal of Hydrogen Energy, 174, 151360.
[2] Chaoui, K., Zanat, K., Elaggoune, W., Henrard, L., & Achehboune, M. (2024). RSC advances, 14(53), 39625-39635.

P27

Investigation of growth-related mechanisms of (100)-(2x1):H diamond by means of first principles calculations

E. Y. Guillaume[1,2,3,4], D. E. P. Vanpoucke[3,4], L. Henrard[1] and K. Haenen[2,4]

[1]*University of Namur, Namur Institute of Structured Matter (NISM), Rue de Bruxelles 61, 5000 Namur, Belgium*
[2]*Hasselt University, Institute for Materials Research (IUMAT), Wide Band Gap Materials group (WBGM), Martelarenlaan 42, 3500 Hasselt, Belgium*
[3]*Hasselt University, IUMAT, Quantum and Artificial inTelligence design Of Materials (QuATOMs), Martelarenlaan 42, 3500 Hasselt, Belgium*
[4]*imec, IUMAT, Wetenschapspark 1, 3590 Diepenbeek, Belgium*

Radical attack and recombination are thought to play an important role in the atomic-scale mechanisms driving the growth of diamond. This work presents an analysis of the reactions involving hydrogen and methyl radicals on a (100) H-passivated diamond surfaces. In more detail, the reactions we investigate include migration of a lone hydrogen on a non-passivated surface, migration of single and double vacancies on a H-passivated surface, along with the study of the growth steps that creates a nucleation seed on the surface. To provide an even bigger picture of the growth, we identified an ensemble of reactions that can etch the said seed.

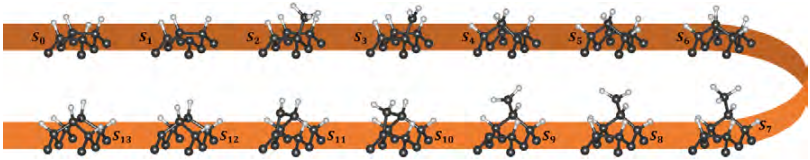

Reaction rates are computed through variational transition state theory, using density functional theory and the climbing Nudged Elastic Band method to accurately determine the energy, geometry, and vibrational spectrum of transition states, irrespective of a tight or loose transition state. Our results highlight that accounting for van der Waals interaction and spin-polarisation is crucial to assess the relative likelihood of the different mechanisms studied here.

$$k(T) = \kappa(\nu^{TS}, E^{TS}) \left(\frac{k_B T}{\hbar}\right) \frac{Q^{*TS}(T)}{Q^{I}(T)} \exp\left(-\frac{[E^{TS} - E^{I}]}{k_B T}\right)$$

$$k(T) = \min_{r \in \mathrm{MEP}} \left\{ \left(\frac{k_B T}{\hbar}\right) \frac{Q^{*TS}(T)}{Q^{I}(T)} \exp\left(-\frac{[E^{TS} - E^{I}]}{k_B T}\right) \right\}$$

Using multi-scale methods (e.g., kinetic Monte-Carlo), these reaction rates have great potential to provide insights into the best conditions to grow single crystal diamond at how temperature, pressure, and radical densities in the reactor influence both the rate and quality of the growth. The approach used in this work can be generalised to other semi-conductor surfaces or crystallographic orientations of diamond.

[1] L. Oberg *et al.*, "Studies of Carbon Incorporation on the Diamond {100} Surface during Chemical Vapor Deposition using Density Functional Theory", J. Phys. Chem. A, vol. 112, No. 45, pp. 11436–11448, 2008.

[2] A. Cheesman *et al.*, "Nitrogen overgrowth as a catalytic mechanism during diamond chemical vapour deposition", Carbon, vol. 178, pp. 606-615, 2021

[3] E. Y. Guillaume *et al.*, "Hydrogen migrations and desorptions on (100)-(2x1):H diamond surfaces", *in review.*

[4] E. Y. Guillaume *et al.*, "Nucleation mechanisms on (100)-2x1:H diamond surfaces", *in preparation.*

P28

Fast-evolving Photochromism in Inorganic Photochromic Materials

W. Hu[1], D. Van der Heggen[1], E. Bossuyt[1], D. Poelman[1,*], P. F. Smet[1,*]

[1]*LumiLab, Department of Solid-State Science, Ghent University, 9000 Ghent, Belgium*

Photochromism typically refers to a reflectance or absorption change (body color change) under or after various radiations. With this merit, they have been used in direct indicator or dosimeter. During an in-depth investigation of these photochromic materials, we observed that many of them undergo rapid bleaching within a few seconds after charging at RT[1]. In some cases, one the absorption bands induced by charging can be bleached fully at a certain temperature, leading to an evolution of the photochromic color. These findings motivated us to further investigate the rapidly evolving photochromic behavior. We therefore designed an in situ time-resolved diffuse reflectance spectroscopy (DRS) setup to study this behavior under different optical stimuli at various temperatures (**Figure 1**). In this work, we successfully elucidate how light and thermal effects influence the rapid evolution of photochromism in LiNbO3:Bi across different temperatures. This work also provides guidelines and strategies for the systematic evaluation of photochromic materials with similar potentials.

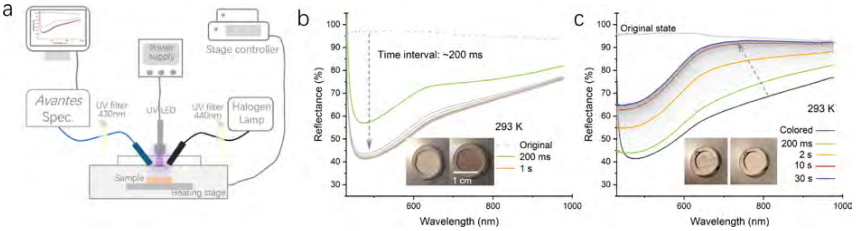

Figure 1: a) Schematic diagram of the home-built time-resolved DRS measurement setup. b) Time-resolved DRS spectra of LNO:Bi under 365 nm (~34 mW cm^{-2}) irradiation at 293 K. The insets are photographs of original state and colored state of LNO:Bi under ambient light. c) Time-resolved DRS spectra of bleaching process of colored LNO:Bi under 100% (~22 mW cm^{-2}, without any intentional attenuation) probe-light intensity at 293 K (the DRS curve of original LNO:Bi is also plotted in the graph as a reference).

[1] Y. Bao, W. Hu, Y. Zhou, et al. 2025 *Sci. China Mater*., **68**, 1064-1073.

P29

On the location of Cu^{2+} in TLD-100H

Eliot Janssens[1], Luana F. Nasciment [2], Philippe F. Smet[1], Henk Vrielinck[1]

[1]*Ghent University, Solid State Sciences, Krijgslaan 285-S1, 9000 Ghent, Belgium*
[2]*SCK CEN, Boeretang 200, 2400 Mol, Belgium*

TLD-100H, with composition LiF:Mg,Cu,P, is a well-established, highly sensitive thermoluminescence radiation detector used in personal dosimetry [1]. It has been established that all dopant elements need to be present in the right concentration to attain high radiation sensitivity [2]. However, the exact role of each dopant and the influence of the microstructure are not yet fully clarified [3,4].

LiF:Mg,Cu,P is known to exhibit an intense Cu^{2+}-related EPR spectrum at room temperature (see Figure 1) independent of the irradiation [3-5]. Its large linewidth and lack of hyperfine structure are indicative of magnetic interactions between Cu^{2+} ions. Further understanding of how Cu^{2+} is incorporated in the LiF lattice and the role of this center in the dosimetric response is still missing. In this work, by combining X- and Q-band EPR with scanning electron microscopy coupled to cathodoluminescence, we shed light on this puzzling situation.

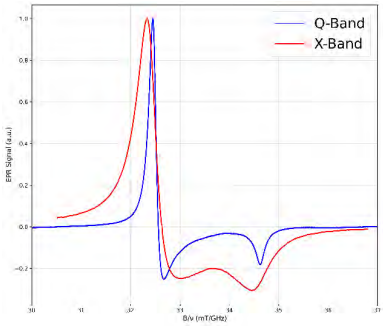

Figure 1: EPR Spectrum measured in X-Band at 9.806 GHz and Q-Band at 34.000 GHz. Both spectra are the same crushed TLD-100H dosimeter.

[1] L. A. DeWerd, J. R. Cameron, Wu Da Ke, T. Papini, and I. J. Das, "Characteristics of a new dosemeter material: LiF(Mg,Cu,P)," *Radiat. Prot. Dosim.*, **6**(1–4), 350–352, 1983. doi:10.1093/oxfordjournals.rpd.a082948.
[2] P. Bilski, M. Budzanowski, and P. Olko, "A systematic evaluation of the dependence of glow curve structure on the concentration of dopants in LiF:Mg,Cu,P," *Radiat. Prot. Dosim.*, **65**(1–4), 195–198, 1996.
[3] T. Gundurao and S. Moharil, "ESR study of phosphorus-related defects in irradiated LiF:Mg,Cu,P and related phosphors," *Radiat. Meas.*, **42**(1), 35–42, 2007.
[4] P. L. Guzzo, B. G. da Nóbrega, B. Obryk, V. S. de Barros, H. J. Khoury, and M. Klosowski, "EPR spectroscopy in LiF:Mg,Cu,P thermoluminescent powder samples irradiated with high gamma doses," *J. Lumin.*, **198**, 284–288, 2018.
[5] F. Sun, L. Jiao, J. Wu, Z. Yang, S. Yuan, and G. Dai, "X-ray diffraction and ESR studies on LiF:Mg,Cu,P phosphor," *Radiat. Prot. Dosim.*, **51**(3), 183–189, 1994.

P30

Tuning the catalytic performance of CO_2 methanolisation catalysts based on bimetallic Gas-phase Cu–Zn nanoparticles

Wenhao Ji [1], Imran Abbas[1], Didier Grandjean[1], Ewald Janssens[1]

[1] *Quantum Solid-State Physics, Department of Physics and Astronomy, KU Leuven, 3001 Leuven, Belgium*

Understanding how the initial structure of bimetallic nanoparticles governs their catalytic performance remains a challenge in nanoscience [1-3]. In this work, we use cluster beam deposition (CBD) to prepare $CuZnO_x$ model catalysts with similar size and composition but different oxidation levels to investigate how the gas-phase formation environment affects their initial structure, chemical state, and catalytic behavior in CO_2 hydrogenation to methanol.

$CuZnO_x$ nanoparticles were synthesized by laser ablation of a $Cu_{70}Zn_{30}$ alloy target using either pure He or 1% O_2/He as condensation gas. Both routes produced 2–4 nm nanoparticles, but with markedly different phases. After deposition on carbon paper, their catalytic behavior was evaluated in a home-made high-pressure flat microreactor under 40 bar in a $3H_2$:$1CO_2$ feed [4]. The sample prepared in 1% O_2/He showed about twice the methanol productivity of the sample prepared in pure He, while both retained similar methanol selectivity.

In situ STEM and grazing-incidence X-ray absorption spectroscopy reveal that these different initial states lead to distinct restructuring pathways under reaction conditions. $CuZnO_x$ nanoparticles prepared in He evolves metallic Cu nanoparticles partially covered by a disordered Cu–ZnO_x overlayer, whereas those prepared in 1% O_2/He are transformed into overlayer-free Cu metal nanoparticles, which contribute to the enhanced performance of the latter catalyst. These results demonstrate that CBD allows a fine tuning of the initial structure of bimetallic nanoparticles that plays a major role in controlling the dynamic Cu–Zn interactions under reaction and their catalytic performance, facilitating the identification of the active phases.

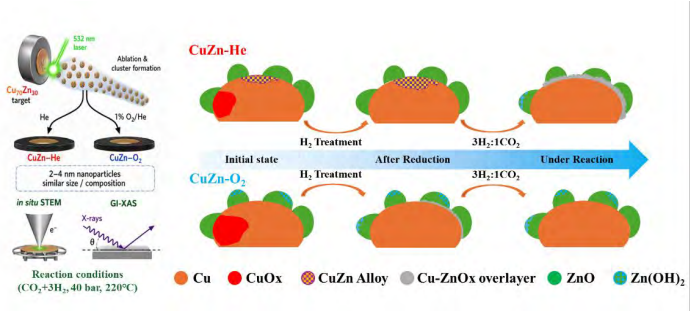

Figure 1: Gas-phase Cu–Zn Nanoparticle-based Catalysts Preparation, Characterization and Evolution under Reaction Conditions.

[1] Zhou H *et al* 2023 *JACS Au* **3**
[2] Mammen M *et al* 2023 *J. Phys. Chem. C* **127**
[3] Zabilskiy M *et al* 2020 *Nat. Commun.* **11** 2409
[4] Abbas I *et al* 2025 *Chem. Eng. J.* **503** 158127

P31

Absorption Enhancement in Hybrid Au-TiO_2 Nanoparticle Assemblies: From Dimers to Disordered Clusters

C. Rousseau[1], **V. Joris[1]**, B. Maes[1] and G. Rosolen[1]

[1] *Micro- and Nanophotonic Materials Group, Research Institute for Materials Science and Engineering, University of Mons, 20 Place du Parc, B-7000 Mons, Belgium*

Hybrid nanostructures [1] combining plasmonic and dielectric nanoparticles (NPs) provide a versatile route to tailor light-matter interactions at the nanoscale. In this context, heteroaggregation, namely the aggregation of distinct NP populations, offers a simple way to form such hybrid assemblies [2]. Here, we investigate whether incorporating titanium dioxide (TiO_2) NPs can enhance the optical absorption of disordered gold (Au) NP assemblies. The analysis is based on full-wave finite-element simulations of Au-TiO_2 dimers, random three-dimensional clusters, and random planar arrays of aligned heterodimers.

At the dimer level, the TiO_2 NP acts as a nearly lossless electromagnetic mediator. By storing and re-radiating the incident field, it modifies the local excitation experienced by the Au NP, leading either to absorption enhancement or suppression depending on the illumination geometry and relative particle position [3]. For NPs with a radius of 100 nm, our results show that, at 520 nm, the most favorable dimer configuration increases the Au absorption by about 43%, whereas an unfavorable one decreases it by about 15%.

This mechanism is then examined statistically in random Au-TiO_2 clusters containing 10 Au and 10 TiO_2 NPs. For each hybrid realization, a matched Au-only reference is obtained by removing the TiO_2 NPs while preserving the Au positions. Over 100 random configurations, TiO_2 addition produces a statistically significant enhancement over most of the visible range, with an increase of about 11% around 520 nm. This improvement results from reduced optical shielding within the Au subnetwork and a more favorable redistribution of the local electromagnetic field.

Finally, random planar arrays of aligned Au-TiO_2 heterodimers are considered to preserve constructive dimer configurations more directly. Depending on illumination geometry and intra-dimer spacing, the visible absorption modulation ranges from weak suppression to enhancements of up to about 32%. Overall, our results show that position-dependent absorption modulations at the Au-TiO_2 dimer level translate, on average, into a positive enhancement in random clusters. This suggests that heteroaggregation is a promising strategy to improve the optical absorption of Au NP assemblies, and that this enhancement can be further amplified in designed two-dimensional geometries where favorable coupling configurations are preserved more effectively.

Acknowledgement: We acknowledge support from the Action de Recherche Concertée (project ARC-23/27 UMONS3).

[1] C. Rousseau et al., 2024 *Computer Methods and Programs in Biomedicine* **257**, 108453
[2] B. M. Smith et al., Nason, 2015 *Environ. Sci. Technol.* **49**(21), 12789-12797
[3] Q. Zhao, Z.-J. Yang, et J. He, 2018 *Front. Phys.***13**(3), 137801

P32

Predicting Ceramic Membranes Performance in Organic Solvent Nanofiltration: A Physics-guided Machine Learning Approach

W. Linsen[1], Y. Roelen[1], P. Piccard[1,2], A. Buekenhoudt[2] and J. Hooyberghs[1]

[1]*UHasselt—Hasselt University, Data Science Institute, Theory Lab, Agoralaan, Diepenbeek, 3590, Belgium*

[2]*VITO N.V.—Flemish Institute of Technological Research, Unit MATCH, Boeretang 200, Mol, 2400, Belgium*

Organic Solvent Nanofiltration (OSN) is a pressure-driven membrane separation technique that selectively filters molecules dissolved in organic solvents based on their molecular size and affinity for the membrane material—rather than differences in boiling point as in distillation. This makes OSN an energy-efficient, environmentally friendly alternative to traditional thermal separation methods. Widespread industrial implementation, however, is hampered by the complex physicochemical interactions between the membrane, solvent, and solutes. Existing theoretical models, including the Spiegler-Kedem model rooted in irreversible thermodynamics, often fail to accurately predict flux (the rate of solvent transport through the membrane) and retention (the degree to which solute molecules are rejected, expressed as a percentage) or rely on empirically fitting free parameters. This absence of a predictive theoretical model results from a lack of insight into the complex underlying transport mechanisms.

This research explores how these interactions govern flux and retention by systematically varying system parameters. These measurements will not only serve to fit and adjust irreversible thermodynamics transport models but will also form the basis for data-driven methodologies [1,2]. Although deep neural networks are well-suited for recognizing patterns in high-dimensional data, they are susceptible to overfitting and physically inconsistent predictions. To overcome this, this research employs a physics-guided machine learning approach: known physicochemical laws and thermodynamic constraints are directly embedded into the neural network's architecture, ensuring that predictions remain physically consistent.

By using Explainable AI, such as feature attribution analyses (e.g., SHAP values), the model remains interpretable: rather than acting as an opaque predictor, a so-called black-box model, it enables identification of the dominant physical driving forces behind membrane transport, serving as a source for new hypotheses and theoretical inspiration. This provides fundamental insights into the complex separation mechanism. We aim to create a robust prediction framework that accelerates the economic valorization of OSN in industry. By optimizing operational costs in their application and minimizing the need for time-consuming pilot experiments, the 'time-to-market' is shortened and the threshold for industrial implementation is lowered.

[1] Piccard P-J, Borges P, Cleuren B, Buekenhoudt A and Hooyberghs J 2025 *J. Membr. Sci.* **735** 124509
[2] Linsen W, Piccard P-J, Hooyberghs J and Buekenhoudt A 2026 J. *Membr. Sci. Lett.* **6** 100111

P33

Development of a Scanning Thermal Microscopy Platform for Thermoelectric Characterization of 2D Materials and Nano-devices

Amirreza Lotfian[1], Pascal Gehring[1]

[1]*Institute of Condensed Matter and Nanoscience, UCLouvain, 1348 Louvain-la-Neuve, Belgium*

Scanning Thermal Microscopy (SThM) is a powerful technique for nanoscale investigation of thermal transport, enabling the quantification of local thermal properties in both bulk and low-dimensional materials [1]. Beyond passive characterization, SThM provides direct access to local heat dissipation in active devices and to thermoelectric phenomena at the nanoscale [1,2]. In particular, combining SThM with external magnetic fields opens new opportunities to study magnetically tunable thermal and thermoelectric effects, relevant for applications ranging from energy conversion to solid-state thermal switches [1].

In this work, we develop a custom SThM platform based on a modified commercial atomic force microscope. The system is extended with the capability to apply controlled inplane magnetic fields up to 500 mT, enabling spatially resolved studies of magneto-thermal effects [1]. The magnetic field is generated using two permanent magnets mounted on independent shafts, whose rotation is driven by high-precision stepper motors, allowing fine control over the field orientation and magnitude at the sample position. The entire platform is housed inside a glove box to ensure a controlled measurement environment and minimize external perturbations. The performance of the setup is benchmarked through measurements of local heat dissipation in integrated CMOS structures.

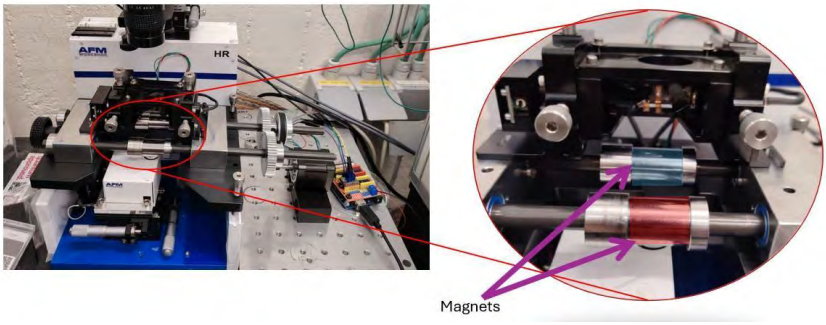

Figure 1: Photograph of the custom SThM platform based on a modified commercial AFM. The inset shows a close-up of the two permanent magnets mounted on rotating shafts, used to apply a controlled in-plane magnetic field at the sample position.

[1] M. Razeghi et al., "Giant Anomalous Ettingshausen Effect and Hybrid LongitudinalTransverse Thermoelectric Cooling in a Nanoscale Magnetic Weyl Semimetal," 2025 *ACS Nano* **19**(46), 39725–39734, doi: 10.1021/acsnano.5c11800
[2] V. Fonck et al., "Characterization of heat transfer in 3D CMOS structures using Sideband Scanning Thermal Wave Microscopy," 2025 *arXiv*, arXiv:2510.27529

P34

Unraveling the Germanium-Vacancy Center in Diamond

E. A. Melan[1,2,3], D. E. P. Vanpoucke[2,3], and L. Henrard[1]

[1]*UNamur, Namur Institute of Structured Matter (NISM), Department of Physics, Rue de Bruxelles 61, B-5000 Namur, Belgium*
[2]*UHasselt, Institute for Materials Research (IUMAT), Qunatum & Artificial intelligence design Of Materials (QuATOMs), Martelarenlaan 42, B-3500 Hasselt, Belgium*
[3]*imec, IUMAT, Wetenschapspark 1, B-3590 Diepenbeek, Belgium*

Most diamonds contain impurities, either intentionally introduced during growth or unintentionally.[1] These impurities can cause lattice deformations, leading to strains in the crystal. They can extend through the crystal lattice and affect a nearby color center. One such color center is the Germanium-Vacancy (GeV) center. It has a highly symmetric D_{3d} structure resulting in a sharp spectral peak which makes it an interesting candidate as a single photon emitter for applications as quantum communication. A lattice deformation can break the highly symmetric structure of the GeV center, and affect the spectral peak.[2]

In this work, density functional theory (DFT) is used to model the ZPL of the GeV center under strain. Two types of strains are studied: hydrostatic strain, and axial strain. Hydrostatic strain does not break the symmetry of the defect. There is, however, a difference in spectral shift under tensile and compressive strain. It has a red- and blue-shift, respectively (Figure 1). Linear strain does break the symmetry of the color center and reduces to a C_{2h} symmetry. The breaking of symmetry, due to both tensile and compressive strain, results in a red-shift of the ZPL. Additionally, the GeV center can be in different charge states and can be influenced differently by strain. Therefore, further theoretical studies are needed to understand the observed optical properties.

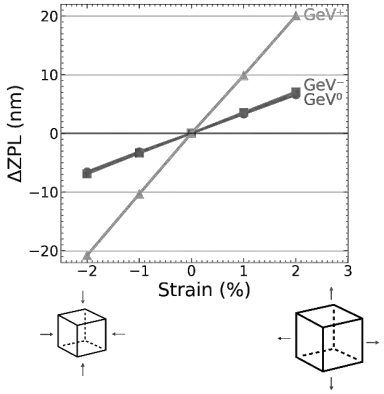

Figure 1: Hydrostatic strain of a germanium-vacancy color center in diamond. Compressive strain results in a blue-shift, and tensile strain in a red-shift, both independent of the charge state of the color center.

[1] E. Y. Guillaume, *et al.* 2025 in *Nanophotonics with Diamond and Silicon Carbide for Quantum Technologies* **Chap. 5** ISBN: 978-0-443-13717-4.
[2] T. G. I. Van Wijk, *et al. Carbon* **234** (2025), 119928.

P35

Study of the Electronic Structure and Optical Properties of Oxygen-Deficient Tungsten Oxide (WO_{3-x}) for Electrochromic Applications

E. Najid[1,2], M. El-Allam[1,2], K. Chaoui[1], L. Henrard[1], I. Derkaoui[2], and M. Achechboune[1,3]

[1] *Namur Institute of Structured Matter, Department of Physics, Namur, Belgium*
[2.] *LPS, Faculty of Sciences Dhar el Mahraz,*
Sidi Mohammed Ben Abdellah University, Fez - Morocco
[3] *School of Applied and Engineering Physics, University Mohammed VI Polytechnic,*
Ben Guerir, 43150, Morocco

Tungsten trioxide (WO_3) is a wide-band-gap semiconductor whose physical and functional properties are strongly influenced by the presence of oxygen vacancies. Its nonstoichiometric form, denoted WO_3-x, is of particular interest for various applications, especially smart windows, due to its remarkable electrochromic properties. In this work, we investigated the electronic and optical properties of WO_3-x using ab initio methods based on density functional theory (DFT). In order to improve the description of excited electronic states, we employed the Hubbard correction (DFT+U) as well as the DFT-1/2 method to obtain a more accurate estimation of the band gap. Through these approaches, we analyzed the effect of oxygen-vacancy concentration on the formation energy and the electronic structure, particularly on the distribution of the density of states and the value of the band-gap energy. Our results show that oxygen vacancies introduce quasi-localized states within the band gap, leading to a reduction in the gap and even to the emergence of metallic behavior, similarly to degenerate semiconductors. Consequently, these defects induce significant changes in the optical properties. Indeed, the metallic character gives rise to the absorption of electromagnetic waves in the visible and infrared regions through surface plasmon excitation in WO_3 nanoparticles, resulting in plasmonic electrochromic properties. Thus, the structural and electronic transformations associated with oxygen vacancies play a key role in modulating the optical response of nanostructured WO_3-x, particularly in the visible and infrared regions.

Keywords: WO_3-x, oxygen vacancies, DFT+U, DFT-1/2, electronic structure, optical properties, plasmonic electrochromism.

P36

Generating, sorting and standardizing microscopy data with artificial intelligence

D. Tomecka[1], S. Khalatabad[2], R. Jaeken[1], T. Nguyen Minh[2], L. Kestens[2], S. Cottenier[2], **M. Sluydts[1]**

[1]ePotentia, Frans van Dijckstraat 59, B-2100 Deurne Antwerpen, Belgium,
michael.sluydts@epotentia.com (https://www.epotentia.com)
[2]Ghent University, Department of Electromechanical, Systems and Metal Engineering,
Tech Lane Ghent Science Park - Campus A, Technologiepark 131, B-9052 Gent, Belgium,
stefaan.cottenier@ugent.be (https://www.ugent.be/ea/emsme/en)

Modern Artificial Intelligence (AI) methods offer the potential to revolutionize the prediction of material properties and the optimization of processes. Creating robust AI models however requires access to large standardized databases [1,2] which are not only rare, but also difficult to combine due to limitations in licensing and degrees of confidentiality. Data which is available is often not standardized and badly labelled making it difficult to use.

We demonstrate self-supervised methods being developed within the AID4GREENEST project [3] to automatically sort and curate large scanning electron microscopy datasets of steels by organizing them into a microstructural space [4]. By analyzing the structure of this space imperfections and imbalances in the datasets are deduced. We then demonstrate synthetic data methods which can generate additional image data by interpolating within microstructure space. In this way models can learn to better treat expected variation in real data and in the future make suggestions towards optimal data production through CHADA documentation [5].

[1] DeCost, B. L., Hecht, M. D., Francis, T., Webler, B. A., Picard, Y. N., & Holm, E. A. (2017). UHCSDB: UltraHigh Carbon Steel Micrograph DataBase: Tools for Exploring Large Heterogeneous Microstructure Datasets. *Integrating Materials and Manufacturing Innovation*, *6*(2), 197–205. https://doi.org/10.1007/s40192-017-0097-0
[2] MicrostructureDB. (2025). [Online]. Available: https://www.microstructuredb.com
[3] AID4GREENEST. (2025). [Online]. Available: https://www.aid4greenest.eu
[4] Larmuseau, M., Sluydts, M., Theuwissen, K., Duprez, L., Dhaene, T., & Cottenier, S. (2020). Compact representations of microstructure images using triplet networks. *Npj Computational Materials 2020 6:1*, *6*(1), 1–11. https://doi.org/10.1038/s41524-020-00423-2
[5] "Materials characterization - Terminology and structured documentation," CEN Workshop Agreement 17815:2025, 2025.

P37

Plasmonic gas-phase Ag–Cu nanoparticles deposited on TiO_2 nanotubes for photocatalytic CO_2 conversion

Daniele Tirotta [1,2], Young Sun Park [1], Ewald Janssen [1], Didier Grandjean [1], Sammy Verbruggen [2], Peter Lievens [1]

[1]*Quantum Solid State Physics (QSP), Department of Physics and Astronomy, KU Leuven, Leuven, 3001, Belgium*

[2]*Antwerp Engineering, Photoelectrochemistry and Sensing (A-PECS), Department of Bioscience Engineering, University of Antwerp, Antwerp, 2020, Belgium*

Carbon Capture and Utilization (CCU) that aims to convert CO_2 into valuable C_1 and C_2 fuels such as CO, methane, and ethylene is an attractive route to solving the global energy and environmental crisis (Fig.1).[1] CO_2 photocatalytic conversion is a promising approach to reach this goal, but the performance of the broadly used TiO_2 semiconductor catalyst is limited by its wide bandgap (3.2 eV), restricting light absorption to a small fraction of the solar spectrum (<5%) [2-3]. Here, we decorate TiO_2 nanotubes (TNTs) with Ag–Cu bimetallic plasmonic nanoparticles (PNPs) to fabricate a visible-light-driven CO_2 conversion photocatalyst whose performance will be enhanced through synergistical mechanisms.

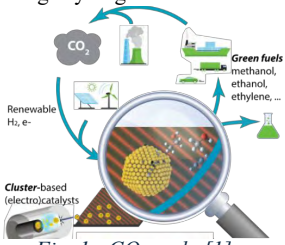

Fig. 1: CO_2 cycle [1]

TNTs fabricated by anodizing titanium foil are decorated with gas-phase ligand-free Cu_xAg_{1-x} PNPs using laser-ablation (LA) and magnetron-sputtering (MS) cluster beam deposition (CBD), enabling control over their size (from 2 to 20 nm), composition (x= 0, 0.1,0.25,0.5,0.75,0.9, 1) and their oxidation level by adding a small fraction of 1 to 5% O_2 to the He carrier gas during the deposition process [4].We will investigate how plasmonic effects and bimetallic interactions in the PNPs influence light absorption, charge carrier dynamics, and reaction selectivity, leading to an improvement of the photocatalytic performance compared to bare TiO_2. A combination of *ex situ* and *in situ* characterization techniques, including scanning transmission electron microscopy (STEM), X-ray photoelectron (XPS) and X-ray absorption (XAS) spectroscopies to probe the PNPs morphology, size distribution and electronic states, as well as *operando* diffuse reflectance infrared Fourier transform spectroscopy (DRIFTS) to monitor the charge carrier dynamics and reaction intermediates, will allow providing insight into the mechanisms governing the selective CO_2 photoconversion in these photocatalysts.

[1] https://www.catchy-etn.eu/catchy-project/
[2] Ciocarlan R.G. et al. 2023, Chem. Sus. Chem.: 16, e202201647
[3] Liao T.W. et al. 2018, Nanomaterials, 8, 30
[4] Chinnabatini V. et al. 2025, Nanoscale: 17, 833-845

P38

Quantifying the Statistical Fidelity of Generative AI in Materials Physics: A Multi-Dimensional Validation Framework

Daria M. Tomecka[1*], S. Khalatabad[2], R. Jaeken[1], B. Lis[1], L. Kestens[2], S. Cottenier[2], M. Sluydts[1]

[1]*ePotentia, Frans van Dijckstraat 59, B-2100 Deurne Antwerpen, Belgium,*
[2]*Ghent University, Department of Electromechanical, Systems and Metal Engineering, Tech Lane Ghent Science Park - Campus A, Technologiepark 131, B-9052 Gent, Belgium*
*tomeckadm@gmail.com

Generative AI offers a transformative solution to data scarcity in electron microscopy, yet its scientific utility depends on its ability to respect the underlying physical laws of material evolution. Within the AID4GREENEST project [1], we present a pipeline that bridges purely visual synthesis and scientifically valid data generation for advanced steels. Our approach centers on a two-step, phase-aware caption generation process that constrains the generative model to physically plausible regions of the material space by sampling processing attributes from phase-specific distributions. This strategy, informed by an initial similarity mapping of the UHCSDB [2] to identify data gaps and anomalies, ensures that synthetic microstructures reflect genuine process-structure correlations rather than impossible parameter combinations.

To audit the integrity of the results, we implement a multi-dimensional validation framework assessing distributional similarity within latent manifolds, discriminative difficulty using adversarial neural classifiers to detect artifacts, and structural fidelity via Fourier-space analysis of morphological symmetries. By comparing these computational metrics against qualitative expert metallurgist assessments, we establish a **robust "Metrology for AI"** that enables the trustworthy integration of generative models into the materials physics R&D cycle.

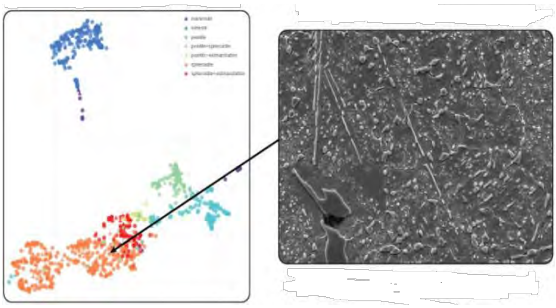

Figure 1: Mapping the microstructure space: Each point represents a single micrograph. On the right, a zoomed-in micrograph is shown; can you determine if it is real or synthetic?

[1] AID4GREENEST [Online]. Available: https://www.aid4greenest.eu
[2] DeCost BL, Hecht MD, Francis T, Webler BA, Picard YN, and Holm EA 2017 UHCSDB: UltraHigh Carbon Steel Micrograph DataBase: Tools for Exploring Large Heterogeneous Microstructure Datasets. *Integrating Materials and Manufacturing Innovation*, **6**(2), 197–205.

P39

Plasmon-enhanced OLED efficiency: a finite-element modeling investigation

L. Weber[1], M. Lobet[1], Y. Olivier[1], and L. Henrard[1]

[1]*Department of Physics, Namur Institute of Structured Matter (NISM), University of Namur, Rue de Bruxelles 61, B-5000 Namur, Belgium*

Plasmon coupling in organic light-emitting diodes (OLEDs) has long been regarded as a dominant loss pathway that limits device efficiency. More recently, however, controlled plasmon interaction has emerged as a promising strategy to enhance both efficiency and operational stability [1,2]. Nevertheless, the systematic optimization of such approaches remains challenging due to the strong dependence of plasmonic resonances on geometrical and material parameters, as well as the interplay of competing optical mechanisms involved (total internal reflections in substrate and organic layers, quenching, and ohmic losses in metallic electrodes). In this context, electromagnetic numerical modeling becomes a key tool for quantitatively investigating light-matter interactions, plasmon energy redistribution, and establish predictive design guidelines for efficiency enhancement. In this work, a three-dimensional finite-element model (FEM) has been developed to quantify both plasmon coupling and light outcoupling efficiency in OLED architectures. As a validation step, the outcoupling efficiency is extracted from the FEM by integrating the far-field intensity over the escape cone and compared with analytical calculations for a reference OLED structure, showing agreement within 2%. This validated 3D model provides a robust platform for the quantitative analysis of plasmonic effects in device geometries and offers a reliable basis for deriving design guidelines aimed at improving the performance of plasmon-enhanced OLEDs.

[1] M. A. Fusella *et al*. 2020 *Nature* **585**, 379
[2] J. A. Wisch *et al.* 2026 *Nat. Photon.* **20**, 24

P40

Semiclassical foundation of universality in chaotic quantum circuits

M. Kieler[1,2], F. Fritzsch[3], and A. Bäcker[2]

[1]*University of Liège, CESAM research unit, Liège, 4000, Belgium*
[2]*TU Dresden, Institute for Theoretical Physics, Dresden, 01069, Germany*
[3]*Max Planck Institute for the Physics of Complex Systems, Dresden, 01187, Germany*

The fundamental correspondence between quantum chaotic single-particle systems and random matrix theory is well-understood via periodic orbit theory. In contrast, we show that many-body systems with explicit subsystem structure possess characteristics different from the single-particle theory.

We present a periodic orbit theory for many-body systems with well defined semiclassical limit. Therefore, we identify periodic orbit families arising exclusively in the many-body setting and implement a central limit theorem characterizing their correlations. With this we demonstrate that spectral correlations in chaotic quantum circuits are characterized by the breaking of individual time translation invariance of periodic orbits in the subsystems into a residual synchronous time translations only. This provides a systematic approach to confirming random matrix universality in deterministic many-body systems.

P41

Quantum Chaos in a Classical Counterpart to the Fermi-Hubbard model through an exact Path-Integral Formalism

Louis Renck[1]

[1]*CESAM, Université de Liège*

Understanding quantum chaos in interacting many-fermion systems remains challenging : unlike many-bosons systems, where quantum-classical correspondence can be established using semiclassical tools such as the van Vleck-Gutzwiller propagator [1], most interacting fermions models still lack a sensible classical limit where Hamiltonian chaos can be defined.

We propose a candidate to the first classical Hamiltonian for the Fermi-Hubbard model with integrability broken by a random onsite potential. Starting from the fermionic Hamiltonian, we apply a Jordan-Wigner transformation and switch to the Schwinger-boson representation to obtain a bosonic form. A recently developed exact bosonic path-integral formalism [2] then provides a classical Hamiltonian symbol defined over a symplectic phase space. We investigate the resulting quantum-classical correspondence by comparing the effective dynamics with the quantum evolution, and we present quantitative checks of chaos based on spectral properties and out-of-time ordered correlators.

[1] T. Engl, J. Dujardin, A. Argu¨elles, P. Schlagheck, K. Richter, and J. D. Urbina, 2014 *Phys. Rev. Lett.* **112**, 140403
[2] F. Bruckmann and J. D. Urbina (2018)

P42

Shape-Dependent NMR Relaxivity of Magnetic Nanoparticles: From Diffusion Regimes to a Predictive Model

F. Fritsche[1], G. Rosolen[2], B. Maes[2], Y. Gossuin[1], and Q.L. Vuong[1]

[1]*Biomedical Physics Unit, Umons, Mons, 7000, Belgium*
[2]*Micro-and Nanophotonic Materials Group, Umons, Mons, 7000, Belgium*

Superparamagnetic magnetite (Fe_3O_4) nanoparticles are widely used as T_2 contrast agents in magnetic resonance imaging due to their ability to induce local magnetic field inhomogeneities and enhance transverse relaxation. While experimental studies suggest that particle shape anisotropy can improve relaxivity [1, 2], its influence on outer-sphere relaxation remains unclear, as standard models assume a dipolar magnetic field and do not account for anisotropic field distributions.

In this work, we numerically investigate water proton relaxation using Monte Carlo simulations in the presence of non-spherical Fe_3O_4 nanoparticles, following the approach described in [3]. The transverse relaxation rate (R_2) is computed at high static field (B_0) as a function of particle size and magnetization orientation for the particle geometries shown in Fig.1. By comparing anisotropic particles with volume-equivalent spheres, we isolate the contribution of shape to relaxivity. Our results show that for particle sizes above ~30 nm, shape has negligible impact on relaxivity. For smaller particles, geometry-dependent effects emerge but are not systematically beneficial, with some anisotropic shapes even yielding lower relaxivity than spheres. Typically, variations in relaxivity range from −20% to +80%, with the largest enhancements observed for elongated particle geometries.

We further introduce a predictive approach based on a weak-field approximation, demonstrating that relaxivity correlates with the variance of the induced magnetic field. This provides a practical pre-synthesis estimator for contrast efficiency and clarifies the conditions under which shape engineering is advantageous. Overall, this work provides a practical framework to evaluate the impact of nanoparticle shape on MRI contrast.

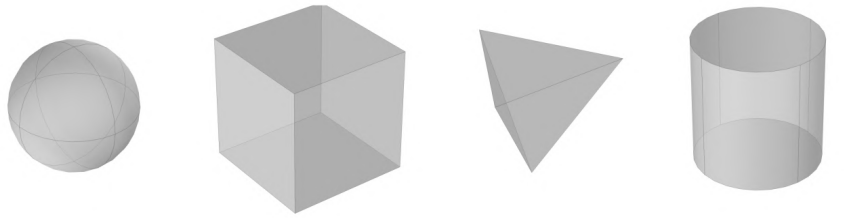

Figure 1: Nanoparticle shapes considered in this study: sphere, cube, tetrahedron, and cylinder. All shapes are defined with equal volume, corresponding to identical iron content.

[1] Andrade R.G.D *et al* 2020 *Int. J. Mol. Sci. 21 2455*
[2] Roca G *et al* 2025 *Adv. Drug Deliv. Rev. 138 68*
[3] Fritsche F *et al* 2025 *J. Chem. Phys. 162 12*

P43

Stochastic impedance in Non-equilibrium systems

B. Meeus[1,2], J. Hooyberghs[1,2], and B. Cleuren[3]

[1]*UHasselt, Faculty of Sciences, Theory Lab, Agoralaan, 3590 Diepenbeek, Belgium*
[2]*UHasselt-Hasselt University, Faculty of Sciences, Data Science Institute*

The real time kinetics of periodically driven stochastic systems are of great interest both from a theoretical point of view, where it sheds light on many of the properties of systems out of equilibrium [1-5], and from a practical point of view, where they provide a window into biological processes [6-8]. Stochastic impedance is developed as a novel way of gathering information about these systems [9].

The theory of stochastic impedance is formulated for periodically driven equilibrium systems. That is, in absence of the driving, the system obeys detailed balance and is as such in equilibrium. The present work aims to extend this framework to *driven non-equilibrium* systems. This would allow the formalism to not only be applied to the already wide extent of biological and chemical processes that are perturbed from equilibrium, but also to transport and search processes, which are of great interest in condensed matter physics and computer science.

[1] McLennan J A Jr 1959 Phys. Rev. 115 1405
[2] Cleuren B, Rutten B and Van den Broeck C 2015 Eur. Phys. J. Spec. Top. 224 879
[3] Proesmans K and Van den Broeck C 2015 Phys. Rev. Lett. 115 090601
[4] Oono Y and Paniconi M 1998 Prog. Theor. Phys. Suppl. 130 29
[5] Hatano T and Sasa S I 2001 Phys. Rev. Lett. 86 3463
[6] SantaLucia J J Annu. Rev. Biophys. Biomol. Struct.k 33 (2004) pp. 415-40
[7] Wolf L K J. Am. Chem. Soc. 127.49 (2005), pp. 17453-17459
[8] Van Oijen A M Current Opinion in Biotechnology 22 (2011), pp. 75-80.
[9] Cleuren B, Proesmans K, Physica A (2019) 122789.

Should you put a ring on it? Or should you get sticky with it? Comparing electrical homogeneity in nanoring and nanostick networks

G. Vanoppen[1], J. Hooyberghs[1,2], W. Deferme[3,4] and B. Cleuren[1]

[1]*UHasselt, Faculty of Sciences, Theory Lab, Agoralaan, 3590 Diepenbeek, Belgium*
[2]*UHasselt-Hasselt University, Faculty of Sciences, Data Science Institute*
[3]*UHasselt, Institute for Materials Research, Martelarenlaan 42, 3500 Hasselt, Belgium*
[4]*IMEC vzw, Division IMOMEC Wetenschapspark 1, 3590 Diepenbeek, Belgium*

Transparent conductive electrodes (TCEs) are essential materials for a wide range of next generation electronic and optoelectronic devices such as touch panels, displays and solar cells [1]. The most commonly used TCEs are based on indium tin oxide (ITO), which is not only rare, expensive and not eco-friendly to extract, but also extremely brittle, making it unsuitable for flexible devices. Therefore, there is a strong demand for alternative TCEs that are not only transparent and conductive, but also flexible and low-cost. Networks of metallic nanowires (NWs) are considered as one of the most promising alternatives to ITO.

While most of the scientific literature focusses on straight NWs (so-called nanorods), nanowires can also be manufactured in a circular shape (so-called nanorings) [2]. Due to their different geometry, nanorings have no dead ends in the percolation network. This could not only result in improved conductive properties but also reduce the occurrence of hotspots, leading to more durable electrodes [3].

Electrical homogeneity quantifies the homogeneity of the power distribution throughout the nanowire network. Networks that have a low electrical homogeneity (i.e. have problematic hotspots) result in electrodes that quicky breakdown under electrical stress. This is because regions with a peak in power density values lead to degradation of wires as a result of Joule heating and electromigration. This results in a snowball effect that destroys other wires and eventually the whole network breaks down. In this work, we propose a method (Figure 1) to calculate the electrical homogeneity and we investigate the effect of multiple design parameters of the network on the electrical homogeneity.

Figure 1: Strategy to calculate the electrical homogeneity. In the left image, we see a few wires that have a high power value. Using the convolution method, we are able to detect these hotspots (center image). The result of this convolution operation (and it's corresponding power density) is used to calculate the electrical homogeneity measure.

[1] Kumar et al 2022 Mater. Today Commun. 33 104433
[2] Li Z et al 2020 Micromachines 11 236
[3] Azani M and Hassanpour A 2018 Chem. Eur. J. 24 19195
[4] Grazioli D et al 2024 J. Compos. Sci. 245 110304

Hyperfine anomaly studies in gold isotopes using laser spectroscopy at CRIS

O. Ahmad[1], X.F. Yang[2], G. Neyens[1], T.E. Cocolios[1], J.G. Cubiss[3], R.P. de Groote[1], C.M. Fajardo-Zambrano[1], K.T. Flanagan[4], R.F. Garcia Ruiz[5], J.S.M Ginges[11], Y.F. Guo[2], H.R. Hu[2], Á. Koszorús[1,6], L. Lalanne[7], P. Lassegues[1], Y.S. Liu[2], K.M. Lynch[4], A. McGlone[4], F. Pastrana[5], J.R. Reilly[8], E. van Dalfsen[1], B. van den Borne[1], J. Warbinek[9], C.J West[11], J. Wilson[10], and Z.X. Yue[2]

[1]*KU Leuven, Instituut voor Kern- en Stralingsfysica, B-3001 Leuven, Belgium*
[2] *School of Physics and State Key Laboratory of Nuclear Physics and Technology, Peking University, Beijing 100871, China*
[3]*School of Physics and Astronomy, The University of Edinburgh, Edinburgh, Scotland, UK*
[4]*Department of Physics and Astronomy, The University of Manchester, Manchester, UK*
[5]*Massachusetts Institute of Technology, Cambridge, MA 02139, USA*
[6]*Belgian Nuclear Research Centre (SCK CEN), 2400, Mol, Belgium*
[7]*Université Paris-Saclay, CNRS/IN2P3, IJCLab, 91405 Orsay, France*
[8]*Systems Department, CERN, CH-1211 Geneva 23, Switzerland*
[9]*Experimental Physics Department, CERN, CH-1211 Geneva 23, Switzerland*
[10]*School of Physics, Engineering and Technology, University of York, Heslington, York, UK* [11]*School of Mathematics and Physics, The University of Queensland, Brisbane, Australia*

The hyperfine anomaly (HFA) originates from finite nuclear-size effects in the hyperfine interaction. It contains contributions from both the finite nuclear magnetization distribution, known as the Bohr-Weisskopf (BW) effect [1], and the finite nuclear charge distribution, known as the Breit-Rosenthal (BR) effect [2,3]. In heavy atoms, the differential BR contribution is expected to be negligible compared to the BW effect (10−4 in the region of gold, (Z = 79)) [4]. In the Au isotopes considered here, the relative HFA is therefore expected to be dominated by the BW contribution. The gold isotopes are a particularly interesting case, since relative hyperfine anomalies between isotopes up to ≈ 10 % have been reported in this chain [5].

We report high-resolution Collinear Resonance Ionization Spectroscopy (CRIS) studies of neutrondeficient ^{181}Au-^{197}Au isotopes, performed at the CRIS experiment at ISOLDE/CERN, using the 6s $^2S_{1/2} \rightarrow$ 6p $^2P_{3/2}$ atomic transition. The precision on the atomic hyperfine coupling constants has been improved by 1-2 orders of magnitude as compared to previous studies [5-8]. This allowed us to study the electronic state dependence of the extracted magnetic dipole moments, μ. The magnetic dipole moments measured independently from the lower and upper hyperfine A factors show a pronounced discrepancy, which becomes larger for isotopes with a larger μ, suggesting a sizable hyperfine anomaly in the electronic states of Au. The present measurements confirm the spin assignments for ^{181}Au-^{183}Au isotopes. Together, the spins and extracted *g*-factors help probe the underlying nuclear configuration and its evolution toward the lightest gold isotopes. These experimental results will be complemented by relativistic many-body atomic calculations of the Bohr-Weisskopf contribution in the relevant electronic levels. This will allow a direct comparison between the observed electronic-state dependence of the hyperfine anomaly and theoretical predictions. These results also extend hyperfine-anomaly studies in gold to 6p $^2P_{3/2}$ atomic level, providing a stringent benchmark for atomic many-body theory and nuclear-structure descriptions near Z = 82.

[1] A. Bohr and V. F. Weisskopf, *Phys. Rev*. 77, 94 (1950).
[2] J. E. Rosenthal and G. Breit, *Phys. Rev*. 41, 459 (1932).
[3] M. F. Crawford and A. K. Schawlow, *Phys. Rev*. 76, 1310 (1949).
[4] H. J. Rosenberg and H. H. Stroke, *Phys. Rev. A* 5, 1992 (1972).
[5] Barzakh, A.E. *et. al*, *Phys. Rev. C* 101, 034308 (2020)
[6] Barzakh, A.E. *et. al*, *Phys. Rev. C*, 064321 (2020)
[7] Cubiss, J *et. al*, *Phys. Rev. Lett.* 131, 202501 (2023)
[8] Harding, R.D *et. al*, *Phys. Rev. C* 102, 024312 (2020)

P46

Accelerating Bayesian Data Integration for Online Tungsten Concentration Inference in Fusion Plasmas

K. Chiñas Fuentes[1], D. Mazon[2] and G. Verdoolaege[1]

[1]*Ghent University, 9000 Ghent, Belgium*
[2]*Commissariat à l'Énergie Atomique et aux Énergies Alternatives, 13108 Cadarache, France*

Tungsten (W) accumulation in the core of a tokamak leads to strong radiative cooling, significantly degrading plasma performance, with maximum tolerable concentrations on the order of 10^{-4}. Bayesian data integration enables the estimation of W concentration profiles with associated uncertainties by combining multiple diagnostics, including soft X-ray (SXR), bolometry, interferometry, and electron cyclotron emission (ECE). This framework has been successfully implemented on both synthetic and experimental data. However, it requires Markov chain Monte Carlo (MCMC) sampling on a strongly correlated, high-dimensional, and non-linear posterior distribution, with analyses requiring several hours, making it unsuitable for online inference.

We present a systematic study of reconstruction strategies for W concentration estimation using synthetic data based on WEST tokamak geometry. Starting from the GPU/JAX-accelerated reimplementation of [1], we achieve a 2.8× wall-time reduction over the original CPU/PyMC baseline. We then benchmark 11 reconstruction configurations spanning exact and approximate Bayesian methods, covering full Gaussian process (GP) priors with MCMC, sparse GP approximations, and variational inference. The reconstruction domain comprises N=1,125 grid points within the last closed flux surface (LCFS) of a 60×60 spatial grid. Wall time spans from 2.6 minutes to 116.9 minutes across configurations, with the fastest method offering a 45× speedup at a 3× RMSE cost — a tradeoff relevant to both offline scientific analysis and real-time monitoring. Contrary to expectations, sparse GP approximations are both slower and less accurate than the full GP at this grid size; however, they could become competitive at larger spatial resolutions. Robustness tests across four synthetic profile geometries show that the Gaussian process prior encodes assumptions about profile shape that break down for hollow profiles. Calibration analysis further reveals that posterior coverage can collapse to near zero on certain noise realisations, which directly impacts uncertainty quantification across both offline and real-time plasma diagnostics.

Future work targets additional approximate Bayesian strategies, including variational free energy sparse GP and variational autoencoders, with the best-performing configuration used to train a neural network surrogate aimed at sub-second real-time deployment.

[1] Hao Wu et al 2025 *Plasma Phys. Control. Fusion* **67** 085001

MR-ToF assisted laser spectroscopy

T. Christen[1], R. de Groote[1], and Á. Koszorús[1, 2]

[1]*Institute for Nuclear and Radiation Physics, KU Leuven, Leuven, 3001, Belgium*
[2]*Belgian Nuclear Research Centre, SCK CEN, Mol, 2400, Belgium*

Precision laser spectroscopy provides a powerful method for investigating fundamental nuclear properties in a model-independent way, including nuclear spins, electromagnetic moments, and changes in mean-square charge radii [1]. These measurements are essential for testing and advancing nuclear theories. However, as experimental campaigns push towards increasingly exotic nuclei with diminishing yields, isobaric beam contamination has emerged as a major limiting factor for both spectral resolution and the range of accessible isotopes. Current laser spectroscopy experiments, such as the Collinear Resonance Ionization Spectroscopy (CRIS) experiment and collinear laser spectroscopy with fluorescence detection (CLSF) at the IGISOL facility, lack the intrinsic capability to suppress these isobaric contaminants. To overcome this limitation, we are planning to integrate a multi-reflection time-of-flight (MR-ToF) device into the beamlines [2]. An MR-ToF device confines ions between opposing electrostatic mirrors, extending the flight path to several hundred meters. Because the trapped ions have the same kinetic energy, the ions separate in time based on their mass-to-charge ratio, isolating the element of interest from the isobaric contaminants. Furthermore, this required mass resolving power is reached in just tens of milliseconds, making the MR-ToF highly compatible with laser spectroscopy timescales.

This contribution provides an overview of the ongoing project, focusing on the development and testing of the offline MR-ToF beamline at KU Leuven. Specifically, we report the first collinear laser spectroscopy measurements of $^{88}Sr^{+}$ performed downstream of the MR-ToF device. Our results reveal a revolution-dependent shift in the resonance frequency, which is attributed to imperfect electrode switching and extraction timing mismatches. Understanding and mitigating these induced kinetic energy variations is essential for ensuring reliable, high-precision MR-ToF-assisted laser spectroscopy. Finally, the future developments needed for integrating this system into radioactive ion beam facilities will be outlined.

[1] Á. Koszorús et al. Nuclear structure studies by collinear laser spectroscopy. 2024 *The European Physical Journal A*, **60**(1):20
[2] M. Schlaich et al. A multi-reflection time-of-flight mass spectrometer for the offline ion source of the puma experiment. 2024 *International Journal of Mass Spectrometry*, **495**:117166

P48

Investigating double bump air showers with the SKA

V. De Henau[1]

[1] *Inter-University Institute For High Energies (IIHE), Vrije Universiteit Brussel (VUB), Brussels, 1050, Belgium*

Cosmic rays are particles travelling in outer space at near light speeds. The origins of cosmic rays are still unknown, with large uncertainties in the transition region between Galactic and extragalactic sources (10^16 - 10^18 eV) [1]. When one of these high-energy particles collides with Earth's atmosphere, it causes an extensive air shower (EAS). However, the exact mechanism describing these collisions still has large uncertainties because the hadronic interaction models at EAS energies are beyond particle collider energies [2]. Most EAS exhibit a characteristic "universal" longitudinal profile (the particle amount as a function of atmospheric depth), with a single peak. The depth at which this peak occurs gives a measurement of the cosmic ray particle mass [3]. Low-mass particles, on average, penetrate deeper into the atmosphere before interacting, producing a shower maximum closer to the ground. These EAS emit radio waves, and by measuring this, we can reconstruct the energy and particle type of the cosmic ray, but due to uncertainties in the hadronic models, this is limited in accuracy. However, a rare phenomenon known as the anomalous shower deviates significantly from this universal profile. These anomalies are caused by secondary particles with high energies compared to the primary particle, traveling a significant distance further in the atmosphere. This causes the longitudinal profile to become elongated, and hence we call these stretched showers. Looking at an even rarer phenomenon caused by an energetic secondary travel even further into the atmosphere, the sub-shower can be displaced significantly enough from the main shower to cause a second bump in the longitudinal profile. These showers are called a double bump shower. These anomalous showers can be used to measure the crosssection of the hadronic interactions, and they hold additional information about the primary cosmic ray. Current cosmic ray experiments lack the resolution to distinguish between these different types of showers. Simulations have shown that the upcoming SKA-Low radio telescope will possess the sensitivity and resolution necessary to detect and reconstruct anomalous showers and thus be the first ever experiment capable of doing so [4].

[1] J. Bluemer, R. Engel, J. R. Hoerandel, (2009), doi:10.1016/j.ppnp.2009.05.002.
[2] D. Maurin *et al.*, (2025), doi:10.1016/j.physrep.2025.11.002.
[3] P. Lipari, (2008), doi:10.1103/PhysRevD.79.063001.
[4] V. De Henau *et al.*, (2025), doi:10.22323/1.501.0236.

Molecules as probes of nuclear structure: laser spectroscopy of ^{223}RaF

C. M. Fajardo-Zambrano[1], M. Athanasakis-Kaklamanakis[1,2,3], L. Lalanne[1,2,4], J. R. Reilly[5,6], O. Ahmad[1], M. Au[6], S. W. Bai[7], C. Bernerd[6], J. Berbalk[1,6], A. A. Breier[8], K. Chrysalidis[6], T. E. Cocolios[1], R. P. de Groote[1], K. T. Flanagan[5,9], R. F. Garcia Ruiz[10,11], P. Imgram[1], A. Koszorus[1], P. Lassegues[1], J. Lim[3], Y. C. Liu[7], K. M. Lynch[5], A. McGlone[5], W.C. Mei[7], G. Neyens[1], L. Nies[6], A. V. Oleynichenko[12], A. Raggio[1], L.V. Skripnikov[12], B. van den Borne[1,2], J. Warbinek[1,2], J. Wessolek[5,6], X. F. Yang[7]

[1]*KU Leuven, Instituut voor Kern- en Stralingsfysica, B-3001 Leuven, Belgium*
[2]*Experimental Physics Department, CERN, CH-1211 Geneva 23, Switzerland*
[3]*JILA and Department of Physics, University of Colorado, Boulder, Colorado 80309, USA*
[4]*Universite Paris-Saclay, CNRS/IN2P3, IJCLab, 91405 Orsay, France*
[5]*Department of Physics and Astronomy, The University of Manchester, Manchester M13 9PL, UK*
[6]*Systems Department, CERN, CH-1211 Geneva 23, Switzerland*
[7]*State Key Laboratory of Nuclear Physics and Technology, Peking University, Beijing, China*
[8]*Institut für Optik und Atomare Physik, Technische Universität Berlin, 10623 Berlin, Germany*
[9]*Photon Science Institute, The University of Manchester, Manchester M13 9PY, United Kingdom*
[10]*Department of Physics, Massachusetts Institute of Technology, Cambridge, MA 02139, USA*
[11]*Laboratory for Nuclear Science, Massachusetts Institute of Technology, Cambridge, USA*
[12]*Affiliated with an institute covered by a cooperation agreement with CERN.*

In the past few years, spectroscopy of radioactive molecules has been performed at ISOLDE (CERN) using the Collinear Resonance Ionization Spectroscopy (CRIS) experiment [1]. Given their structure and chemical properties, radioactive molecules are promising candidates for studies in different fields, including for more efficient extraction of refractory elements from ISOLDE targets [2].

Following the successful high-resolution studies of ^{225,226}RaF [3,4], the CRIS experiment at ISOLDE performed the first hyperfine-resolved resonance ionization spectroscopy of ^{223}RaF, yielding the first measurement of the EQM in a short-lived radioactive molecule ($t_{1/2}$ = 11.4 days) for ^{223}Ra (I = 3/2). Additionally, the change in charge radii of ^{223,225,226}Ra have been extracted from spectroscopy of RaF molecules with a precision comparable to atomic studies [5]. Finally, the magnetic dipole moment and finite magnetization contribution of ^{223,225}RaF were extracted in a nuclear model-independent way.

This contribution will focus on the measured nuclear moments of ^{223}RaF and compare them with atomic and ionic measurements reported in the literature. Our measurement, in combination with state-of-the-art relativistic coupled-cluster calculations of the electric field gradient in the molecule [6,7], provides an accurate and precise value for the ^{223}Ra quadrupole moment. Thus, serving as a reference for the extraction of quadrupole moments of other isotopes. This work also demonstrates how molecular laser spectroscopy could offer a new pathway for extracting unknown nuclear moments of radioactive isotopes, not accessible in atomic form, using suitable radioactive molecules.

[1] Garcia Ruiz, R.F., et al. 2020 *Nature* **581**(7809), 396-400
[2] Arrowsmith-Kron, G et al 2024 *Rep Prog Phys.* **12**, 87(8).
[3] Wilkins, S. G., et al 2025 *Science* **390**(6771), 386-389
[4] S.-M. Udrescu, et al 2024 *Nature Physics* **20**(2)
[5] Lynch, K. M., et al 2018 *Phys. Rev. C* **97**(2), 024309
[6] Petrov, A. N., & Skripnikov, L. V. 2020 *Phys. Rev. A* **102**(6), 062801
[7] Skripnikov, L. V. 2020 *J. Chem. Phys.* **153**, 114114

P50

The ScIDEP Muon Radiography Project at the Egyptian Pyramid of Khafre

D. Geeraerts[1], S. Aly[2], M. Gamal[2], A. Hecht[4], R.T. Kouzes[5], A. Mahrouss[2], A. Aftoiu[3], D. Stanca[3], M. Tytgat[1], C. Vancea[3], J. Valencia[4], Z. Wang[1]

[1]*Inter-University Institute for High Energies, Vrije Universiteit Brussel, Brussels, Belgium.*
[2]*Institute of Basic and Applied Science, Egypt-Japan University of Science and Technology, Alexandria, Egypt.*

[3]*Horia Hulubei National Institute for Physics and Nuclear Engineering, Magurele, Romania.*
[4]*Department of Nuclear Engineering, University of New Mexico, Albuquerque, New Mexico, USA.*

[5]*Pacific Northwest National Laboratory, Richland, Washington, USA.*

Despite centuries of research, the Egyptian pyramids at Giza continue to raise questions about their internal structure and construction. The Great Pyramid of Khufu features an intricate network of chambers and passageways, whereas the Pyramid of Khafre, the second-largest pyramid on the Giza Plateau, seems to have a relatively simpler interior design, prompting speculation about the possible existence of hidden voids.

Muon radiography uses cosmic-ray muons to detect density variations inside large objects: muons penetrate large amounts of material with attenuation proportional to the crossed matter density, enabling the mapping of the target's internal density by comparison with free-sky measurements [1]. The ScIDEP (Scintillator Imaging Detector for the Egyptian Pyramids) Collaboration is developing muon telescopes with the aim of mapping the internal density distribution of the Pyramid of Khafre using transmission muon radiography [2]. Two distinct detector designs are currently being built and investigated: (i) large-area PVT scintillator plates with fiber readout and (ii) modular plastic scintillator b ars. The collaboration plans to position one detector inside the pyramid, in the King's burial chamber located at the pyramid's base, and another detector outside. This setup, combining data from multiple angles, allows for a three-dimensional reconstruction of potentially unknown internal features.

A Geant4 simulation framework has been developed to aid in the design and optimization of the ScIDEP muon telescopes and to simulate the expected muon flux through the pyramid. The framework includes a 3D model of the Pyramid of Khafre, with its known internal structure, along with a complete detector description that incorporates realistic scintillator properties and optical photon transport. This contribution highlights the ScIDEP project, covering the detector concepts in development, the simulation framework, and first results on track reconstruction and muographic imaging performance.

[1] L. Cimmino, *Principles and perspectives of radiographic imaging with muons*, J. Imaging **7** (2021) 253.
[2] M. Gamal *et al.*, *The ScIDEP muon radiography project at the Egyptian Pyramid of Khafre*, J. Appl. Phys. **138** (2025) 044901.

P51

First Study of the Dee Integration, Module Testing and Noise Performance of One endcap of CMS Phase - II Outer Tacker System

Majid Hussain[1]

[1]*Université Catholique de Louvain (UCL), Belgium*

The Large Hadron Collider (LHC) accelerator is going to be upgraded to the High-Luminosity LHC (HL-LHC) to achieve instantaneous luminosity exceeding a factor of 5 –7.5 compared to the current performance, which requires a corresponding upgrade of the CMS tracker (then called Phase-2 tracker). The upcoming tracker system will consist of two parts: an inner tracker (IT) and an outer tracker (OT), to ensure stable performance during high pileup collisions and L1 trigger functionality will be implemented for the OT. The upgraded outer tracker will contain two-barrel regions, and two endcaps made of double disks (TEDD) for a nearly hermetic detector. In one endcap region, five double disks will be installed, and the structure is made up of "dees", that integrated into two types of modules (2S and PS).

The TEDD integration centres set up a detailed testing process to ensure that the dees, their services, and modules on the dee structures work reliably. Before starting the integration, the modules are first tested on the reception test stand individually. Then they are integrated with the electrical and optical services on the dee structures. Last, so-called sector tests are run to observe and evaluate the behaviour of the silicon sensors.

This poster presentation will present exercises of the module integration on dee, the procedure of double disk assembly, as well as module testing, and noise measurement under the different operating conditions to meet the requirement that the detector will work very well in HL-LHC environment.

Collinear laser spectroscopy of germanium isotopes at IGISOL

A. Kayaalp[1], Á. Koszorús[1,2], G. Neyens[1], R.P. de Groote[1], and the IGISOL collaboration[3]

[1]*Institute for Nuclear and Radiation Physics, KU Leuven, B-3001 Leuven, Belgium*
[2]*Belgian Nuclear Research Centre, SCK CEN, B-2400 Mol, Belgium*
[3]*Department of Physics, University of Jyväskylä, FI-40500 Jyväskylä, Finland*

High-resolution laser spectroscopy can probe nuclear spins, magnetic dipole (μ) and electric quadrupole (Q_s) moments, and changes in mean-square charge radii ($\delta\langle r^2\rangle$) from hyperfine structures and isotope shifts of short-lived nuclei [1]. These observables provide complementary information on both single-particle and collective properties of the atomic nuclei. We present the plans for a collinear laser spectroscopy (CLS) campaign at IGISOL, using the chemically non-selective ion-guide technique [2] to deliver Ge isotopes.

In the *fpg*-shell, the germanium chain (Z = 32) lies in the γ-soft/triaxial mid-shell, exhibiting shape coexistence in ^{72}Ge [3] and rigid triaxial deformation in ^{76}Ge [4]. Recent CLS campaigns have measured $\delta\langle r^2\rangle$ of $^{68–74}$Ge [5] and moments of ^{69,71,73}Ge [6]; the planned campaign will extend these measurements to $^{77–83}$Ge, approaching the N = 50 shell closure. Reaching ^{83}Ge (N = 51) will determine the magnitude of the N = 50 charge-radii kink at Z = 32, trace the evolution of quadrupole collectivity, and deliver the first electromagnetic moments of odd-A ^{77,79,81,83}Ge and their long-lived isomers. These measurements will constrain the $\nu g_{9/2}$ occupancy along with the $\nu p_{1/2}$, $\nu p_{3/2}$, $\nu f_{5/2}$ orbitals in the *fpg* valence space, and clarify tentative spin assignments. Near the closure, the tentative $(9/2^+)$ ground-state and $(1/2^+)$ intruder assignments in ^{81}Ge will be examined; the $(1/2^+)$ isomer involves excitations across N = 50 and mirrors the intruder $(1/2^+)$ isomer observed in the N = 49 isotone ^{79}Zn [7]. Beyond the closure, ^{83}Ge will probe single-particle structure above N = 50. Together, these observables will benchmark shell-model interactions (JUN45, jj44b, and cross-shell PFSDG-U near and beyond N = 50) alongside Gogny-IBM predictions.

[1] Yang X F *et al* 2023 *Prog. Part. Nucl. Phys.* **129** 104005
[2] Moore I D *et al* 2014 *Hyperfine Interact.* **223** 17
[3] Ayangeakaa A D *et al* 2016 *Phys. Lett. B* **754** 254
[4] Ayangeakaa A D *et al* 2019 *Phys. Rev. Lett.* **123** 102501
[5] Wang S J *et al* 2024 *Phys. Lett. B* **856** 138867
[6] Kanellakopoulos A *et al* 2020 *Phys. Rev. C* **102** 054331
[7] Yang X F *et al* 2016 *Phys. Rev. Lett.* **116** 182502

P53

A time-offset stacking search for neutrino emission associated with gamma-ray bursts

E. Magnus[1,2], N. van Eijndhoven[1,2], and K. de Vries[1,2]

[1]*Inter-University Institute For High Energies (IIHE), Vrije Universiteit Brussel (VUB), Pleinlaan 2, Brussels, 1050, Belgium*

The IceCube Collaboration discovered a diffuse flux of high-energy astrophysical neutrinos in 2013 [1]. More than a decade later, only a handful of sources have been identified, including the blazar TXS 0506+056, some X-ray bright Active Galactic Nuclei (such as NGC 1068), and diffuse emission from the Galactic Plane [2,3,4]. However, it remains unclear what fraction of the observed flux these sources account for, leaving the origin of most astrophysical neutrinos unknown.

Gamma-ray bursts were among the earliest proposed source classes for high-energy neutrinos. However, searches by neutrino detectors, such as ANTARES and IceCube, have placed strong limits on neutrino emission coincident with the GRB trigger times [5,6]. Most of these analyses relied on short and conservative time windows, potentially missing neutrino emission occurring at larger time offsets relative to the GRB trigger.

In this work, we explore an alternative temporal search strategy that extends the observation window up to ± 40 days around the GRB trigger time, in accordance to a similar study in [7]. We employ a time-delay stacking method, originally proposed in [8] and here developed into a more sensitive implementation. The method tests the hypothesis that GRBs emit neutrinos at fixed time offsets from the trigger time by stacking neutrino-GRB time differences over many bursts and searching for deviations from a uniform background distribution.

This project is currently in a preparatory phase, focusing on sensitivity studies and optimization of the time windows. The final goal is to apply this method to IceCube data to probe non-standard temporal correlations between GRBs and high-energy neutrinos.

[1] IceCube Collaboration 2013 *Science* **342** 1242856
[2] IceCube Collaboration 2018 *Science* **361** 147-151
[3] IceCube Collaboration 2026 *ApJL* **1000** L37
[4] IceCube Collaboration 2023 *Science* **380** 1338-1343
[5] IceCube Collaboration 2024 *ApJ* **964** 126
[6] ANTARES Collaboration 2021 *MNRAS* **500** 4, 5614–5628
[7] ANTARES Collaboration 2017 *Eur.Phys.J.C* **77** 1, 20
[8] N. van Eijndhoven 2008, *Astropart. Physics* **28** 6, 540-546

P54

DFT+TN: A new method to accurately model complex materials from first principles

S. Ganne[1], D. Vrancken[1, 2], D. Verraes[1, 2], T. Braeckevelt[1], L. Devos[2], L. Vanderstraeten[2], J. Haegeman[2], V. Van Speybroeck[1]

[1]*Center for Molecular Modeling, Ghent University, Zwijnaarde, 9052, Belgium*
[2]*Department of Physics and Astronomy, Ghent University, Gent, 9000, Belgium*

Modern technological applications rely on materials with precisely controlled electronic and magnetic properties. However, predicting these properties computationally remains challenging for an important class of materials where electrons interact strongly with each other. These "strongly correlated" materials exhibit extraordinary behaviours such as superconductivity at relatively high temperatures and transitions between conducting and insulating states, making them promising candidates for next-generation technologies including quantum computers and energy-efficient electronics.

Current computational methods like Density Functional Theory, whilst successful for many materials, often fail to accurately predict the properties of strongly correlated systems. This limitation significantly hinders the rational design of new functional materials. We have developed a systematic computational approach that addresses this challenge by combining multiple advanced techniques in a novel framework.

Our method begins with standard electronic structure calculations and systematically constructs simplified but accurate models that capture the essential physics of electron correlations. These models are then solved using state-of-the-art numerical techniques developed for quantum manybody systems. Initial applications to quasi-one-dimensional materials demonstrate substantial improvements in calculated electronic properties compared to conventional methods, with results showing excellent agreement with experimental measurements [1].

This work establishes a robust, parameter-free computational tool for predicting the properties of strongly correlated materials, accelerating the discovery and design of novel materials with tailored functionalities for technological applications.

[1] Vrancken D, Ganne S, Verraes D, Braeckevelt T, Devos L, Vanderstraeten L, Haegeman J and Van Speybroeck V 2Quantitative Description of Strongly Correlated Materials by Combining Downfolding Techniques and Tensor Networks 2025 *J. Chem. Theory Comput.* **21** 7830–44

The Belgian Physical Society General Scientific Meeting 2026 is supported by: